TRIBHUVAN UNIVERSITY

INSTITUTE OF ENGINEERING

PULCHOWK CAMPUS

THESIS NO: 078/MSPSE/015

Rolling Bearing Fault Diagnosis on Vibration-Based Condition Monitoring of Induction Machines Using Machine Learning Approaches

by

Prakash Dahal

A THESIS

SUBMITTED TO THE DEPARTMENT OF ELECTRICAL ENGINEERING IN PARTIAL FULFILLMENT OF THE REQUIREMENTS FOR THE DEGREE OF MASTER OF SCIENCE IN POWER SYSTEM ENGINEERING

DEPARTMENT OF ELECTRICAL ENGINEERING

LALITPUR, NEPAL

APRIL, 2025

COPYRIGHT©

त्रिभुवन विश्वविद्यालय
TRIBHUVAN UNIVERSITY
इन्जिनियरिङ्ग अध्ययन संस्थान
INSTITUTE OF ENGINEERING
पुल्चोक क्याम्पस
PULCHOWK CAMPUS
DEPARTMENT OF ELECTRICAL ENGINEERING
Pulchowk, Lalitpur

Accredited by University Grants Commission (UGC) Nepal 2020

Institute of Engineering Electrical Engineering Department Pulchowk Campus

CERTIFICATE OF APPROVAL

The undersigned certify that they have read, and recommended to the Institute of Engineering for acceptance, a thesis entitled "**Rolling Bearing Fault Diagnosis on Vibration-Based Condition Monitoring of Induction Machines Using Machine Learning Approaches**" submitted by **Prakash Dahal** in partial fulfilment of the requirements for the degree of **Master of Science in Power System Engineering**.

.....

Asst. Prof. Anil Kumar Panjiyar
Department of Electrical Engineering
Pulchowk Campus, Lalitpur
(Supervisor)

.....

Asst. Prof. Dr. Kamal Chapagain
Department of Electrical and Electronics
Engineering, Kathmandu University
(External Examiner)

.....

Asst. Prof. Dr. Bishal Silwal
Program Coordinator
MSc. in Power System Engineering
Pulchowk Campus, Lalitpur
(Supervisor)

.....

Assoc. Prof. Dr. Basanta Kumar Gautam
Head of Department
Department of Electrical Engineering
Pulchowk Campus, Lalitpur

April 2025

ABSTRACT

This dissertation analyzes motor vibration signals from a squirrel cage induction machine for the detection and diagnosis of rolling bearing faults. Machine learning diagnostic models including support vector machines (SVM), random forest classifiers (RF), logistic regression (LR) and gradient boosting machines (GBM) are employed to identify bearing faults such as outer race fault, inner race fault and damaged bearing cage fault. All these methods make the fault diagnosis by statistical feature extraction in both the time and frequency domains as well as the envelope signal of each of these domains. Then, in order to clearly visualize such diagnostic performance, optimized domain features were represented for each of the machine learning models using permutation importance feature selection techniques. The prepared datasets are segregated into two forms: 75% in the training group for models and another portion of 25% for their model testings with blind validation. A normalized confusion matrix is used to assess each machine learning model's performance, producing performance measures including accuracy, precision, recall and F1-score. These measures offer a thorough evaluation of how well the model detects rolling bearing problems in real-world operational scenarios.

This research enhances the effectiveness and reliability of condition monitoring for induction machines with vibration spectrum analysis and intelligent machine learning, i.e. SVM, RF, LR and GBM. The innovation of this research is the encouragement of predictive maintenance approaches for enhancing rolling bearing fault diagnosis, which can increase the availability of the machine and reduce the maintenance cost.

Keywords: Squirrel Cage Induction Machine, Rolling Bearing Faults, Condition Monitoring, Motor Vibration Spectrum Analysis, Machine Learning Approaches

ACKNOWLEDGEMENT

I am grateful to the thesis supervisors, Program Coordinator Assistant Professor Dr. Bishal Silwal and Assistant Professor Anil Kumar Panjiyar, who have been guiding me continuously and sharing invaluable insights, which were of great assistance in this thesis work. Their knowledge and encouragement have given much needed leverage in steering the research. In fact, I also feel greatly indebted to the Head of the Department, Department of Electrical Engineering, Associate Professor Dr. Basanta Kumar Gautam, for better coordination, offering valuable feedback, and keeping a very healthy academic environment.

My sincere gratitude also goes to the entire staff of the Department of Electrical Engineering, the Institute of Engineering, Pulchowk Campus, for the availability of resources and the academic environment in a timely fashion that would enhance academic growth and learning effectively.

I am thankful for being provided the chance to take part in student mobility under the Capacity Enhancement in Electrical Equipment Condition Monitoring and Fault Diagnosis project, which was co-funded by the European Union's Erasmus+ Programme. To me, this offered much in the way of my academic experience as well as the vision of other cultures and traditions on the higher education landscape. This project gave me the opportunity to complete the priceless learning abroad experience. I would like to express my heartfelt sense of gratitude to the Department of Electrical Power Engineering and Mechatronics, Tallinn University of Technology, Tallinn, Estonia, especially to Professor Dr. Toomas Vaimann, Professor Dr. Ants Kallaste, and Professor Dr. Hadi Ashraf Raja for their suggestions and kind support throughout this research work.

I am sincerely thankful to Er. Chandan Pokhrel for his support and guidance throughout this thesis. I am also grateful to my family and friends, who have been very supportive, patient, and understanding of the tough times but enriching experiences. They have always been a moral support and strength throughout my academic journey. This thesis would not have been possible without the contribution and support of those mentioned above, and thanks to all for believing in me, an integral part of the journey.

TABLE OF CONTENTS

LIST OF FIGURES

LIST OF TABLES

LIST OF ABBREVIATIONS

AC	Alternating Current
AUC	Area Under Curve
BPFI	Ball Pass Frequency Inner race
BPFO	Ball Pass Frequency Outer race
BSF	Ball Spin Frequency
DFT	Discrete Fourier Transform
DTC	Direct Torque Control
EMF	Electromotive Force
EMG	Electric Machine Group
EPRI	Electrical Power Research Institute
FFT	Fast Fourier Transform
FN	False Negative
FP	False Positive
FTF	Fundamental Train Frequency
GBM	Gradient Boosting Machine
GLCM	Grey Level Co-occurrence Matrices
IAS	Industry Applications Society
IWO	Invasive Weed Optimization
LR	Logistic Regression
MCSA	Motor Current Signature Analysis
MEMS	Micro Electro Mechanical System
MVSA	Motor Vibration Spectrum Analysis
PI	Permutation Importance
PSD	Power Spectral Density
RBF	Radial Basis Function
RF	Random Forest
RMS	Root Mean Square
ROC	Reciever Operating Characteristics
SCIM	Squirrel Cage Induction Motor
SMOTE	Synthetic Minority Oversampling Technique
SVM	Support Vector Machine
TN	True Negative
TP	True Positive
VFD	Variable Frequency Drive

CHAPTER ONE: INTRODUCTION

1.1 Background

Electrical machines and drive systems make a significant contribution towards efficiency and productivity in most industries and make complex processes simple, secure and easier to use. With technological advancement, electrical machines and drive systems have seen increased application and a routine maintenance schedule must be adopted in an attempt to avert malfunctions. Induction motors have become most prevalent in use with less maintenance, less size, high dependability, adaptability for variation in speed and high performance in any working environment. Application of induction motors for efficiency and economy in residential, industrial and commercial use is preferred and can deliver reliable service in most of environments. Traditional maintenance routines include routine inspections which can generate wastage of resources. Predictive maintenance procedures have become essential with the advancement of contemporary technologies in order to maximize resource use and boost productivity. Performance of equipment in various industries requires condition monitoring and predictive maintenance strategy to avoid failures. Installation of a trustable condition monitoring system increases technical asset reliability and efficiency in overall system operation.

Fault detection methods utilizing machine learning algorithms have improved the identification of rolling bearing problems in mechanical components of electrical machines. According to statistics, faults in mechanical parts contribute to approximately 50% of failures in such machines [1]. Among these faults, rolling element bearing faults are most prevalent and can cause significant mechanical failure. Machine state monitoring is significant in failure prediction and maintenance scheduling at the appropriate time for electrical machines. Electrical machine fault detection techniques include Motor Current Signature Analysis (MCSA), Park Vector Analysis, Motor Vibration Spectrum Analysis (MVSA), Temperature Monitoring, Stator Voltage Monitoring and Harmonic Analysis of motor speed and torque [2].

This thesis develops a comprehensive plan for diagnosing and detecting rolling bearing issues in an induction machine with a squirrel cage. Condition monitoring systems use advanced signal processing techniques and machine learning algorithms to diagnose and detect faults in order to do predictive maintenance.

1.2 Problem Statement

Induction machines have a significant role in residential, commercial and industrial applications for efficiency and dependability. Nevertheless, rolling bearing problems in induction machines including outer and inner races, rolling balls and bearing cages happen frequently and can cause vibrations, a loss of efficiency and catastrophic failure if they are not detected in time. High maintenance costs and unscheduled downtime are caused by these defects. Early fault detection is significant in terms of operational dependability and reduced maintenance costs.

The purpose of this thesis is to develop the rolling bearing fault diagnosis system in squirrel cage induction machines using motor vibration signal and advanced machine learning algorithms such as support vector machines (SVM), random forest Classifier (RF), logistic regression(LR) and gradient boosting machines (GBM).

1.3 Objectives

Main Objective

To develop the machine learning models and algorithms for a vibration-based condition monitoring system to detect and diagnose rolling bearing faults, i.e., outer race, inner race and damage bearing cage faults in squirrel cage induction motors (SCIM).

Specific Objectives

1. To analyse the effects of rolling bearing faults under the different loading conditions on the condition monitoring of a induction machine.

2. To compare the performance of different machine learning models using various performance evaluation metrics.

3. To Identify the most effective machine learning model for detection and diagnosis of rolling bearing faults in SCIM.

1.4 Scope

- Generation of time-domain signals, frequency domain signals and envelopes of both time and frequency domain signals in various motor states under various loading conditions.

- The extraction of the statistical features from each time domain signal, frequency domain signal and both of their envelope of time and frequecy domain signals. The statistical features includes mean, standard deviation, median, kurtosis, root mean square, skewness, maximum value and absolute sum for all types of above mentioned signals. Additionally, the time-domain signal whose crest factor, mean of frequency domain power spectral density and maximum values of frequency domain power spectral density are also extracted.

- Building the various machine learning models capable of classifying the actual state of machines based on extracted input statistical features with proper number of useful feature selection as per model requirements.

- Evaluate the performance of each of the machine learning models under proper input features selected condition with using various performance evaluation metrices. Also making proper comparision of models performance between them to identify the optimal model for detecting and diagnising rolling bearing faults in SCIM.

1.5 Limitation

- The research only focuses on diagnosis of most frequently occuring rolling bearing faults such as outer race, inner race and damaged bearing cage faults in squirrel cage induction motors. Other bearing faults such as rolling element fault, corroded lubricant fault and bearing current fault are not touched upon here.

- For this research, the developed algorithm is designed to identify major rolling bearing faults using the statistical features that were extracted from time-domain, frequency-domain and envelope signals of each of these domains. But, the other bearing frequency spectral features are not included.

1.6 Thesis Organization

The thesis is organized into five chapters. This section enlists a brief outline of each chapter and its contents.

- This chapter gives a brief introduction of the dissertation. The problem statement is described and followed by the objectives, scope and limitation of the thesis.

- Chapter 2 explores the necessary literature review done for this thesis which includes the fundamentals of induction machines theories, various types of induction

motor faults, fault diagnostic and condition monitoring techniques, effects of rolling bearing faults in induction manchine and research gaps on rolling bearing fault diagnosis in SCIM.

- Chapter 3 describes the research methodology of the dissertation, including the experimental setup and overall thesis workflow.

- Chapter 4 presents the results obtained, analyzes how bearing faults affect stator current under various loading scenarios and conducts a final analysis based on the effectiveness of different machine learning algorithms to determine the best optimal model for rolling bearing fault diagnosis and detection.

- Chapter 5 concludes the thesis work.

Finally, this thesis will end with a list of references and the relevant appendices.

CHAPTER TWO: LITERATURE REVIEW

The thorough literature review conducted for this dissertation is presented in this chapter. It covers the following topics: the fundamental theories of induction machines, the effects of rolling bearing faults, the different types of induction machine faults, condition monitoring and fault diagnostic techniques and research gaps in bearing fault diagnosis, including how they operate and the types of issues they can cause.

2.1 Induction Machine

One of the electrical machines most frequently found in industrial settings is the induction machine. Indeed, motors of this type are so deeply penetrating that some industrial installations can be termed as all-induction-motor types. In polyphase types, induction machines offer single-phase and three-phase variants, their most common division in practice, in which the largest single-phase induction motors seldom go up to a rating of 3 horsepower. An induction machine operates both as a motor and a generator, but the performance characteristics for these two operations are quite dissimilar. Due to issues with voltage and frequency control, it is often far less efficient when used as a generator than when utilized as a synchronous machine. Numerous commercial and industrial applications now use three-phase induction motors as their principal drive. Several reasons can be highlighted as to why induction motors have gained such favor. They are recognized as inexpensive and of simple construction due to the elimination of brushes and a commutator, which reduces maintenance requirements. This simplicity promotes robustness and reliability, also making them well-suited to continuous operation under severe conditions. The squirrel-cage type is by far the most common form of induction machine, accounting for about 85% of power consumption in industrial applications [3].

2.1.1 Construction

Because of its robustness and dependability in various sectors, the squirrel cage induction motor or SCIM for short, is the most used three-phase induction motor. A general SCIM comprises two parts: the stator and the rotor. The stator is the stationary part that is manufactured with high-quality alloy steel laminations to minimize eddy current losses. The major components are the outer frame, the stator core and the stator windings. The outer frame is supported structurally and protected against internal components mostly in casting material in smaller motors and fabricating material in the larger ones. The stator core is manufactured from silicon steel stampings and carries the alternating magnetic field. Each stamping is insulated by a thin layer of varnish to reduce hysteresis and eddy

current losses. These stampings normally have a thickness in the range of 0.3 to 0.5 mm and are slotted on the inner side to carry the windings. The three-phase stator windings are linked to a power source. The motor's speed will be determined by the number of poles in the windings. The speed increases with fewer poles and decreases with more poles. The rotor in SCIM consists of the rotating part and to reduce these energy losses, the rotor core is also constructed using thin silicon steel laminations. It comes as a whole cylinder with projected slots on the outside for the housing of conducting bars made up of either aluminum or copper alloy. The squirrel cage design mainly has longitudinal conducting bars inserted into the slots joined together at each end by end rings. Because of this configuration, the stator's rotating magnetic field may induce current in the bars, enabling efficient functioning. Another common practice is to skew the bars to reduce noise and ensure smooth torque delivery by minimizing fluctuations in torque as each bar passes beneath the stator slots. Typically, a rolling bearing system in SCIM consists of a bearing cage, rolling components, an outer race and an inner race. The inner race is fixed on the shaft of the motor while the outer race is placed into the bearing seat. These bearings make rotation smooth and frictionless. To prevent wear on the raceways where the rolling components come into contact with the rings, proper lubrication with grease or oil is crucial. The SCIM is less expensive, easier to develop and requires less upkeep. Hence, it sees wider applications in the industry wherever high reliability is paramount. Figure 2.1 below illustrates the different components of a squirrel cage induction machine.

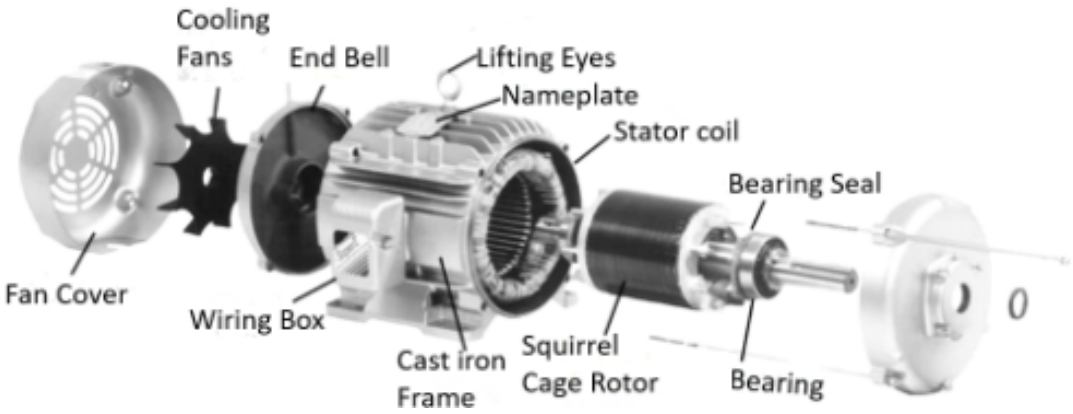

Figure 2.1: Various Parts of Squirrel Cage Induction Machines from [4]

2.1.2 Operation

The fundamental idea behind how a squirrel cage induction motor works is electromagnetic induction. A rotating magnetic field is produced when the stator windings are powered by a three-phase AC source. This rotating magnetic field is the reason for the motor's

operation and is mathematically represented by:

$$N_s = \frac{120\ f}{p} \tag{2.1}$$

where f is the AC supply's frequency in Hertz (Hz), N_s is the synchronous speed of the spinning magnetic field in revolutions per minute (rpm) and p is the number of pole pairs in the stator winding.

Faraday's law of electromagnetic induction states that an electromotive force would be generated in the rotor bars when the rotating magnetic field entered the rotor. This produces EMF results in the flow of a current in the rotor conductors, which may basically be made from aluminum or copper. The rotor rotates because of the interaction between the induced currents in the rotor and the magnetic field produced by the stator. It's crucial to remember that "slip" occurs when the rotor speed is always a little slower than the synchronous speed of the rotating magnetic field. Slip (s) can be expressed as:

$$s = \frac{N_s - N_r}{N_s} \tag{2.2}$$

where N_r – Actual speed of the rotor in rpm.

This slip is critical in producing torque, the greater the load, the more the slip and the induction of more current in the rotor, thereby increasing the torque output. A series of conductive bars implanted in the laminated iron core of the squirrel cage rotor architecture helps to lower eddy current losses. Because the top and bottom faces of the conducting bars are often skewed, noise is reduced and torque is applied smoothly, improving performance. Other than its primary function as a motor, an SCIM is capable of operating as a generator when driven above synchronous speed. In this mode, it converts the mechanical energy back into electrical energy, which can be fed into an electrical grid or used for other applications. In general, the overall design and principles of operation make SCIM a trustworthy area of industrial application by virtue of simplicity and efficiency.

2.2 Faults in Induction Machine

Even though induction machines are effective and often used in industries, they can have a number of problems that can negatively impact their lifespan, maintenance needs and operational performance. Induction machine faults are categorized as illustrated in Figure 2.2.

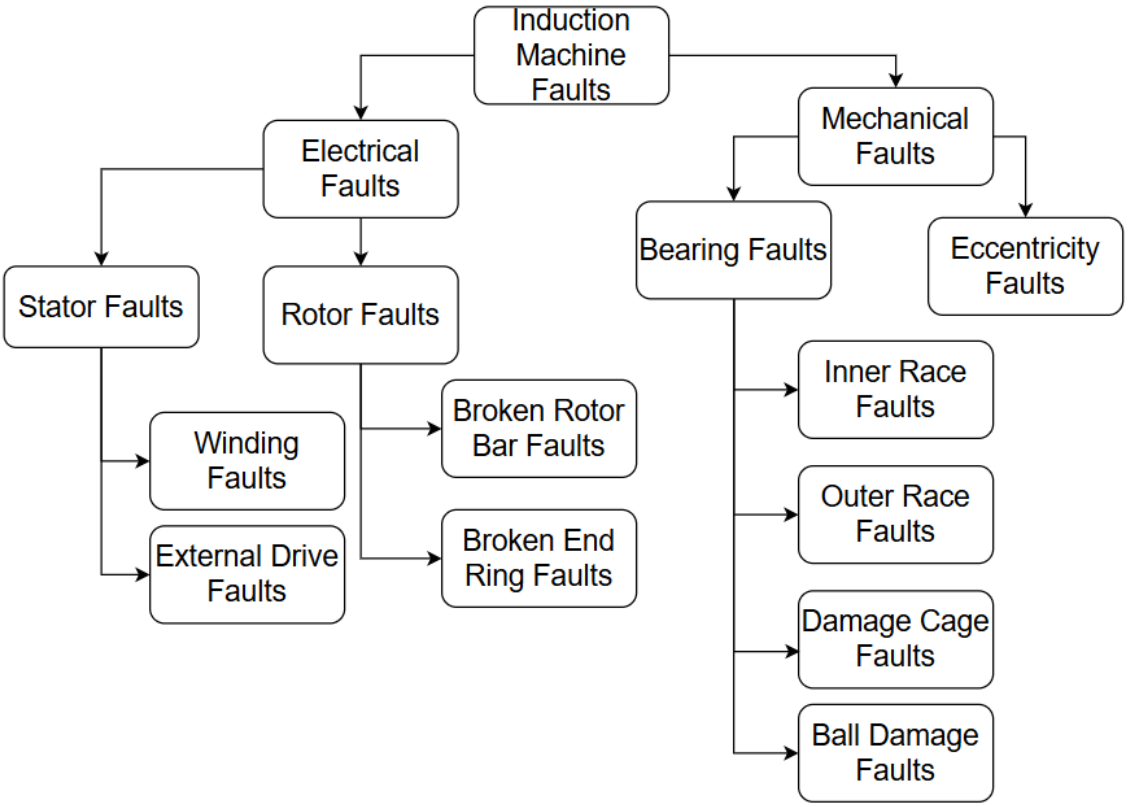

Figure 2.2: Fault Classification of Induction Machine from [5]

Due to their role as a bridge between the mechanical and electrical domains, induction motors are vulnerable to both mechanical and electrical issues. Typically, these malfunctions fall into one of three primary categories: environmental, mechanical and electrical. The categories are described in depth in Table 2.1, which also includes examples of defects and their root causes. There are a number of factors that influence the frequency and distribution of these failures, which mainly include the size of the machine, type of machine and rated voltage. Mechanical issues, which include broken rotor bars, rotor eccentricity, bearing failures and damaged end rings, make up a significant portion of all failures of these kinds [6]. Induction machines typically have bearing-related problems, which make up around 40% of all motor-related problems [7]. Bearing problems are common and can have a significant impact on the motor's performance, making their detection and diagnosis crucial. Bearings are among the critical elements in rotating machinery and are subject to various types of damage that may be caused by contamination, corrosion or poor lubrication practices. These contaminants like dust and moisture can penetrate the bearings causing structural damage that manifests itself as premature wear and eventual failure. The most important factor in reducing friction and providing protection against corrosion, improper lubrication can increase wear by higher orders of magnitude and drastically reduce

Table 2.1: Induction Machine Fault Classification

Categories of Faults	**Induction Machine Faults**	**Causes of faults**
Electrical	Overloading, Unbalanced Supply Voltage, Inter-turn Short Circuit, Earth Fault, Broken Rotor Bar	Overloading can cause excessive current, which may cause the stator insulation to fail and the windings to experience inter-turn short circuits.
Mechanical	Wear in bearing, Air-gap misalignment, Mass imbalance	These faults may originate from component defects or wear. Additionally, the motor and drive assembly's condition influences failure risks.
Environmental	High ambient temperature, External moisture, vibrations	Such issues often arise from improper installation practices or adverse environmental conditions in the installation area.

the service life. In addition, material fatigue under unidirectional loading can result in the formation of surface cracks in bearings, while a variety of mechanical-related problems, such as misalignment and manufacturing defects, further degrade the performance. The various types of rotor faults include damage to the end rings and broken rotor bars. As a result, operational instability may emerge from an unequal air gap between the stator and rotor [8]. Stator failures usually occur due to specific problems associated with winding, such as short circuits or deterioration in insulation due to thermal and electrical stressors. Continuous monitoring and diagnosis of such different types of fault in induction motors is indispensable for their reliability and performance maintenance. The various fault types that may occur with induction machines have to be understood in depth for effective maintenance strategies and operational efficiency. Induction motor lifetime and efficiency are improved in industries via the use of strong diagnostic techniques and preventative actions.

The stator is primarily responsible for supply-related issues in squirrel cage induction motors. Once the defects are sufficiently established and a critical threshold has been crossed, they may be identified and managed using basic protection devices by keeping an eye on the supply voltage and current quality. Faults at their incipient stage may be detected only through the close observation of either overall or localized parameters. Faults specific to the motor's electrical and mechanical systems constitute a considerable share of overall failures and tend to worsen over time. Among these, mechanical issues particularly those associated with bearings form the largest proportion of faults. In accordance with IEEE-IAS and Electrical Power Research Institute (EPRI) standards, the comprehensive fault

distribution in medium-voltage induction motors is depicted in Figure 2.3.

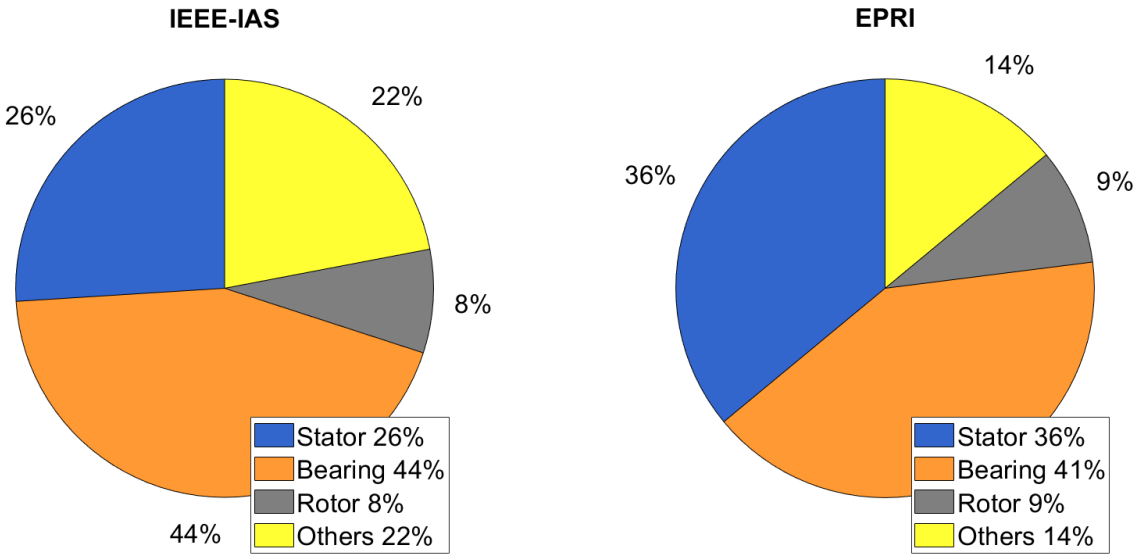

Figure 2.3: Percentage Faults Contribution according to IEEE Standard [6, 7]

2.3 Rolling Bearing Faults

In larger induction machines, the percentage of bearing-related faults becomes considerably lower due to the extensive use of sleeve bearings in those systems. However, in small induction machine, the bearing related fault are more pronounced due to their rolling type construction. Both standards in Figure 2.3 indicate that combined bearing and stator-related defects account for over half of all failures. Additional details on fault contributions for various voltage classes of machines are available in [9]. According to statistics, mechanical problems account for half of all electrical machine failures, which can lead to increased noise, vibrations, and ultimately equipment failure [1]. In rotating machines, bearings are crucial parts that are especially susceptible to mechanical damage, which causes a large percentage of these failures. Strict production guidelines ensure quality. However, operational factors such as unexpected overloads, inadequate lubrication and improper installation often reduce their lifespan [10]. Basically, bearings are widely exposed to environmental and operating factors that may provoke failures and destroy them. Design and production quality standards are followed strictly. However, the influence of internal and external factors at work may diminish their operational cycles. Most common defects, including material defects and mechanical damage, come from poor installation, manufacturing defects or misalignment. That is why a preliminary check for manufacturing defects should be performed in bearings before installation and motor operation to

minimize certain risks. The key parameters must be closely watched to avoid catastrophic failure consequences.

One can use a mathematical relation to determine the frequency resulting from a faulty bearing's natural frequency, which depends on its geometry. This relation can be used to locate the cage, rolling elements, outer and inner raceways, as shown in Figure 2.4 and the ball bearing cross-section in Figure 2.5. Faulty frequencies for these cases can be defined

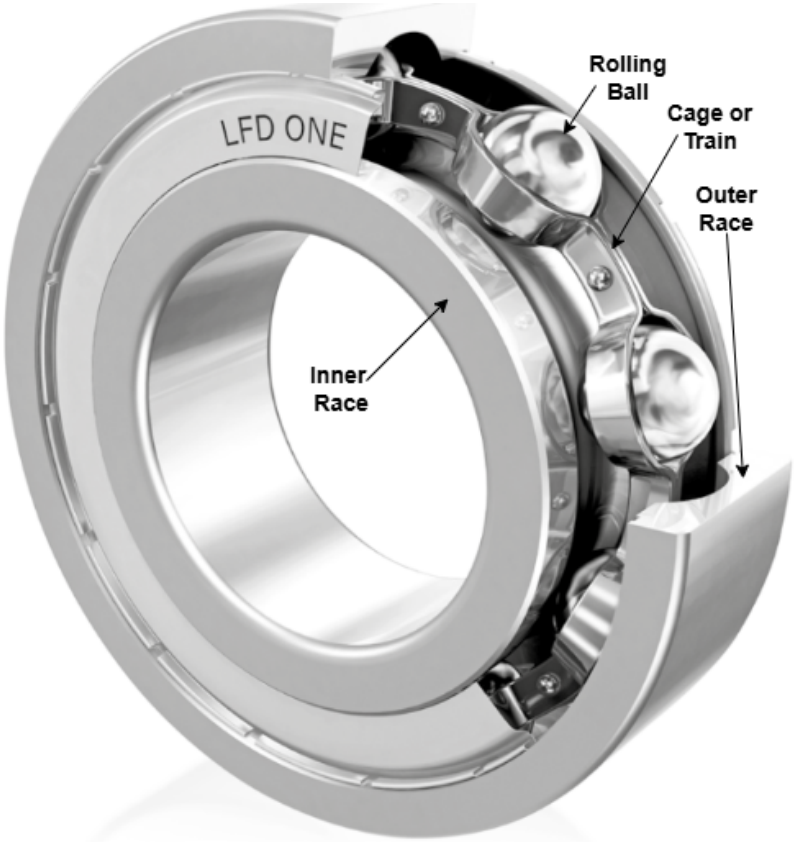

Figure 2.4: Construction of Rolling Bearing [11]

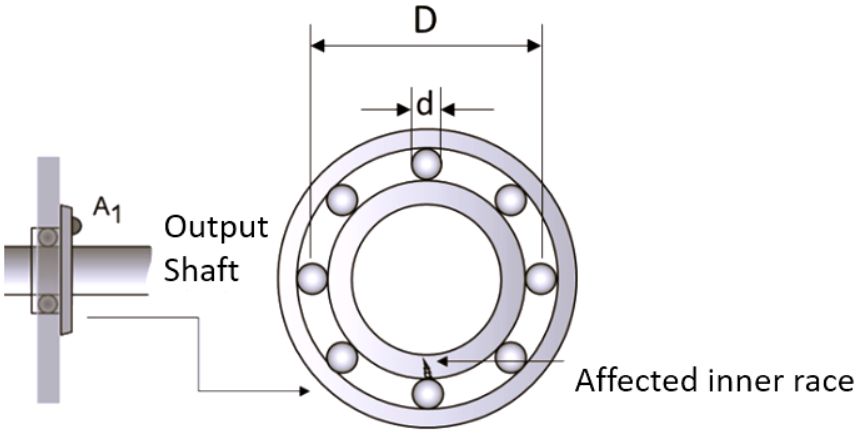

Figure 2.5: Ball Bearing Cross-section[12]

as follows:

1. Ballpass frequency, outer race (BPFO):

$$\text{BPFO} = \frac{nf_r}{2}\left(1 - \frac{d}{D}\cos\varphi\right) \tag{2.3}$$

2. Ballpass frequency, inner race (BPFI):

$$\text{BPFI} = \frac{nf_r}{2}\left(1 + \frac{d}{D}\cos\varphi\right) \tag{2.4}$$

3. Cage speed or fundamental train frequency (FTF):

$$\text{FTF} = \frac{f_r}{2}\left(1 - \frac{d}{D}\cos\varphi\right) \tag{2.5}$$

4. Ball spin frequency (BSF):

$$\text{BSF} = \frac{Df_r}{2d}\left[1 - \left(\frac{d}{D}\cos\varphi\right)^2\right] \tag{2.6}$$

The bearing fault frequency equations are as follows:

$$f_{\text{bb}} = |f_s \pm mf_{i,o}| \tag{2.7}$$

$$f_{i,o} = \frac{n_{\text{bb}}}{2} f_r \left[1 \pm \frac{d}{D}\cos\varphi\right] \tag{2.8}$$

For n between 6–9, the above equation can be simplified for outer and inner race faults as:

$$f_{\text{bbo}} = f_s \pm 0.4knf_r, \quad k = 1, 2, 3, \ldots \tag{2.9}$$

$$f_{\text{bbi}} = f_s \pm 0.6knf_r, \quad k = 1, 2, 3, \ldots \tag{2.10}$$

where d – diameter of ball in mm, D – bearing pitch diameter in mm, f_r – motor shaft speed in Hz, n – number of rolling elements in bearing, φ – bearing contact angle (in radians), f_{bb} – rolling bearing fault frequencies, $f_{i,o}$ – characteristic vibration frequencies, f_{bbo} – outer race fault frequencies of bearing, m–Positive integer, f_{bbi} – inner race fault frequencies of bearing.

Since rolling bearings are very critical in rotating machines, much damage and failure tend to occur to them. They, therefore need to be monitored. Regular monitoring such as temperature checks, noise and vibration analysis and periodic evaluation of lubricant quality can serve to reduce the occurrence of bearing failure. The major causes of rolling bearing faults in SCIM are described below.

2.3.1 Mechanical Damage

Most of the faults occurring in bearings are manifestations of mechanical damage arising from either manufacturing or some unforeseen operating conditions of the motor. Usually, the rolling elements, bearing cage or inner and outer races sustain this kind of damage. A bearing cage that has been damaged is seen in Figure 2.6. Inappropriate design, misaligned

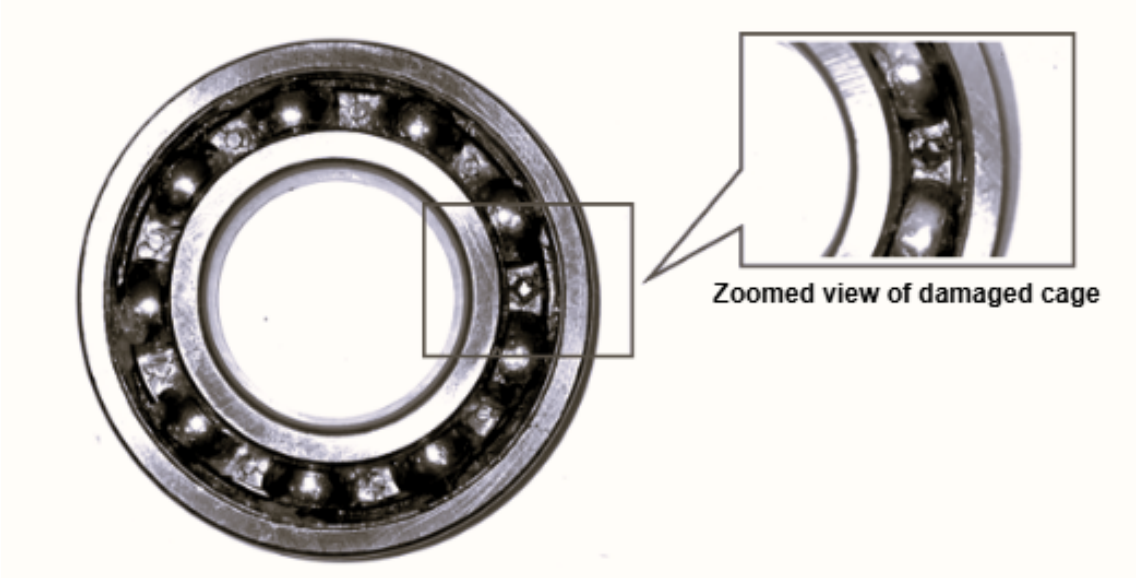

Figure 2.6: Damaged Cage in Rolling Bearing [13]

bearing races, unequal rolling element dimensions or problems during the manufacturing or assembly process might also result in these mechanical failures. First, a preliminary inspection must be performed on the bearing. Among other criteria, its looking appearance by rotational smoothness and provided clearances correspond to those outlined in the given technical documentation shall be examined prior to its putting up.

2.3.2 Material Fatigue

Material fatigue often results from repetitive loads that cause the bearing's surface to break. During the application of the external force to the rings, the material strength weakens and forms cracks. The crack deepens with time and eventually the bearing becomes unserviceable. The number of rotations a bearing can withstand before the first signs of material fatigue appear on the rolling components or rings is known as its endurance. Figure 2.7 shows one instance of fatigue failure of a bearing part.

Figure 2.7: Material Fatigue of a Rolling Bearing [13]

The most important causes of material fatigue are: continuous overload, poor maintenance and contaminated surfaces. The size of the operational load and rotational speed are influential in this phenomenon, its beginning and development. Firstly, microcracks develop in the subsurface. The surface of the bearing starts to crack over an extended area during the development of the process and becomes rough and uneven. Usually, there is an increase in vibration and noise. In addition, the bearing's operating temperature rises. To avoid such failures, periodic inspections and good lubrication of the bearing are necessary.

2.3.3 Ambient Contamination

Where the stress on the rings is higher, the lubricant is less efficient when damp air gets within a bearing. In addition, lubricants may become contaminated with water or other chemicals which further deteriorates their performance. With the deterioration of the properties of the lubricant, bearing corrosion may occur. Corrosion is a process in which the material interacts with the environment, resulting in the dissolution of the material. Proper lubrication has a lot of importance in terms of the performance and life span of the operational bearing. The impact of the rolling components against the bearing races and cages

is lessened by the thin oil layer created by properly chosen lubricant. Besides, it protects the bearing from early wear and corrosion. Inadequate lubrication will make the bearing to be either greased not enough or excessively. Too little lubrication raises friction and crack growth rate whereas, too much may be liable for slipping of the shaft resulting in structural failure.In Figure 2.8, bearing corrosion is demonstrated. The bearings will most

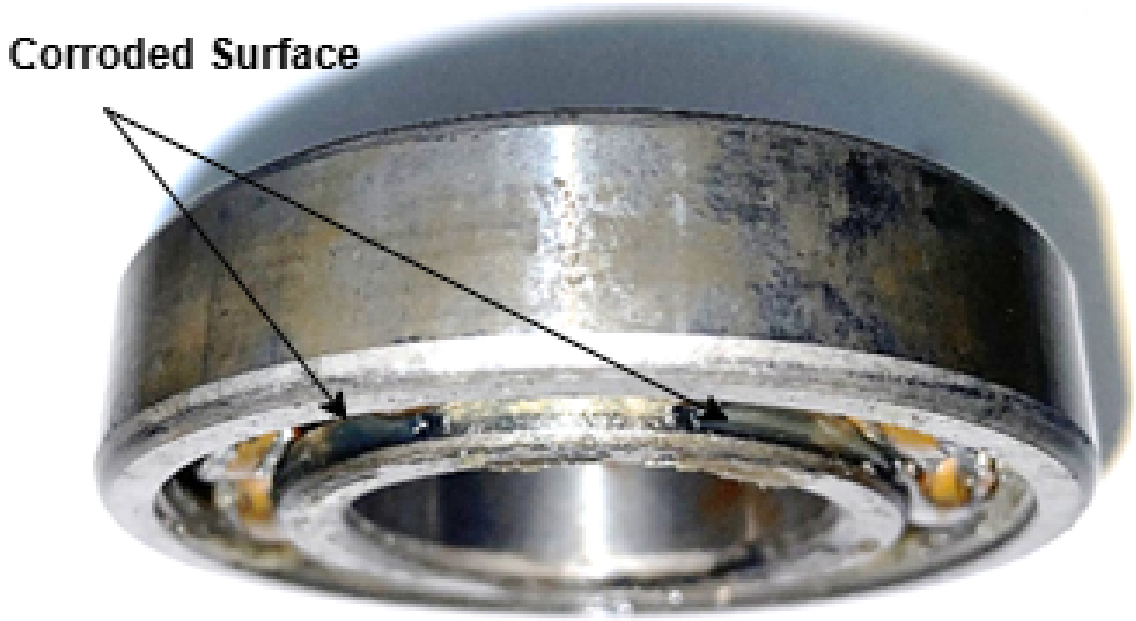

Figure 2.8: Corroded Surface of a Rolling Bearing [13]

probably get contaminated by dust, sand and other abrasive particles that might cause structural damage such as scratches and cracks. When the rolling components push the particles into the rings, these impurities may also cause significant dents to form. One of the key causes of such damage is the improper selection of a bearing cage that fails to prevent the intrusion of these particles. The only way to reduce these problems is the use of corrosion-resistant lubricants and performing the assembly in a clean environment, without contaminated components.

2.3.4 Bearing Currents

Shaft currents may often attack bearings and leave markings on their surfaces. Higher load concentrations at these locations typically cause damage where the lubricant coating is thinnest. Fluting sometimes shows up as multiple lines across the bearing rings when there are conditions of low voltage with a constant rotational speed. This is one of the common problems that may be caused by shaft currents. The other two are frosting and pitting. The frosting on the other hand occurs when the motor operates at changing speeds. In most cases, pitting relates to low speed and high-voltage sources which result in crater

formation on the surface. Secondly, a matte finish that is similar to the pitting happens but here the craters are much more minute. Commonest shaft currents damages are in figure 2.9 and figure 2.10. The initial sign of a potential issue related to shaft currents

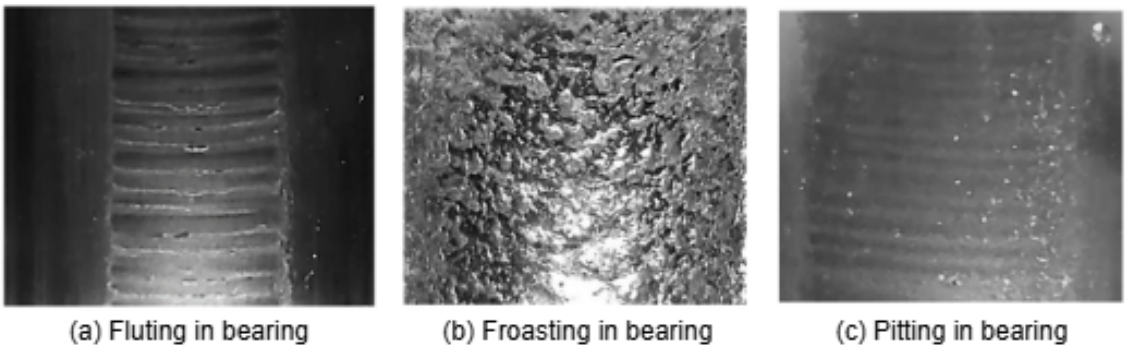

Figure 2.9: Zoomed View of Damages caused by Shaft Current [13]:(a) Fluting, (b) Froasting, and (c) Pitting

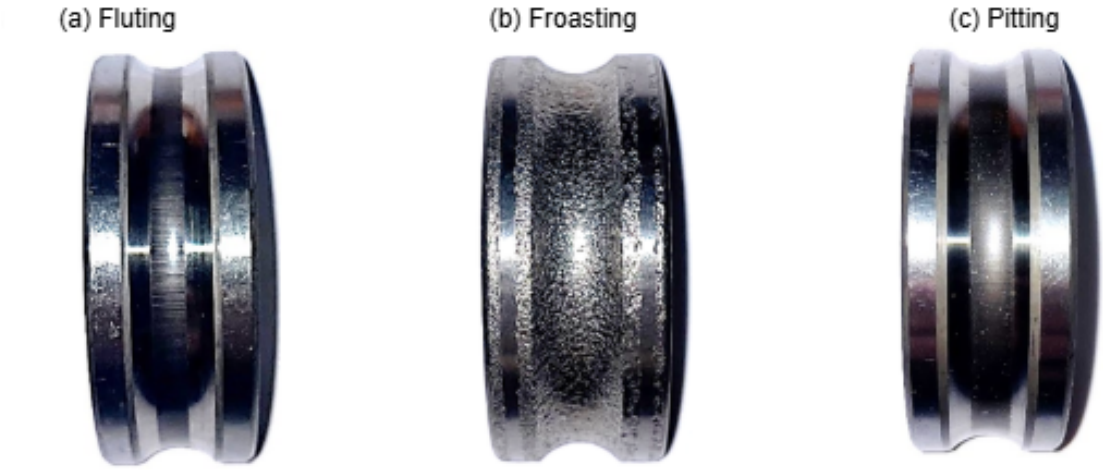

Figure 2.10: Common Damages caused by Shaft Current[13]:(a) Fluting, (b) Froasting, and (c) Pitting

is the darkening of the lubricant. As seen in Figure 2.11, oxidation is the source of this, and sparking from electrical discharges causes it to happen. The initial evidence of shaft currents is usually darkening of the lubricant. This occurs due to oxidation and is triggered by sparking related to electrical discharges. The result of this action is not evident in the early stages and damage can only be detected by dismantling the bearing and microscopic examination of the rings and rolling elements. Somewhat later in the development of the fault, however, the appearance of damage due to currents becomes clearly different from that of other types of bearing damage. It is, therefore, very important that bearings are carefully examined at maintenance when bearing or shaft currents are suspected and particularly where such problems can be expected.

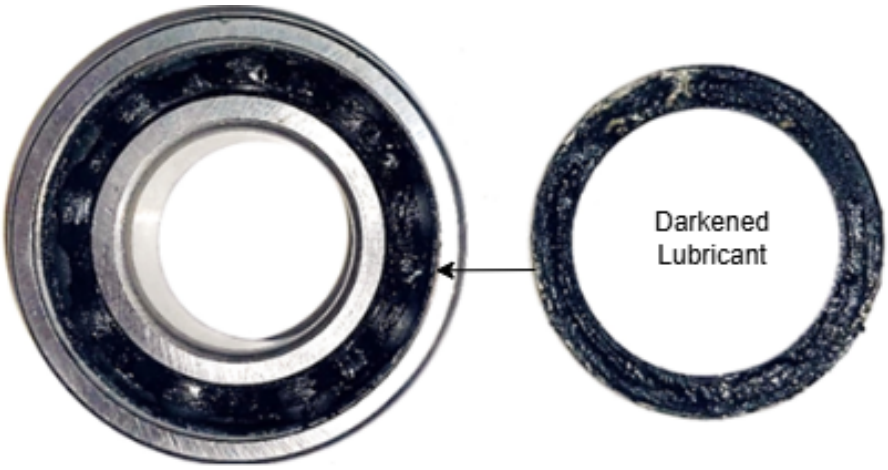

Figure 2.11: Darkened Lubricant [13].

This damage is not apparent in the early stages and can only be found by disassembling the bearing and looking for minute anomalies in the rolling components and rings. At a later stage in its development, the damage caused by currents becomes visually different from other forms of bearing damage. Thus, it is important that bearings be inspected closely at maintenance when bearing or shaft currents are suspected especially under those circumstances where the occurrence of such trouble can be anticipated.

2.4 Rotor Faults

The most frequent fault occurring in the operation of the machine is rotor faults. One of the common issues regarding rotor faults is the damage to rotor bars and end rings. These faults are caused by natural wear and tear that occurs over a period of time. Thermal expansion aggravates the problem by causing cracks in the rotor bars. This occurs because of the unequal expansion between copper and steel laminations; copper, being a better conductor of heat, expands faster than steel at higher temperatures, thus creating more stress and eventually cracks.

2.4.1 Eccentricity faults

Centrifugal forces have often been reported to be responsible for rotor damage usually in relation to eccentricity. An uneven air gap between the rotor and stator is one way to characterize the eccentricity. When the air gap surpasses 10% of the nominal value, it is considered faulty [14]. It is important to note that improper installation, missing bolts, shaft misalignment and rotor imbalance can easily cause eccentricity.

In general, the eccentricity in motors may happen due to the static, the dynamic or the elliptical types. Of course, these might combine when the centre of rotor and stator besides the rotation axis, happen to be each displaced. Figure 2.12 illustrates the three main types of eccentricity.

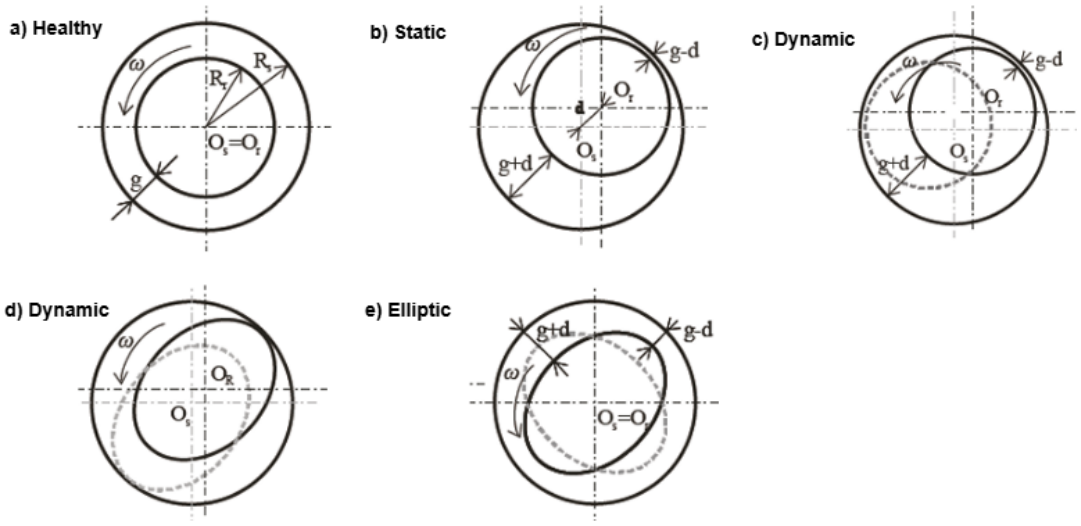

Figure 2.12: Rotor Eccentricities [15]: a) Healthy, b) Static, c) and d) Dynamic, e) Elliptic Eccentricities

Static Eccentricity (SE): It is the type of eccentricity that happens in motors the most frequently. During this phenomenon, the axis of rotation for the rotor becomes fixed and hence does not change parallel to the stator axis over a period of time.

Dynamic Eccentricity (DE): The air gap between the rotor and stator changes over time as a result of rotor movement in dynamic eccentricity.

Elliptical Eccentricity (EE): This condition indicates that when the stator and rotor centers are aligned, but there exists an elliptical rotor, hence a non-uniform air gap is caused due to time-varying angular variation.

Certain equations can be used to calculate mathematically the air gap for various types of eccentricity. Such calculations are important in the assessment and management of eccentricity in electrical machines for their reliable operation. The following formulas

can be used to calculate the width of the air gap for various eccentricities:

$$g_{\text{SE}} = R_s - R_r + \sqrt{R_r^2 - (d\sin\beta)^2} \tag{2.11}$$

$$\delta_{\text{DE}} = \frac{|O_W.O_r|}{g} \tag{2.12}$$

$$g_{\text{EE}}(t) = R_s - \sqrt{\left[(R_r + d)\cos\left(\frac{\omega t}{p} - \beta\right)\right]^2 + \left[(R_r - d)\cos\left(\frac{\omega t}{p} - \beta\right)\right]^2} \tag{2.13}$$

where d is the deviation, β is the initial eccentricity angle, g is the air gap, R_s is the stator radius and R_r is the rotor radius. O_s is the stator symmetry center, O_W is the rotating center and p is the number of poles.

2.4.2 Broken Rotor Bar fault

When one or more bars break in the squirrel-cage rotor, the rotor's current flow is interrupted, resulting in the BRB fault. This happens essentially because of thermal stresses brought on by every heating and cooling cycle or because of mechanical fatigue caused by torque variations or manufacturing defects in the rotor materials. Therefore, it includes several characteristic effects such as torque ripple, increase of vibrations, overheating and decrease in motor efficiency. BRB faults are usually detected by the MCSA technique. This technique depends on identifying the characteristic sideband frequencies in the stator current spectrum, which may be found using:

$$f_{\text{BRB}} = (1 \pm 2ks) f_s \tag{2.14}$$

where k =1, 2, 3, …, N is the harmonic order, f_s – supply frequency, and s–slip.

2.5 Stator Faults

Stator problems in electrical motors are normally related to winding issues which are crucial to the operation of the motor and yet very fragile. This explains why the protection of windings is crucial at the design and operational stages of the motor. A motor should not be put into operation before careful checks are made to ensure that the windings are not damaged are properly connected and sufficiently insulated.

2.5.1 Winding Failures

Short-circuit failures, which typically begin as turn-to-turn faults, are among the most frequent kinds of winding failures. Phase-to-phase or phase-to-ground short circuits are

two major defects that might emerge if this is not addressed promptly. One of the biggest challenges in the electrical machinery business is the early detection of an inter-turn defect. Inter-turn short circuits have the potential to cause serious harm, including total motor failure, even in their early stages. Some typical short circuit modes of wye-connected stators are shown in Figure 2.13. The four main elements that accelerate the process of

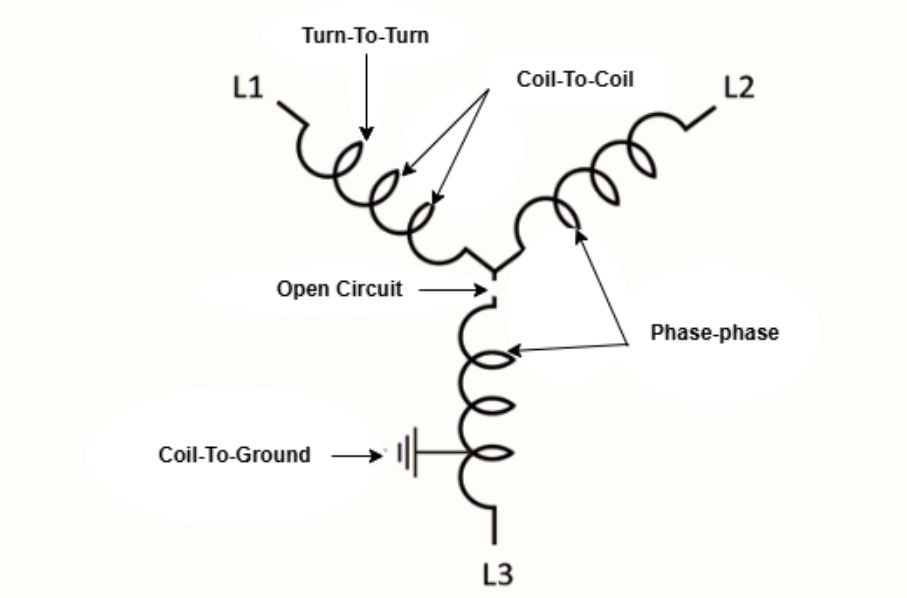

Figure 2.13: Common Modes of Short Circuit in Y-connected Stator [16]

winding insulation deterioration are thermal, electrical, ambient, and mechanical stresses or TEAM stresses.

Thermal Stresses: Unduly high temperature is the most common form of failure. Many induction motors are subject to very high starting current-related temperatures that exceed critical limits, eventually degrading the insulation system.

Electrical Stresses: Supply voltages, transient over-voltages, unstable grounding and incorrect machine ratings can all lead to a weakening of insulation. Motors operating with fast-switching inverters are particularly vulnerable to these stresses.

Ambient Stresses: Adverse environmental conditions include humidity, moisture, dirt, aggressive chemicals and other particulates that may affect insulation either in isolation or in combination with other stresses.

Mechanical Stresses: Those are the centrifugal or magnetic forces that act on the insulation along with poor handling at manufacture and installation. Other causes, almost

always very important but hardly considered, are the failures happening because of manufacturing. For instance, some defects in design or assembly may involve irregularities in air gaps, badly distributed current in windings or improper positioning of windings.

All these sometimes bring about operating defects such as increased vibrations causing friction among copper conductors and hence damage to insulation. These faults create asymmetries which are responsible for additional harmonic components in the system and are given by the harmonic frequency equation:

$$f_h = f_s(1+2ks), \quad k = 1,2,3,\ldots,N \tag{2.15}$$

where s stands for slip, f_s for supply frequency and f_h for harmonic frequency.

Besides, thermal imbalances inside the motor can result in hot spots increasing the deterioration of insulation. This can be significantly lessened with early detection through proactive monitoring, thus reducing the impact of the damage and allowing efficient maintenance and life extension of the motor.

2.6 Fault Diagnostics and Condition Monitoring Techniques

The prevention of induction motor failures is vital due to their essential role in industrial domains. Machine maintenance techniques may be roughly divided into three categories, as shown in Figure 2.14: predictive maintenance, preventive or planned maintenance and corrective or breakdown maintenance [17]. Corrective or breakdown maintenance as shown by Figure 2.14(a) and also commonly referred to as reactive maintenance which is the repair of equipment after an actual failure has occurred [19]. It can be adopted for relatively small, non-vital workstations where sudden failures do not cause major losses either economically or operationally.

Preventive or scheduled maintenance on the other hand as shown in Figure 2.14 (b), aims at preventing failures from occurring through regular inspections and service routines according to a predefined plan. This method has serious drawbacks. While it may extend the operational life span of machinery, it cannot make critical predictions about the life span of equipment and their usage or provide prognostic capabilities. Besides, preventive maintenance in most cases is either partial or complete production shutdowns for scheduled checks against inefficiency at increased operating costs.

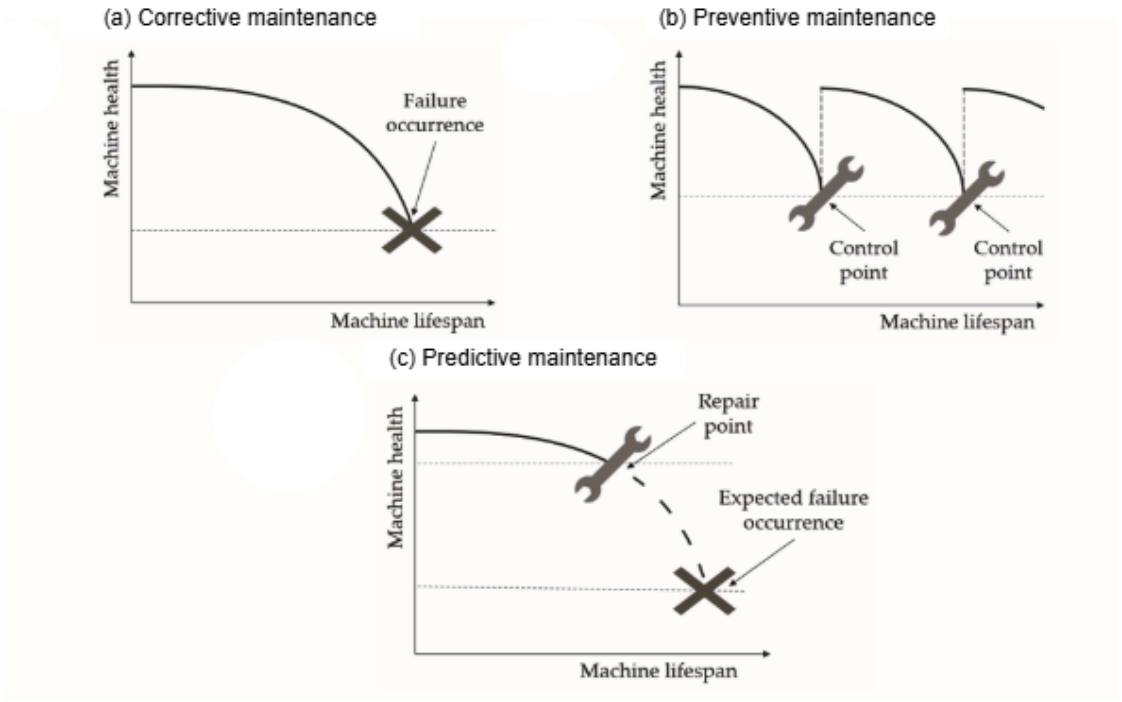

Figure 2.14: Various Maintenance types [18]:(a) Corrective maintenance, (b) Preventive maintenance, (c) Predictive maintenance

As solutions to these problems, predictive maintenance has come into prominence. As illustrated in Figure 2.14 (c), this proactive strategy utilizes condition monitoring techniques to anticipate possible failures by real-time operation data. Predictive maintenance decreases shutdown costs and reduces downtime by optimizing resource usage, hence effectively performing in present-day industries [20].

For dependable and effective functioning of electrical machines, important parameters including current, vibration, temperature, and magnetic flux must be continuously monitored. Specific fault patterns in these signals provide early warnings about impending failures. Conclusively, condition-based monitoring should be employed to achieve informed decisions about active machine maintenance. Early fault detection of electrical machines is very vital in order to prevent catastrophic failure that eventually can cause an overall disruption and lead to tremendous loss. For such purposes, numerous fault diagnosis and condition monitoring techniques have so far been proposed that can be further classified below:

2.6.1 Motor Current Signature Analysis (MCSA)

The application of Motor Current Signature Analysis (MCSA) for fault diagnosis in induction machines is explained in the paper [21]. It uses signal processing techniques to

analyze the stator current spectrum of both healthy and problematic machines and case studies demonstrate its usefulness. Through Matlab-Simulink simulation and a fault test rig experiment, the paper [22] also provides a comprehensive comparative study of motor current signature analysis techniques for broken rotor bar and air gap eccentricity detection in induction motors across four categories, including Fourier, parametric and eigen analysis, wavelet and current space vector techniques. It also compares the benefits and drawbacks of each technique. The instantaneous space phasor module, Fourier transform-based spectral analysis, wavelet transform-based multi-resolution analysis and fuzzy logic-based current phasor evaluation are among the methods for stator current analysis that are formally investigated and proposed in the paper [23]. These methods are used for nonintrusive detection and classification of multiple severity levels of stator winding short circuit faults in induction motors using motor current signature analysis (MCSA) to increase operational reliability and efficiency.

2.6.2 Vibration Analysis

The importance of vibration analysis using Micro Electro-Mechanical System (MEMS) based accelerometers in the diagnosis and detection of electrical and mechanical faults in induction motors is emphasized in the paper [24]. It cites the benefits of MEMS technology in terms of size, power consumption and cost, which shows how mechanical faults like looseness and misalignment and vibration variations controlled by voltage harmonics can be a good indicator of hidden motor faults. Vibration analysis is an effective and general technique for diagnosing mechanical and electromagnetic faults of induction motors that provides valuable information on internal conditions such as winding and core, air gap eccentricity and external conditions such as voltage unbalance and waveform distortion. The paper [25] demonstrates that electromagnetic vibrations, typically caused by non-sinusoidal voltage, faulty adjustable speed drives or in-motor faults can be accurately diagnosed based on vibration data and theoretical calculations and industrial test cases confirm the diagnostic capability of this approach. The most frequent problems with induction motors are bearing problems and while vibration monitoring is useful for early diagnosis, it is typically subject to expert interpretation. In research paper [26] explores a data-driven approach from three-axis vibration signals and statistical measures identifying peak-to-peak and RMS values as main indicators of motor condition. The research article [26] demonstrates that bearing problems may be accurately diagnosed with about 100% accuracy in recognizing defective and healthy states of motors using simple machine learning methods like Decision Trees and K-Nearest Neighbors.

2.6.3 Thermal Analysis

With experimental validation demonstrating accuracy and effectiveness for non destructive and maintenance-oriented fault detection, the paper [27] focuses on mechanical fault diagnosis of induction motor faults such as air gap eccentricity, shaft misalignment and cooling system malfunction that have a tendency to increase stator temperature. Diagnostic indicators are generated by analyzing thermal images using a thermal pixel counting algorithm and are categorized using an adaptive neuro-fuzzy inference system. In order to identify faults in induction motors for different load and fault conditions, the paper [28] suggests a hybrid machine learning-based fault diagnosis technique that combines thermal imaging, Grey Level Co-occurrence Matrices (GLCM), Invasive Weed Optimization (IWO) and intelligent classification algorithms. The model demonstrates sufficient potential for expansion to broader infrared image processing applications by achieving high accuracy, precision, sensitivity and F1 score of motor fault detection, such as broken rotor bars, bearing and stator faults, by obtaining texture features from thermal images and dimensionality reduction with IWO.

2.6.4 Acoustic Analysis

The application of acoustic signal analysis to identify early faults in induction motors is reviewed in this paper [29]. Time and frequency domain approaches are also discussed, along with features extracted from raw acoustic data. Intelligent condition monitoring systems that use AI and machine learning to improve fault diagnosis accuracy are also identified and recent developments in this field are summarized. In order to represent the electrical to acoustic form energy transfer by magneto-mechanical and vibro-acoustic paths, the paper [30] describes a numerical approach of acoustic noise analysis of electromagnetic origin in induction motors by using a combination of finite element and boundary element methods to model magnetic forces, mechanical deformation, and resulting acoustic emissions. It also shows that the use of the boundary element method reduces computational cost by eliminating massive meshing of the surrounding air domain.

2.6.5 Electromagnetic Field Analysis

This paper [31] investigates electromagnetic performance of normal and single broken bar fault operating open loop pulse width modulated inverter-fed induction motor under normal and faulty states using Finite Element Method approach emphasizing diagnosis capability in sensing airgap magnetic fields for comparative analysis to be performed with the aid of ANSYS Maxwell in identifying minuscule variances in patterns of electromagnetic field between normal and faulty motor models

2.6.6 Infrared Detection

With feature dimensionality reduced by principal component analysis and optimized through Mahalanobis distance, this article [32] suggests a two-dimensional discrete wavelet transform-based infrared thermography method for non-destructive diagnosis of bearing faults in induction motors, such as inner or outer race faults and lubrication deficiencies. The method is then classified using support vector machines, complex decision trees and linear discriminant analysis. Support vector machines performed the best out of them, proving to be a viable technique for identifying self-adaptive bearing faults and avoiding catastrophic system shutdowns.

2.6.7 Stray Flux Detection

A kinematic chain comprising a 0.746 kW induction motor, belt and pulley transmission mechanism, and alternator as load was used to validate the new, non-intrusive and low-burden diagnostic method for misalignments and defective rotor bars that is proposed in the paper [33]. The method relies on the calculation and measurement of amplitude of stray flux based statistical parameters from startup transient measured signals. Using orbit analysis of time flux signals as fault signatures, this article [34] introduces a new stray flux sensor on the inner surface of the rear end plate of a three-phase induction motor to detect the presence and trend of common faults. Experimental verification under various load conditions shows how effective the technique is in diagnosing faults like misalignment, inter-turn short circuits and unbalanced voltage supplies, making it useful for predictive maintenance in industry.

Most advanced condition monitoring methods rely on these approaches either directly or indirectly. Electrical machines are complex by nature and due to the interaction of many parameters, an exact fault might be difficult to pinpoint. Numerous studies have been conducted in this sector, with a focus on methods including MCSA, vibration analysis, temperature analysis and electromagnetic field analysis. Because it is noninvasive, simple to use and compatible with a wide range of signal processing instruments, MCSA continues to receive the most citations in the literature among them. Almost all condition monitoring algorithms are based on one or more signal processing techniques. Application of various signal processing techniques for analyzing transient and steady-state signals is comprehensively covered in references [35, 36]. The occurrence of faults in electrical machines is highly dependent on several parameters of the motor, including but not limited to its type, size, rated voltage, among other specifications. To enhance reliability in these machines, several operational parameters should be monitored. The Table 2.2 shows suitable signals for fault signature in electrical machine.

Table 2.2: Suitable Signals for Fault Signature Detection in Electrical Machines [16]

Fault Signatures	**Winding Short Circuit [37, 38]**	**Rotor Broken Bars [39]**	**Eccentricity [40, 41]**	**Bearing Faults [42]**
Vibration	⊙	⊙	⊙	●
Current	●	●	⊙	●
Temperature	⊙	⊙	⊙	×
Magnetic flux changes	●	●	●	⊙
Chemical analysis	⊙	×	×	×
Torque changes	●	●	⊙	×

Legend: ● = Highly effective for condition monitoring, ⊙ = Moderately effective for condition monitoring, × = Not suitable for condition monitoring.

2.7 Electromagnetic Effect on the Rolling Bearing Faults

Due to mechanical vibrations and electromagnetic coupling, bearing failures in squirrel cage induction motors (SCIMs) significantly affect the stator current, flux, and voltage [43]. They are caused by flux modulation, harmonic production and air-gap eccentricity. The motor's electromagnetic performance fluctuates due to changes in the rotor-to-stator air gap induced by mechanical vibrations brought on by bearing problems, including outer race faults, inner race faults, rolling element damage faults and bearing cage damage faults [44]. The stator current spectrum contains harmonic components as a result of the mechanical asperities modulating the electromagnetic flux distribution. The sideband frequencies resulting from bearing faults can be described mathematically as:

$$f_{\text{sideband}} = f_s \pm k f_d \tag{2.16}$$

where the supply frequency is represented by f_s, the bearing defect frequency by f_d, and the harmonic order is represented by an integer k. These sidebands are critical markers used for fault diagnosis in induction motors. The bearing defect frequencies depend on the mechanical rotor frequency, f_r and this frequency is expressed by:

$$f_r = (1 - s)\,\frac{f_s}{p} \tag{2.17}$$

where s donotes motor slip and p denotes number of pair of poles. This indicate f_r is entirely depends on slip.The major electromagnetic effects of bearing faults are explained as below:

2.7.1 Air-Gap Eccentricity and Flux Distortion

Air-gap eccentricity can be of two forms due to bearing faults:

- **Static Eccentricity**: A persistent mismatch between the rotor and stator.
- **Dynamic Eccentricity**: Periodic variations in the air gap caused by the rotor's time-varying displacement.

The mutual inductance L_m between the stator and rotor fluctuates as a result of these eccentricities. A Fourier series may be used to simulate the mutual inductance [45]:

$$\Delta L_m(t) = \sum_{k=1}^{n} c_k \cos\left(2\pi k f_c t + \varphi_k\right) \tag{2.18}$$

where f_c is the characteristic defect frequency, c_k are coefficients depending on fault severity and φ_k are phase shifts. The resulting flux distortions due to changes in the air gap induce sideband frequencies in the stator current spectrum which can be written as:

$$f_{\text{sideband}} = f_s(1 \pm 2ks) \tag{2.19}$$

where s is the motor slip and f_s is the supply frequency. In SCIMs, these sidebands are important for identifying bearing problems.

2.7.2 Electromagnetic Modulation Mechanisms

Bearing faults modulate the stator current waveform through amplitude modulation (AM) and frequency modulation (FM). These modulations are described as follows:

Amplitude Modulation (AM)

Periodic changes in the air gap affect the flux linkage, which results in amplitude changes in the stator current. This phenomenon is known as amplitude modulation. The stator current's amplitude may be written as follows:

$$I(t) = I_0 + \Delta I \cos(2\pi f_s t + \varphi) \tag{2.20}$$

where f_s is the supply frequency, φ is a phase shift associated with fault severity, I_0 is the base current and ΔI is the modulation amplitude.

Frequency Modulation (FM)

When frequency fluctuation in the stator current are introduced by rotor instability, then the frequency modulation takes place. The rotor slot passing frequency (f_{rsf}) is one of the important frequencies that is modulated. This frequency is expressed as follows:

$$f_{\text{rsf}} = n_r f_r \tag{2.21}$$

where f_r is the rotor frequency and n_r is the number of rotor slots. Frequency fluctuations in the stator current, which are utilized to diagnose faults, are caused by these oscillations in the rotor speed.

2.8 Research Gap

In order to maintain effective operations and minimize downtime, diagnosing rolling bearing problems in induction machines is a crucial responsibility. Although recent developments in machine learning show promise for enhancing vibration-based monitoring systems, several challenges and research gaps still limit their effective application. Some identified research gaps are described as follows:

2.8.1 Real-Time Diagnostic Capabilities

Most of the machine learning based fault diagnosis methods require offline training and inference which fails to meet the industrial requirements. Furthermore, vibration data analysis is always time-consuming and computationally intensive. This has remained one of the significant bottlenecks for the deployment of deep learning-based fault diagnostic methods in real-time scenarios [46] . Thus, future works shall be directed towards proposing frameworks for edge computing to realize the real-time fault diagnosis.

2.8.2 Feature Extraction and Data Fusion

The effectiveness of fault diagnosis depends substantially on the technique of feature extraction and fusion from multi-sensor data. Accordingly, traditional techniques like wavelet transform and envelope analysis often have limited diagnostic efficacy due to the intrinsic nonlinearity and non-stationary nature of vibration signals [47]. Besides, advanced multi-sensor fusion techniques should be explored including Dempster-Shafer evidence theory, so that the systems are robust under a wide variety of operating conditions.

2.8.3 Generalization Across Different Operating Conditions

Most of the research done at present focuses on particular fault types or controlled settings, further limiting the general applicability of the results. Validation studies for machine learning models must be conducted in authentic industrial settings that replicate a range of defect scenarios. This includes investigating how varied operating circumstances affect the effectiveness of ML algorithms in diagnosing rolling bearing problems.

2.8.4 Integration of Multi-Modal Data

Most of the developed fault diagnosis methods are based only on vibration signals. There is a growing interest in incorporating multi-modal data sources such as temperature and acoustic emissions to improve the accuracy of diagnosis. The effective integration of various data types using intelligent algorithms may lead to a significant improvement in the capabilities of fault detection.

2.8.5 Model Interpretability and Usability

It is challenging for practitioners to have faith in the results, even while the interpretability of the model declines as machine learning models get more complicated. Indeed, future research should be done on interpretable models that give clear insights into the decision-making processes behind fault diagnoses. This would ensure that user confidence increases and contribute to wider diffusion in industrial applications.

CHAPTER THREE: METHODOLOGY

This chapter discusses the research workflow which starts with vibration data collection from SCIM with healthy and faulty bearings under various loading conditions through a laboratory experimental setup system, then work continues through feature engineering to extract various statistical features in the time and frequency domains along with their envelope signals and finally research ends with detection and diagnosis of rolling bearing faults by developing various machine learning models.

3.1 Approach

The methodology approach that has been adopted in this dissertation is summarized in the Figure 3.1. In order to comprehend the concepts, ideas, needs and development of

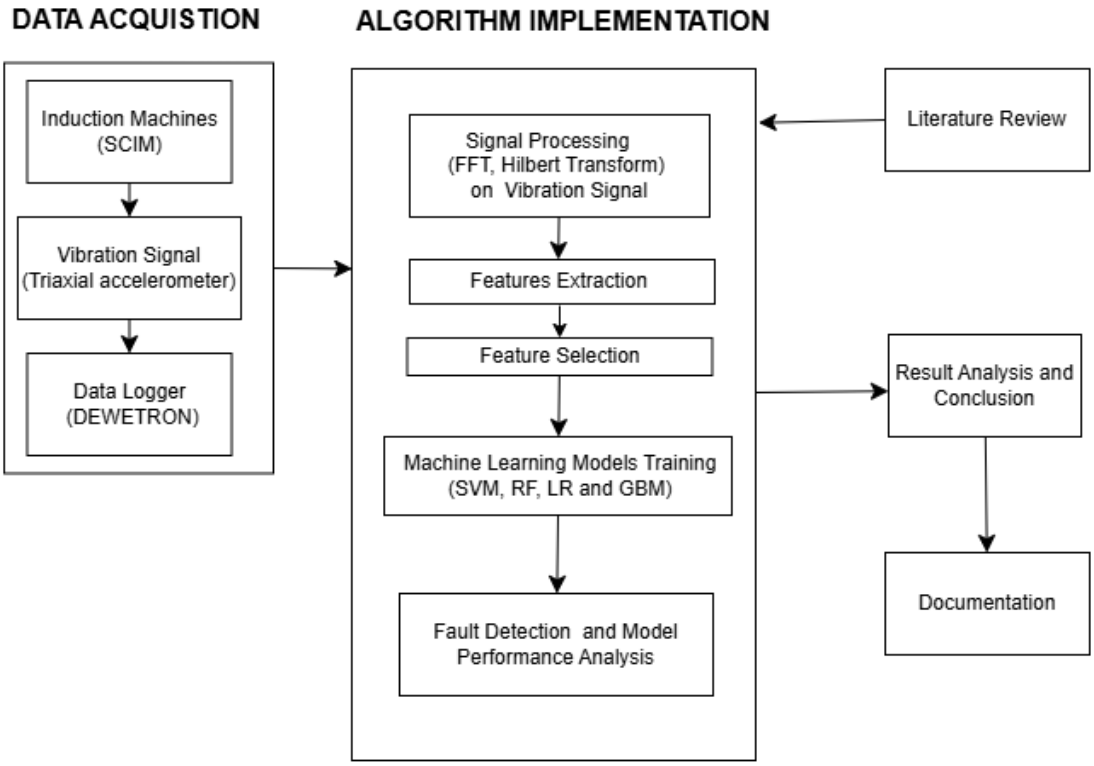

Figure 3.1: Methodology Approach

the machine learning model for fault diagnostics and condition monitoring, a literature research was conducted first. Next, an experimental setup system at Tallinn University of Technology (Taltech), Tallinn, Estonia, was used to gather vibration data for various machine states under various loading circumstances. After processing the vibration signals in several domains using the hanning window function, fast fourier transform and hilbert

transform, different statistical characteristics were recovered from the signals in each domain. In order to train and test the various developed machine learning algorithms, such as support vector machines, gradient boosting machines, random forest classifiers and logistic regression for fault detection and diagnosis of rolling bearing faults, the appropriate features were then chosen using permutation importance techniques in accordance with the requirements of the machine learning model. This is followed by presenting detailed discussion and conclusion with documentation of the all works and findings.

3.2 Data Acquisition

The experimental methods used by Tallinn University of Technology (TalTech) at Tallinn, Estonia's Electric Machine Group (EMG) are described in this section. The vibration data collected from these experiments serves as the foundation for this research.

3.2.1 Experimental Setup

A test bench used in this study to examine bearing problems in induction machines is shown in Figure 3.2. It consists of testing machine, loading machine, accelerometer and

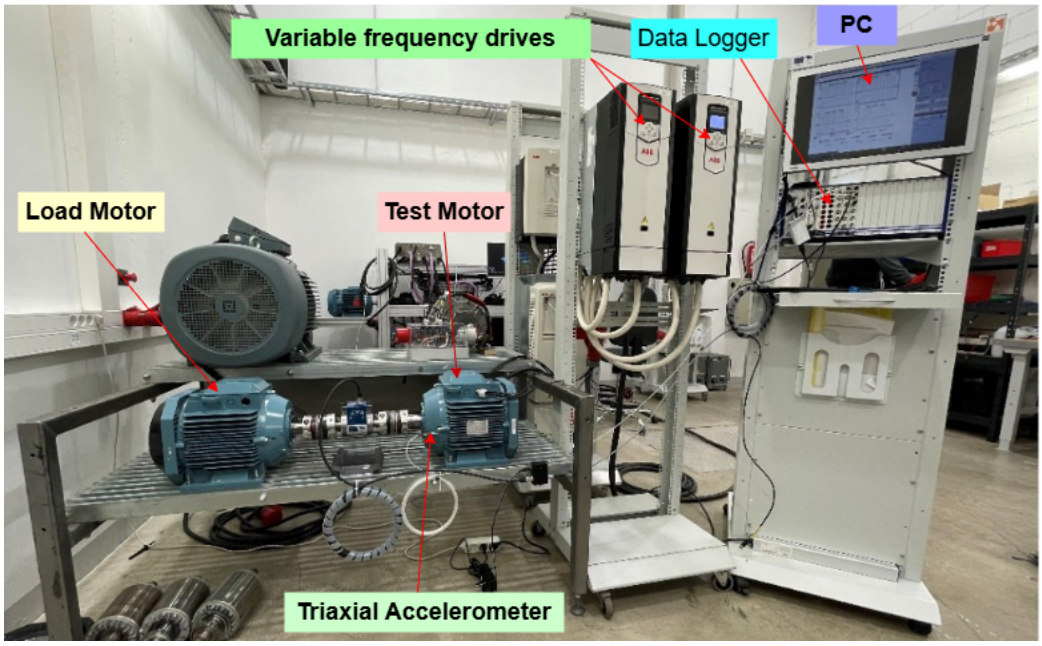

Figure 3.2: Experimental Test Bench [48]

data acquisition system. The data loggeras as a Dewetron DEWE2-M18 system was used for data collection and signal processing. Figure 3.3 displayed the motor nameplate specifications, Table 3.1 displayed the specifications for the testing and loading motors and Table 3.2 displayed the rolling bearing specifications.

Table 3.1: Induction Machine Specification

Parameters	Symbols/Units	Value
Number of poles	P	4
Number of Phases	Φ	3
Connection		Δ
Voltage	V	400
Current	A	15.3
Power	kW	7.5
Speed	rpm	1460
Power factor	cos ϕ	0.79

Table 3.2: Bearing Specification

Parameters	Symbol	Value
Drive End Side Bearing		
Bearing Type	LFD ONE	6208 Z
Outer Diameter	mm	80
Inner Diameter	mm	40
No. of Balls	Nos	9
Weight	kg	0.402
Non Drive End Side Bearing		
Bearing Type	LFD ONE	6206 Z
Outer Diameter	mm	62
Inner Diameter	mm	30
No. of Balls	Nos	9
Weight	kg	0.210

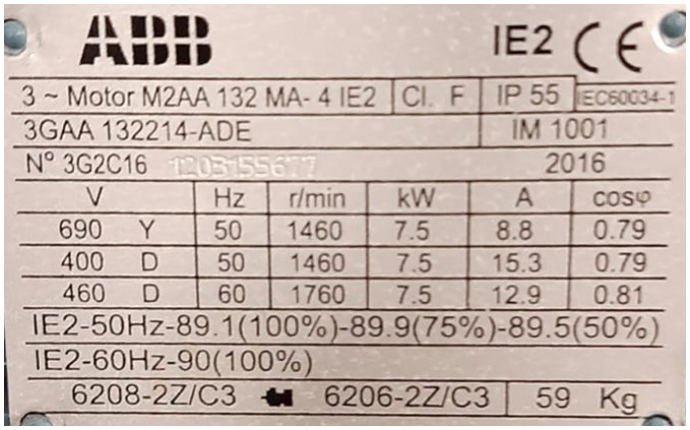

Figure 3.3: Test Motor Nameplate

The experimental configuration consists of two identical motors linked together through their shafts using a flanged coupling. The test machine undergoes a variety of machine state situations, including healthy motor, outer race fault, inner race fault and damaged bearing cage fault. The first motor, which was in good condition, loads the machine. Both motors were powered by a variable frequency drive that controlled both motors such that ABB ACS600 was VFD for the loading machine and ABB ACS800 was VFD for the test machine. During the tests, the loading level was regulated using the loading machine with the Variable Frequency Drive (VFD) utilizing Direct Torque Control (DTC) technology. After the system stabilized, vibration signals were captured for around 60 seconds using a data logger acting as a Dewetron transient recorder, sampling at a rate of 20 kHz. Because the consequences of bearing problems were mostly seen in vibration rather than the current spectrum, the vibration spectrum is essential for assessing bearing damage. A triaxial accelerometer was installed on the shaft to monitor vibration for this reason. The specification of the accelerometer was shown in Table 3.3.

Table 3.3: Description of Acclerometer (Sensor)

Sensor	Triaxial accelerometer
Sensitivity	50 mv/g
K -Shear	±100g

Acceleration measurements were expressed in 'g' units, and the placement of the accelerometer is shown in Figure 3.4. Current, voltage, torque, speed, and vibration were

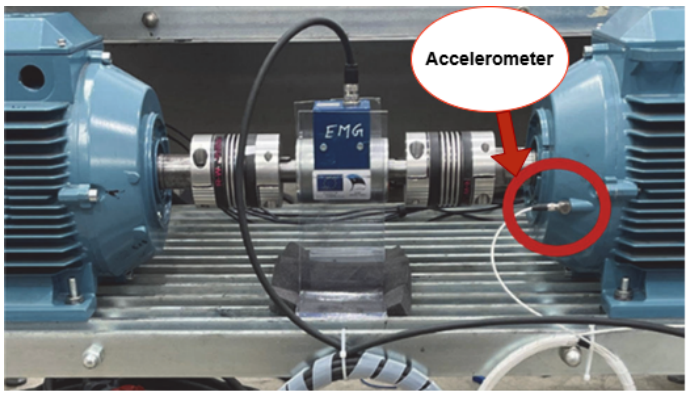

Figure 3.4: Placement of Triaxial Accelerometer [49]

among the factors that were recorded in the datasets created throughout this project. Grid-fed, scalar and DTC control modes were among the several control modes used for data collecting. Also, data was collected under various load conditions: 0%, 25%, 50%, 75%, and 100%. Aiming to boost efficiency, this approach does not need to study the whole signal but only some regions where fault effects are highly pronounced. The focus was to

identify these critical signal segments in order to train the models and extract meaningful patterns. Thus, this gave complete datasets with all information in minute detail about both healthy and faulty conditions. The vibration signals were found to be more effective in fault detection at an earlier stage for mechanical fault as bearing fault.

3.2.2 Experimental Procedure

The vibration data collection under healthy and faulty conditions of rolling bearings of SCIM whose experimental procedure was carried out using the following experimental setup scheme illustrated in Figure 3.5.

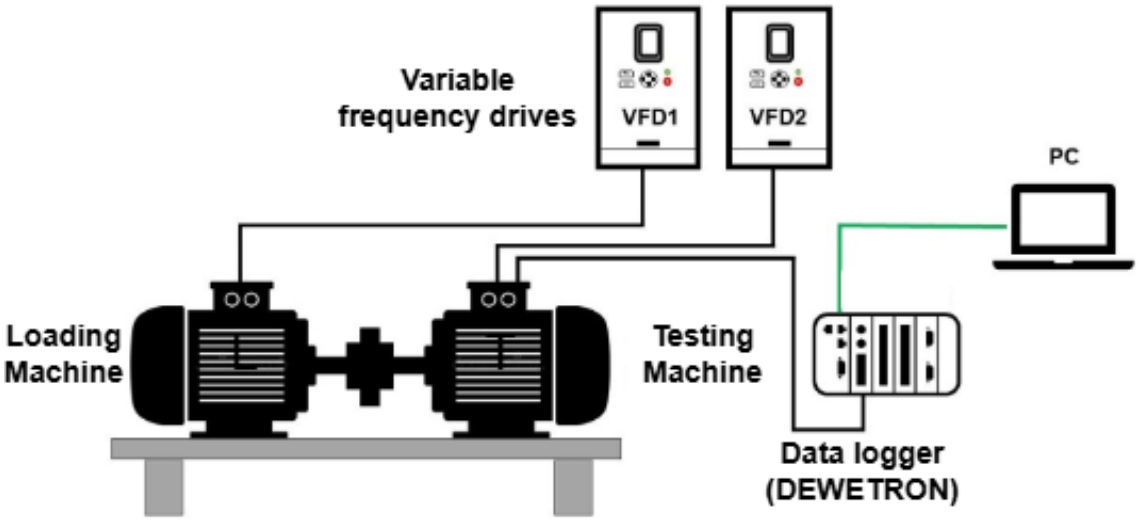

Figure 3.5: Block Diagram of Experimental Setup

The overall procedure is described as below:

- A total of 20 tests were conducted as part of the experimental procedure.
- Initially, vibration data of the test machine during its steady phase were recorded for 60 seconds under healthy bearing conditions.
- These recordings were performed at varying load levels: 0%, 25%,50% ,75% and 100% of the test machine's nominal load.
- The bearings were then purposefully damaged on a different test bench to create certain problems, such as damaged bearing cage faults, inner race faults and outer race faults.

- Using the main experimental setup, vibration signals were recorded for each of these fault conditions under all loading conditions as healthy case.

- All vibration recordings were stored as `.mat` files, compatible with MATLAB software.

3.3 Features Extraction

To extract features from time and frequency domain vibration signals as well as from their envelope signals, a sliding window approach was employed for all machine states and all loading conditions. The difference between the start and finish times was used to compute the signal's overall duration, which came out to be about 60 seconds.

$$\text{Total Duration (T.D)} = \text{End time} - \text{Start Time} = 60\,\text{seconds}. \tag{3.1}$$

A window length of 4 seconds was defined, corresponding to:

$$\text{Window Length (W.L)} = 4 \times 20,000 = 80,000\,\text{data points}. \tag{3.2}$$

Where, the signal's sampling rate of 20 kHz.

The window was shifted by 2,000 data points equivalent to:

$$\text{Slide Time (S.T)} = \frac{2000}{20,000} = 0.1\,\text{seconds}. \tag{3.3}$$

The initial time was set to 2 seconds, this process had iteratively repeated overlapping segments of the signal. The total duration of the usable signal for the sliding windows:

$$\text{Usable Duration (U.D)} = \text{T.D} - \text{Start Time} - \text{W.L} = 60 - 2 - 4 = 54\,\text{seconds}. \tag{3.4}$$

The total number of windows was calculated as:

$$\text{No. of Windows} = \left\lceil \frac{\text{U.D}}{\text{S.T}} \right\rceil + 1 = \left\lceil \frac{54}{0.1} \right\rceil + 1 = 541. \tag{3.5}$$

This allowed features to be extracted from each of these windows. A total of 541 windows for each machine state with particular loading conditions were produced. The vibration signals were not practically recorded for the signal length of 60 seconds in experiment for all machine states and all loading conditions. In some case, the duration was may

be exactly 60 seconds, while in others, it was a little over this value or a bit less. Sliding windows generated for feature extraction in the datasets thus varied from 537 to 569. For consistency and standardization of the analysis, a uniform value of 530 windows was chosen for all cases of vibration signals in this research. This procedure is illustrated in Figure 3.6. The vibration signal was transferred in frequency domains from time using a

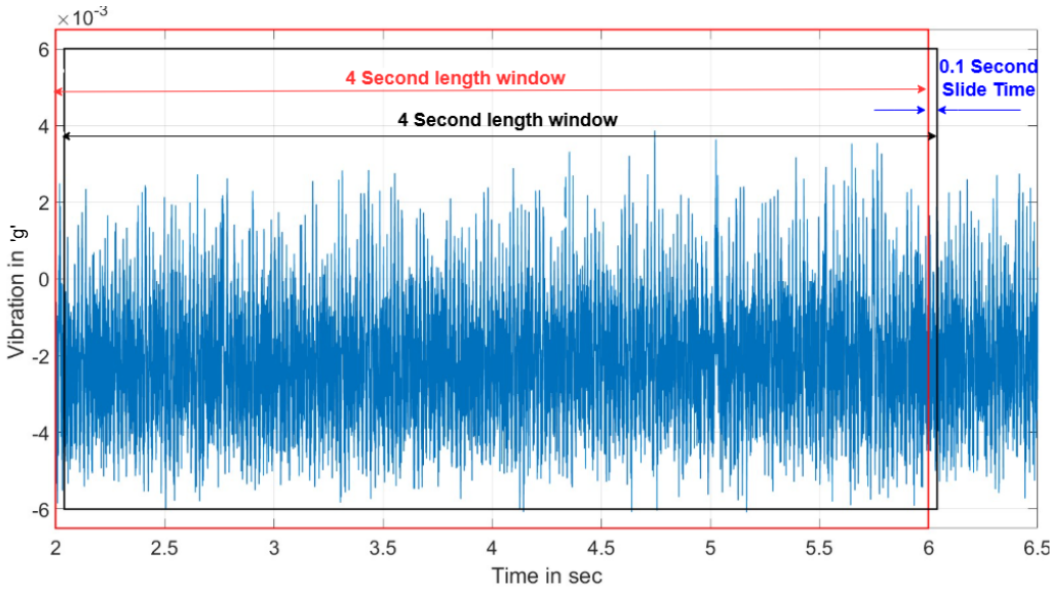

Figure 3.6: Vibration Signal Windowing

fast Fourier transform (FFT) in the study. The discrete fourier transform (DFT) is mathematically calculated by the FFT by:

$$X[k] = \sum_{n=0}^{N-1} x[n] e^{-j\frac{2\pi kn}{N}} \tag{3.6}$$

where N is the number of samples, k is the frequency index, and $X[k]$ is the frequency components. The windowed signal in this thesis was converted into the frequency domain using the fast fourier transform (FFT). To minimize spectral leakage, the Hann window function was employed. The mathematical definition of the Hann window is:

$$w(n) = 0.5\left(1 - \cos\left(\frac{2\pi n}{N}\right)\right) \tag{3.7}$$

where N is the total number of samples and $w(n)$ is the window function. Figure 3.7 displays the original vibration time domain signal for the healthy case in a direct torque control environment for the 100% loaded case. Above is the original time-domain signal after the application of the hanning window in Figure 3.8. Features like instantaneous amplitude and phase may be extracted by using the Hilbert transform to get the envelope of a vibration signal in either the frequency or time domain. The definition of the Hilbert

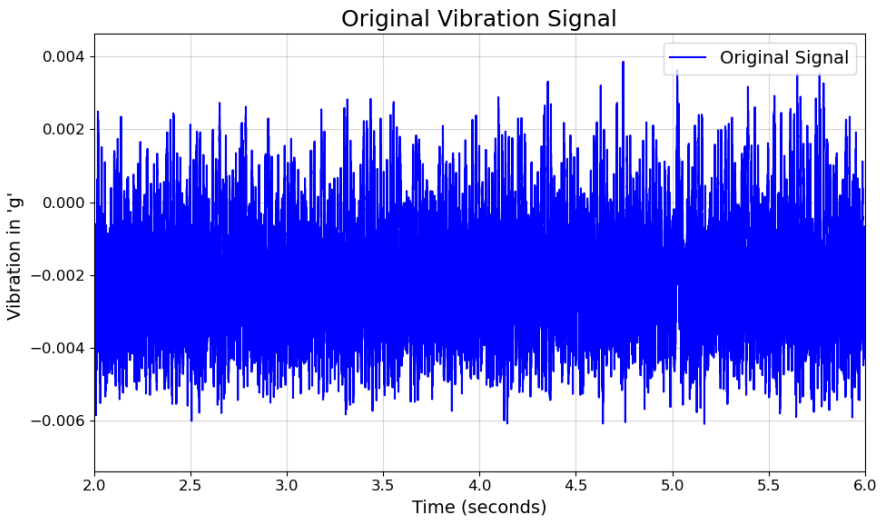

Figure 3.7: Original Vibration Signal for Healthy Motor at 100% Loading

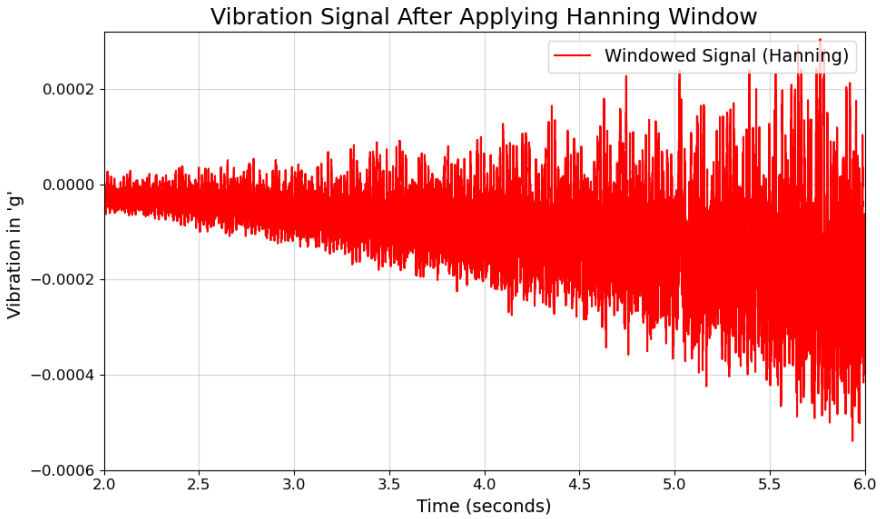

Figure 3.8: Hanned Vibration Signal for Healthy Motor at 100% Loading.

transform of a signal $x(t)$ is:

$$\hat{x}(t) = \mathcal{H}\{x(t)\} = \frac{1}{\pi}\mathcal{P}\int_{-\infty}^{\infty}\frac{x(\tau)}{t-\tau}\,d\tau \tag{3.8}$$

where $\mathcal{H}$ denotes the hilbert transform and $\mathcal{P}$ indicates the cauchy principal value of the integral. The instantaneous amplitude of the signal is then used to compute its envelope:

$$a(t) = \sqrt{x(t)^2 + \hat{x}(t)^2} \tag{3.9}$$

The statistical features had been extracted using every 530 number of windows in all motor states and loading scenarios of the induction machine. The mean, standard deviation, median, kurtosis, root mean square, skewness, maximum value, sum of absolute values and crest factor were among the time-domain features that were retrieved. In the frequency domain, the features to be extracted were mean, standard deviation, median, kurtosis, root mean square, skewness, maximum value, sum of absolute values, mean power spectral density and maximum power spectral density.

Hilbert transform was performed to obtain statistical features of envelopes of time and frequency-domain signals. The envelope-based features that considered were mean, standard deviation, median, kurtosis, root mean square, skewness, maximum value and sum of absolute values in both time and frequency domain envelope signals. These features were taken from vibration signals that were recorded in four different operating conditions: a healthy motor, an outer race fault, an inner race fault and a bearing cage defect that was damaged. Data collection was carried out under different loading conditions such as 0%, 25%, 50%, 75%, and 100% load levels. For each vibration signal time window, these statistical features were computed and organized in an Excel file for methodical further study. In Figure 3.9, the feature extraction procedure was depicted.

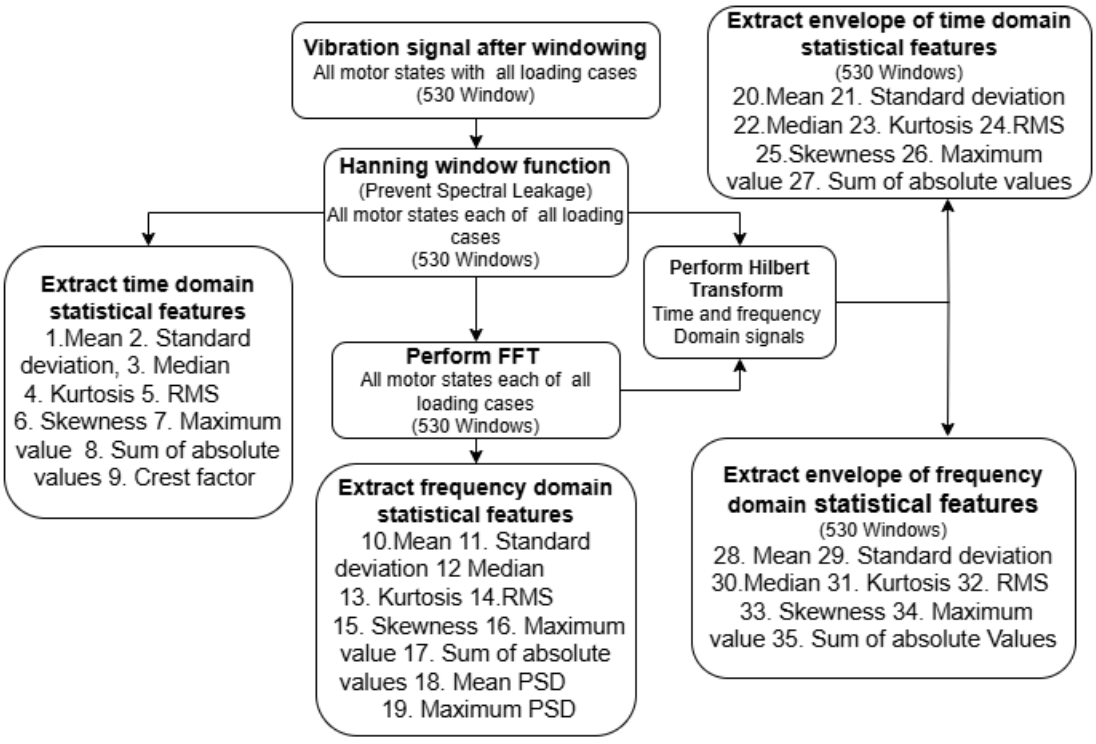

Figure 3.9: Feature Extraction Procedure

3.3.1 Dataset Structure

The raw vibration signal dataset structure and extracted input statistical features dataset structure are explain as below.

Raw Vibration Dataset Structure

Table 3.4 displays the structure of the vibration data that was obtained from the induction motor's bearing with all machine states under various loading circumstances. The data is in .mat format.

Table 3.4: Vibration Raw Dataset Structure

Number of data in loading conditions (x)										**Output (y)**
0%		**25%**		**50%**		**75%**		**100%**		
Amp	**Time**	**Amp**	**Time**	**Amp**	**Time**	**Amp**	**Time**	**Amp**	**Time**	**States**
256	256	256	256	256	256	256	256	256	256	Healthy
256	256	256	256	256	256	256	256	256	256	Outer race
256	256	256	256	256	256	256	256	256	256	Inner race
256	256	256	256	256	256	256	256	256	256	Damage cage

This data set contains vibration signals collected in five independent cases of loading (0%, The vibration signals in this dataset were obtained in five separate loading scenarios (0%, 25%, 50%, 75% and 100%) for the machine condition categorization as healthy motor, outer race fault, inner race fault and damaged bearing cage. All conditions have 256 numbers of amplitude and time-domain samples obtained from 20 KHz sampling for 60 second length vibration signal.

Extracted Feature Dataset Structure

The extracted input features dataset was structured in 10,600 records for each of feature in excel form as shown in Table 3.5. The dataset includes statistical characteristics taken from five loading circumstances (0%, 25%, 50%, 75% and 100%) and several machine health statuses (healthy motor, outerrace fault, innerrace fault and broken cage). Each combination of machine state and loading condition contains 530 samples per statistical feature, with a total of 35 features. This results in a well-balanced dataset structured for supervised learning, totaling 10,600 data samples per feature. The dataset provides a comprehensive representation of machine behavior, enabling effective fault detection using machine learning models.

Table 3.5: Structure of Extracted Statistical Features Dataset

Machine State	% Loading	Number of Statistical Feature Values			
		T_mean	T_sd	T_median	... up to 35 Features
Healthy	0%	530	530	530	530 per feature
	25%	530	530	530	530 per feature
	50%	530	530	530	530 per feature
	75%	530	530	530	530 per feature
	100%	530	530	530	530 per feature
Outer Race	0%	530	530	530	530 per feature
	25%	530	530	530	530 per feature
	50%	530	530	530	530 per feature
	75%	530	530	530	530 per feature
	100%	530	530	530	530 per feature
Inner Race	0%	530	530	530	530 per feature
	25%	530	530	530	530 per feature
	50%	530	530	530	530 per feature
	75%	530	530	530	530 per feature
	100%	530	530	530	530 per feature
Damaged Cage	0%	530	530	530	530 per feature
	25%	530	530	530	530 per feature
	50%	530	530	530	530 per feature
	75%	530	530	530	530 per feature
	100%	530	530	530	530 per feature

3.4 Feature Selection

Feature selection is focused on finding the most significant features for machine learning and enhancing model performance by eliminating bias and overfitting. In this research, the permutation importance approach was employed. To train and evaluate machine learning models like SVM, RF, LR and GBM, more important features were selected and a permutation importance plot was created. In this method, firstly train the model and obtain its baseline performance, then for one feature randomly shuffle its values and re-test the model to record any drop in performance, that being the feature's permutation importance value. The process was repeated for all of the features to rank them based on their permutation importance which is helpful for feature selection and also enhances model interpretability.

3.5 Fault Diagnostics using Machine Learning Methodologies

The major fault diagnostic machine learning methodologies used in this dissertation were described below:

3.5.1 Support Vector Machine (SVM)

In this thesis work, diagnosis of induction motor bearing fault was done using SVM model in a structure ranging from data acquisition using excel files to stratification, taking into consideration fault type and loading percentage, feature scaling with StandardScaler and then dealing with the class imbalance by means of SMOTE. Feature selection had been performed based on permutation importance, selecting only the top five most discriminative features. The hyperparameter tuning was carried out by using GridSearchCV, along with a 5-fold cross-validation on C-0.1, 1, 10 and 100. The kernel types (linear, RBF, polynomial) and gamma values were scaled and automatic. Finally, a trained SVM model on chosen features forecasted the fault condition and performances were evaluated via confusion matrix classification reports for precision, recall, and F1 scores. This model also used 75% for training and 25% for the validation dataset. Such a structured approach ensures robust and reliable SVM-based fault diagnosis in industrial applications.

3.5.2 Gradient Boosting Model (GBM)

In order to improve the overall model's performance, a number of decision trees were developed using the Gradient Boosting Classifier model approach. Initially, the number of estimators was set to 200, with a learning rate of 0.1 and each tree was taken to a depth of 5. In the model, the parameters were balanced between model complexity and predictive accuracy to avoid overfitting, which means that the model has the ability to capture the underlying pattern in the data. Also, early stopping was set with a validation fraction of 10%, stopping if it did not improve in 10 consecutive iterations. Thus, it prevents overfitting by stopping too much training of the model. StandardScaler, which standardizes features by eliminating the mean and scaling to unit variance, was used to carry out the scaling. The boosting models need this step. This model also used 75% for training and 25% for the validation dataset.

3.6 Model Validation and Performance Matrices

A confusion matrix that was acquired following each model's validation was used to assess each of the created machine learning models. The confusion matrix yielded the following performance metrics: F1-score, recall, accuracy and precision. These concepts have the following definitions:

Accuracy: Accuracy is the number of times a model has produced the right forecast out of all the examples that were examined. It considers both correctly identified positives and negatives. It provides a general idea of how well the model performs across a range of

areas. A greater accuracy score indicates that the model is making an increasing number of accurate predictions. Hence, it can also do well with new unseen data. It is calculated as

$$Accuracy = \frac{TP + TN}{Total\ Observation} \tag{3.10}$$

Precision: Precision depicts the exactitude of the model in predicting the positive cases by comparing the actual number of the true positives versus the total numbers that the model predicted as being positive, adding the false instances. A higher precision score therefore means that it makes fewer errors when identifying a case as being positive, raising the reliability on its positive prediction. It is calculated as:

$$Precision = \frac{TP}{TP + FP} \tag{3.11}$$

Recall: Recall means how good the model is at correctly finding every actual positive case in a dataset. That ratio is the amount of true positives or accurately predicted positives, to the total number of real positives or false negatives, that the model is expected to miss. If recall is high, this then implies that the model is good in detecting positive cases and capturing relevant examples without missing them. The recall is evaluated by using equation:

$$Recall = \frac{TP}{FN + TP} \tag{3.12}$$

F1 – score: The F1-score may be thought of as the accuracy and recall harmonic means. When both metrics are significant, this yields a single figure that strikes a balance. Precision looks at how accurate the positive predictions are while recall is about how well the model finds all the instances. F1-score is perfect when the precision and recall are both 1, which says that the model is outstanding in making as many positive predictions correctly and capturing all relevant examples in the dataset. The F1-Score is mathematically evaluated by using equation::

$$F1 - score = 2\frac{Recall * Precision}{Recall + Precision} \tag{3.13}$$

CHAPTER FOUR: RESULTS AND DISCUSSION

Using the methods outlined in Chapter 3, the results are presented in this chapter.

4.1 Feature Extraction

As explained in Section 3.3, each vibration signal was split into four-second vibration windows in order to extract features from the vibration signals of various motor states under various loading situations. This resulted in 530 windows in total. Applying the hanning window function for each of the windows for all motor states and loading situations was followed by feature extraction on the time domain signal. Figure 4.1 displays the time domain signal following the application of the hanning window in the event of a damage bearing cage fault at 100% loading. From this obtained time domain signal, the time domain statistical features were extracted from all of the windows for all motor states and all loading conditions. After applying hanning window function to time domain signal, the fast fourier transform was performed to obtain frequency domain signal for all of windows for all motor states with all loading conditions. The frequency domain signal after performing fast fourier transform in case of damage bearing cage fault at 100% loading is shown in Figure 4.2.

From obtained both time and frequency domain signals, the hilbert trainsform was carried out to obtain envelope signal of both time and frequency domain signals. From this frequency domain signal, frequency domain statistical features were extracted for all of windows for all motor states with all loading conditions. The envelope of time domain signal and frequency domain signal after applying hilbert transform in case of damage bearing cage fault at 100% loading are shown in Figure 4.3 and 4.4. From these both envelope of time and frequency domain signal, envelope of both time and frequency domain statistical features were extracted for all of the windows for all motor states with all loading conditions. The total 35 number of statistical feature were extracted for each of loading conditions for each of machine state. The one feature has 530 data for one loading condition of each of machine state. The total amount of data in a single feature obtained was 10600 for each of the five loading conditions (0%, 25%, 50%, 75% and 100%) for four motor states: healthy, outer race fault, inner race fault and damage bearing cage fault. As a result, the total dataset size for training and testing the various machine learning models created for rolling bearing defect diagnosis and detection was 10600×35.

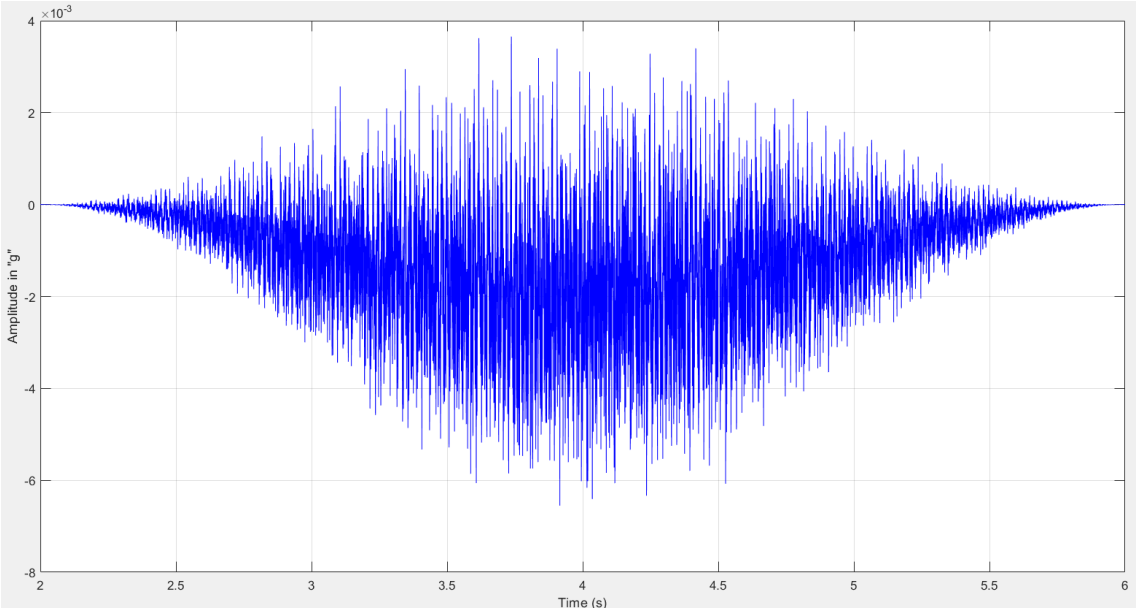

Figure 4.1: Time Domain Vibration Signal After Applying Hanning Window for Damage Bearing Cage Fault at 100% Loading

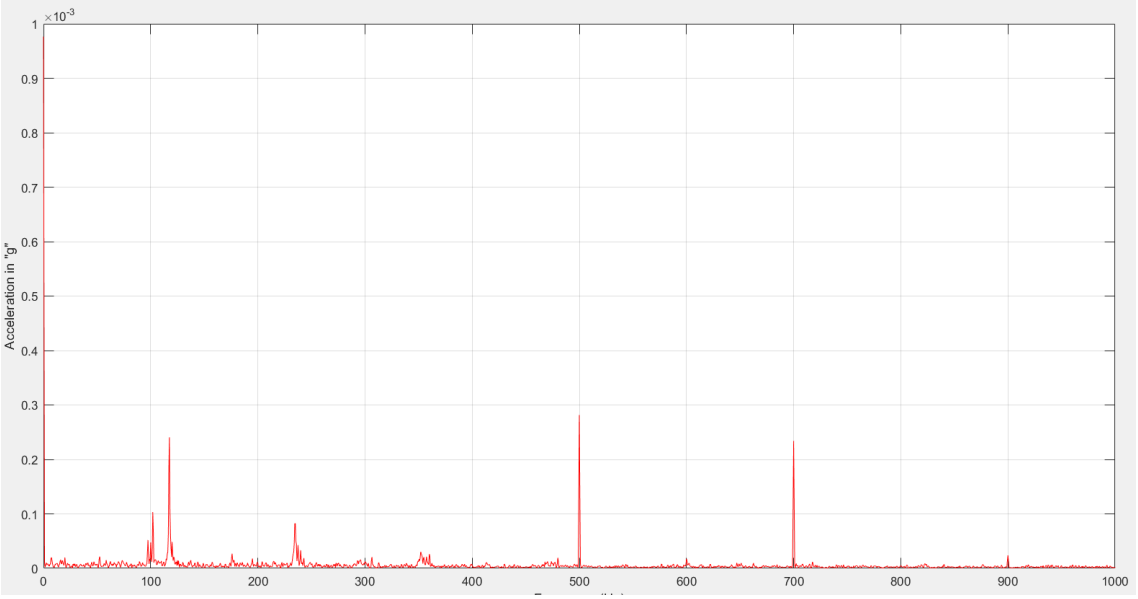

Figure 4.2: Frequency Domain Vibration Signal After Applying Hanning Window for Damage Bearing Cage Fault at 100% Loading

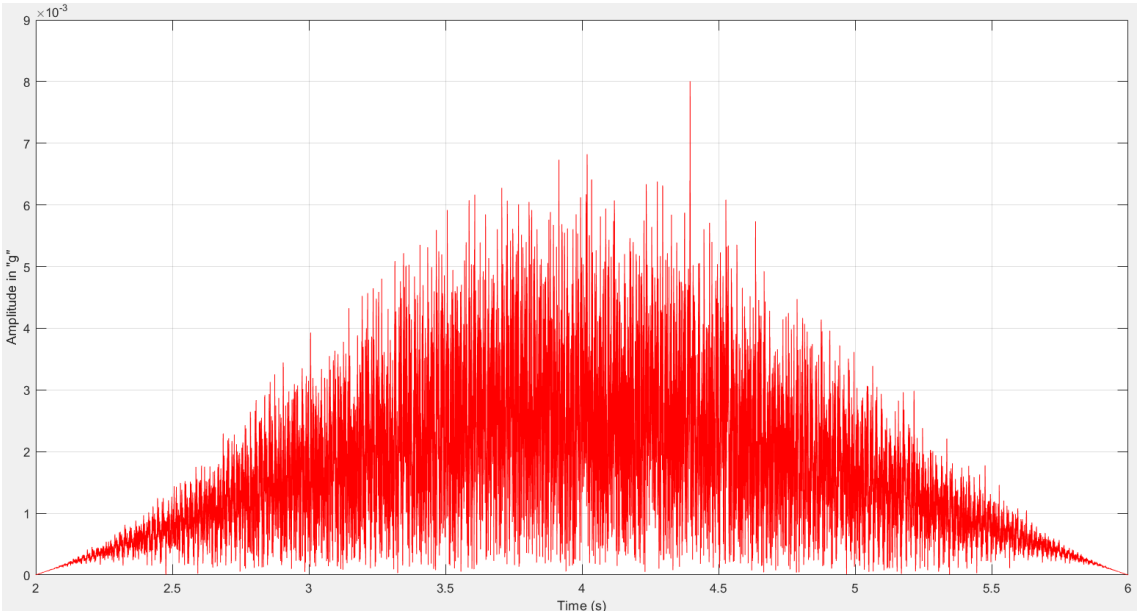

Figure 4.3: Envelope of Time Domain Vibration Signal After Applying Hanning Window for Damage Bearing Cage Fault at 100% Loading

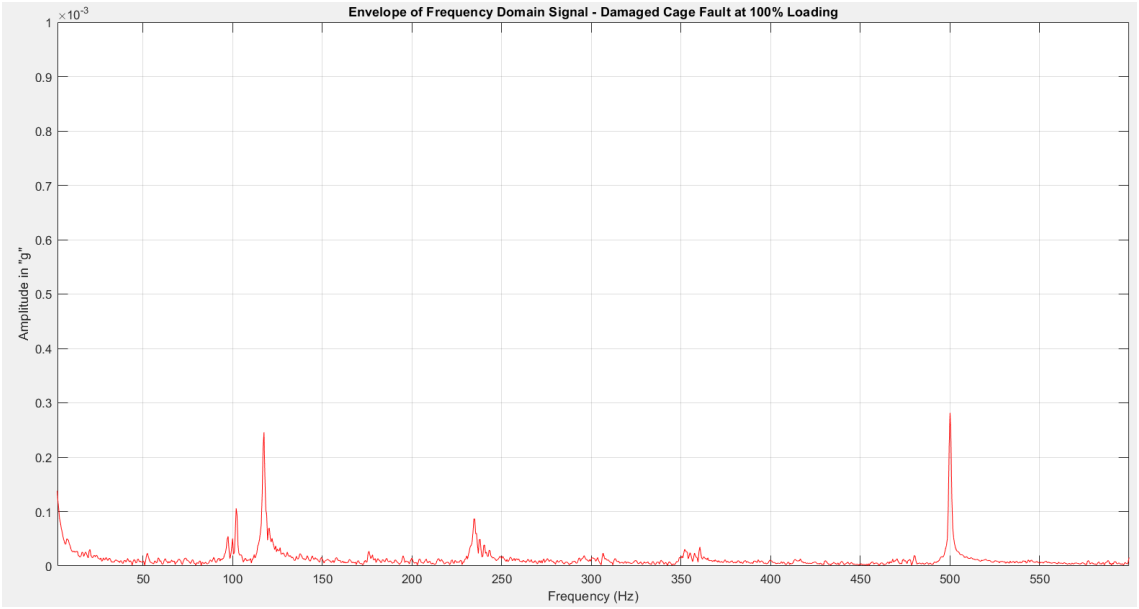

Figure 4.4: Envelope of Frequency Domain Vibration Signal after Applying Hanning Window for Damage Bearing Cage Fault at 100% Loading

4.2 Stator Current Analysis under Different Machine States

The stator current spectrum under various machine states such as healthy motor, outer race bearing fault, inner race bearing fault and damaged cage bearing fault are shown in Figure 4.5, 4.6, 4.7, 4.8 and 4.9 under different loading level as 0%,25%,50%,75% and 100%. Under no-load condition, the sidebands in the motor state frequency spectrum could not be detected by the fast fourier transform analysis. This restriction results from the fact that the sidebands strongly overlap with the current signal's fundamental component due to low value of motor slip when there is no load. Analysing the magnitude and frequencies of side band, we can easily identify different types of rolling bearing fault using motor current signature analysis.

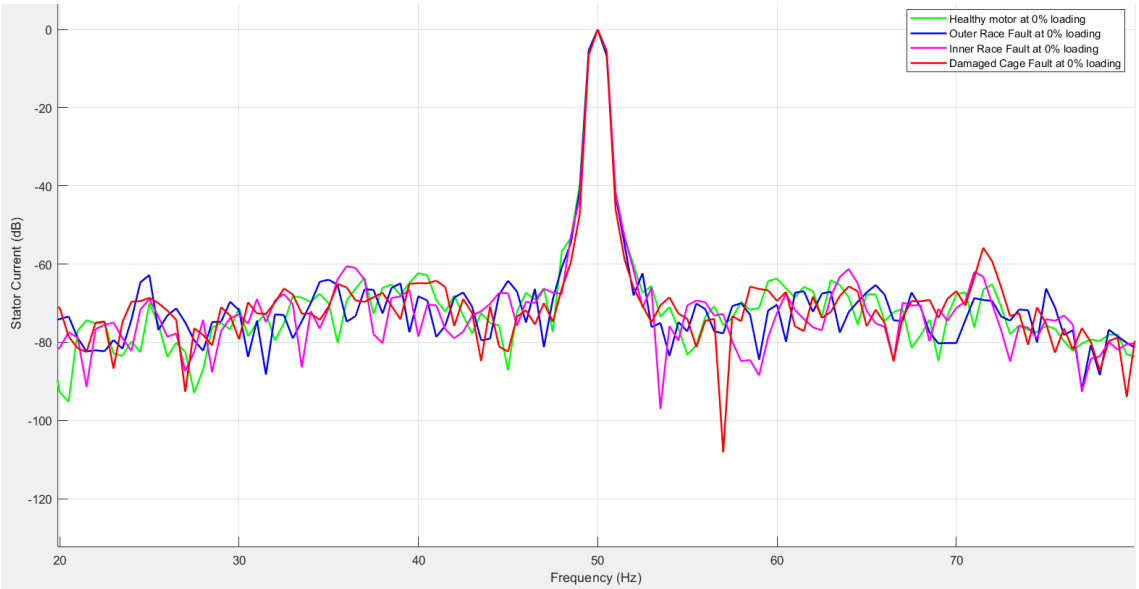

Figure 4.5: FFT spectrum of stator current signal at no load

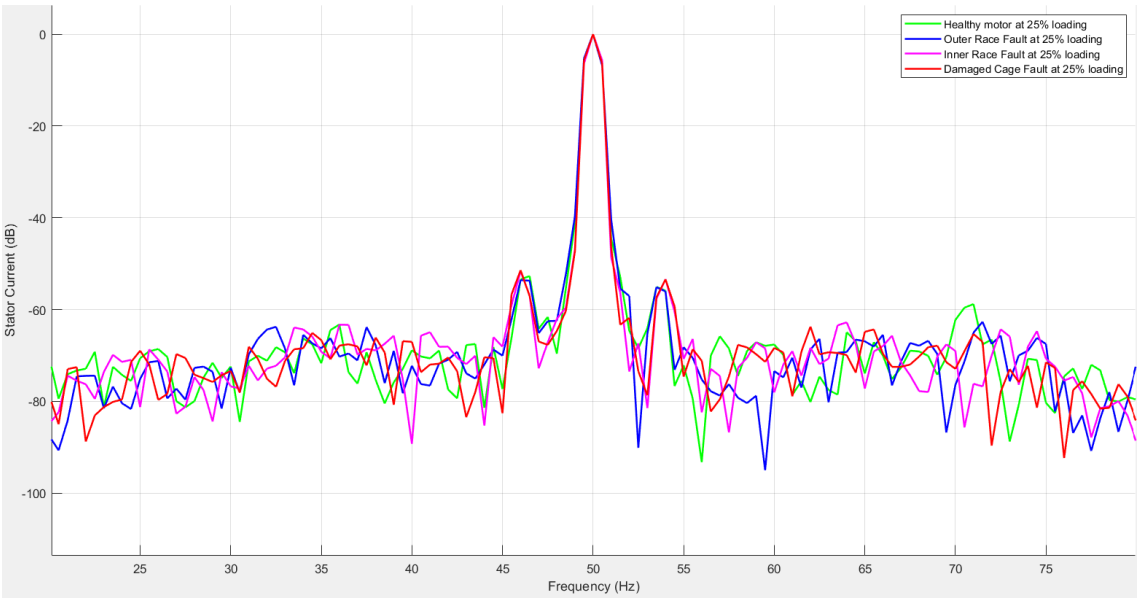

Figure 4.6: FFT Spectrum of Stator Current Signal at 25% Load

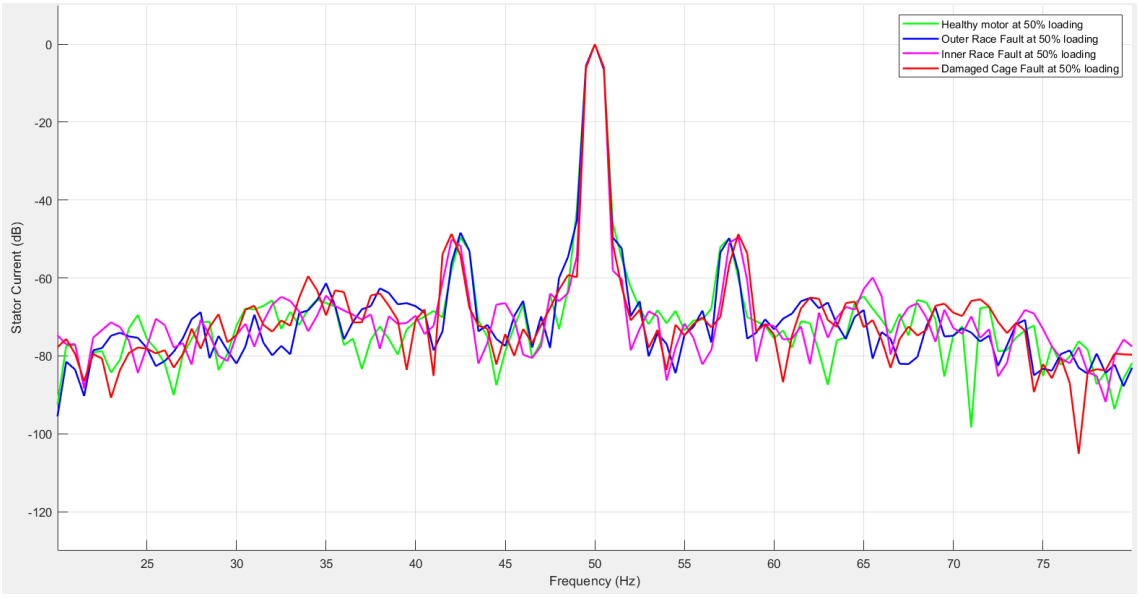

Figure 4.7: FFT Spectrum of Stator Current Signal at 50% Load

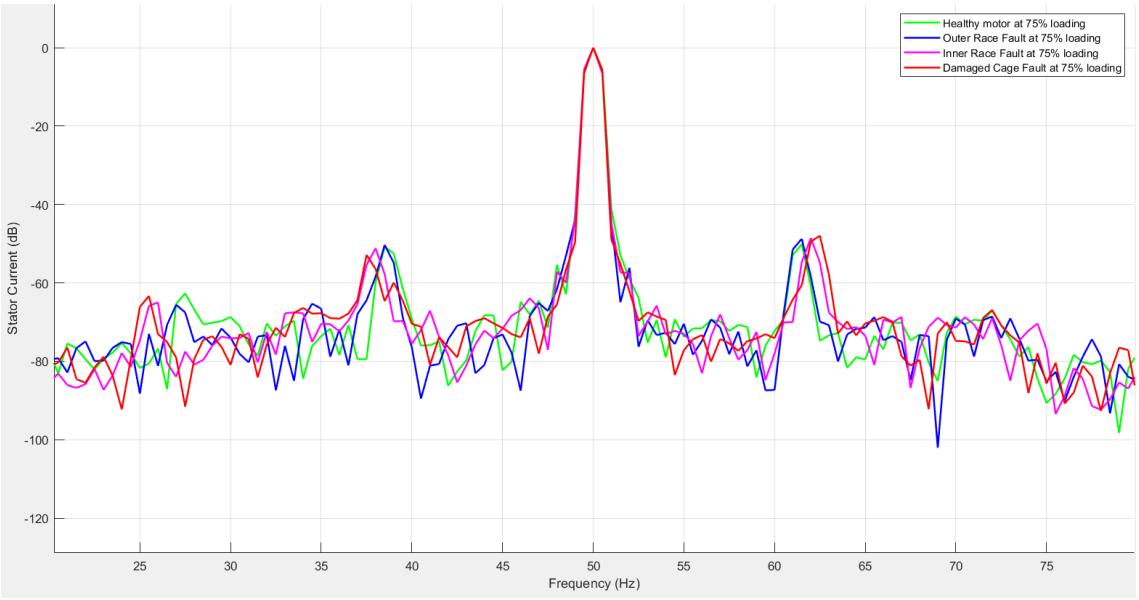

Figure 4.8: FFT Spectrum of Stator Current Signal at 75% Load

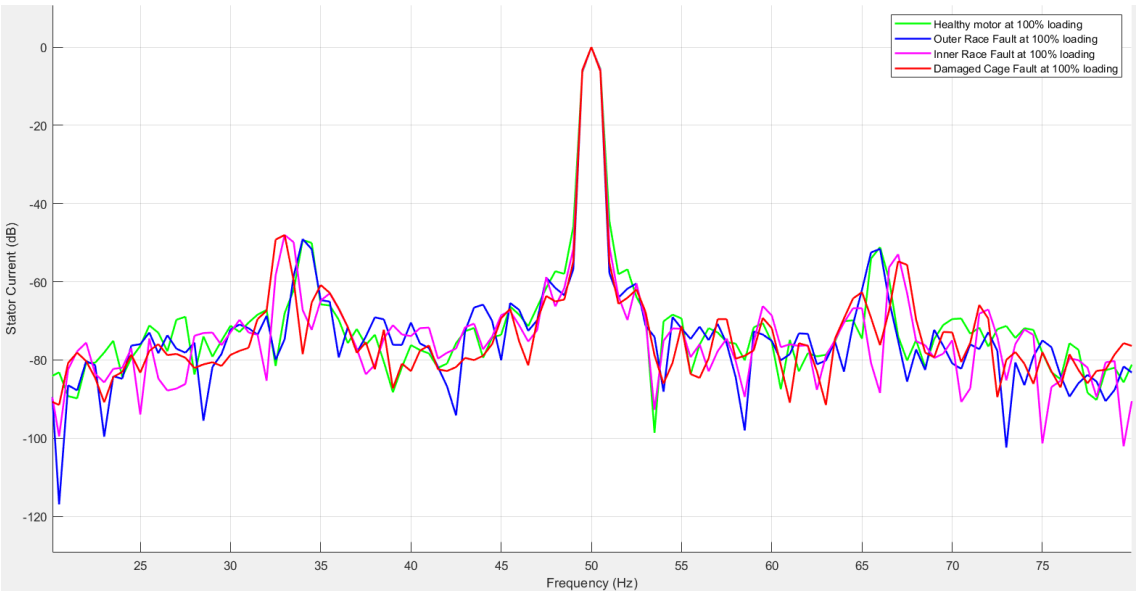

Figure 4.9: FFT Spectrum of Stator Current Signal at 100% Load

4.3 Stator Current Analysis of Bearing Faults under Various Loading Conditions

The rolling bearing fault belongs to mechanical faults that produce vibration resulting eccentricity and torque oscillation that influence stator current and distribution of the magnetic field. The effect on stator current due to various bearing fault such as outer race fault, inner race fault and damage bearing cage fault under different loading condition are shown in Figure 4.10, 4.11 and 4.12 as the current spectrum. It was observed that the side bands of current spectrum moved farther away from the fundamental component as

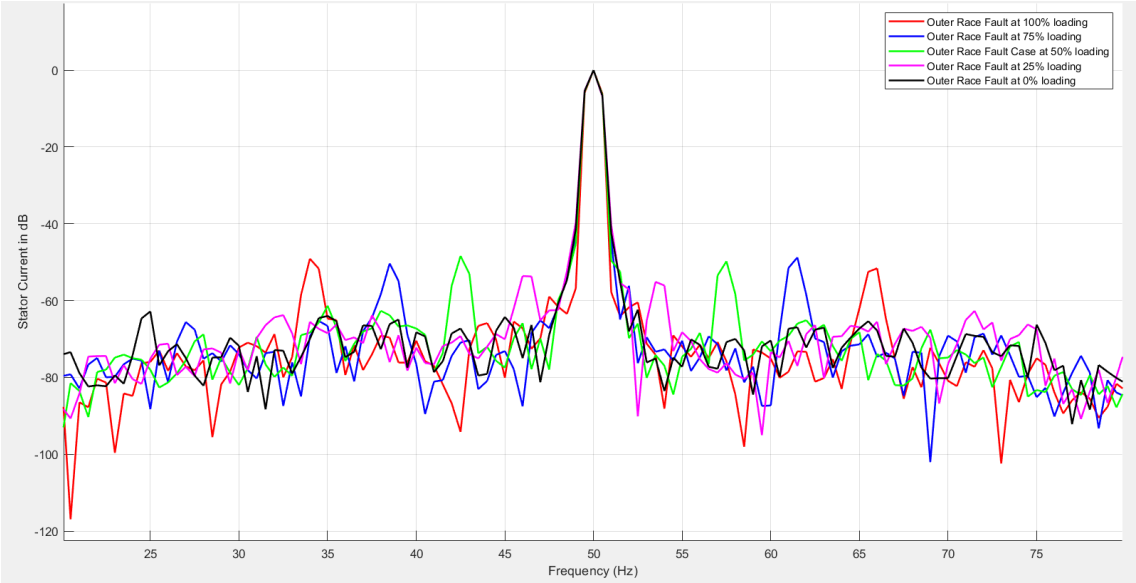

Figure 4.10: Stator Current in dB due to Outer Race Fault with loading Conditions

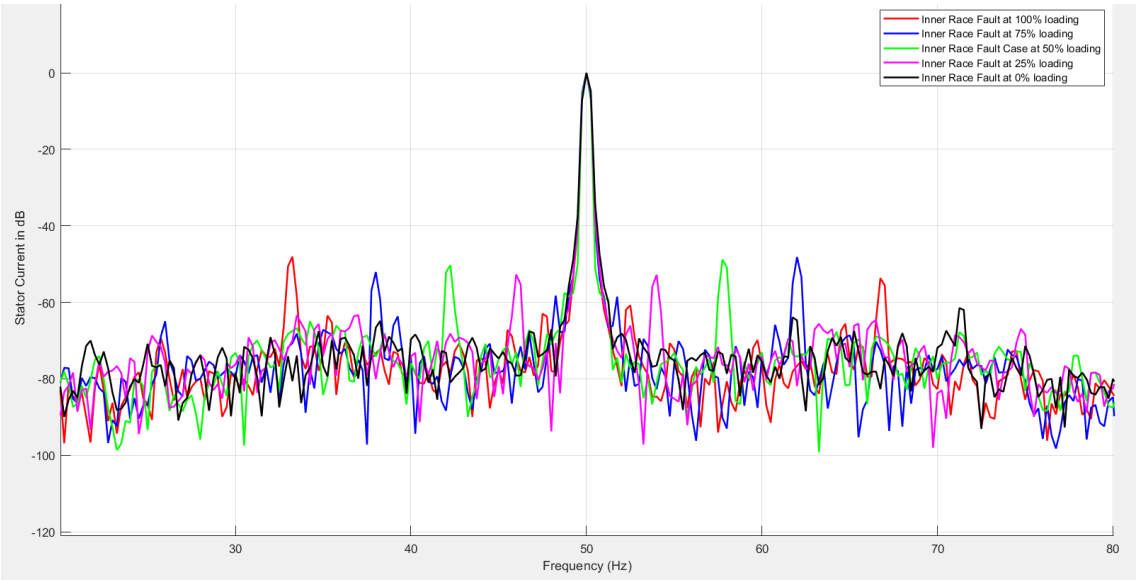

Figure 4.11: Stator Current in dB due to Inner Race Fault with loading Conditions

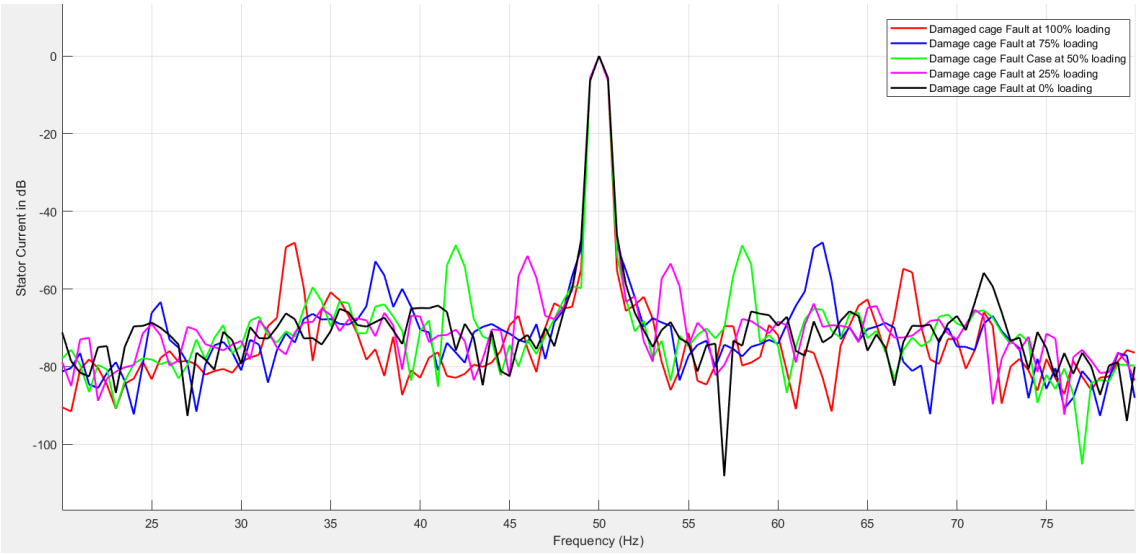

Figure 4.12: Stator Current in dB due to Damage Cage Bearing Fault with loading Conditions

the machine's loading increases and side bands are not visible under no load condition. This is because, according to equation 4.1, the machine's slip rises as the load increases, increasing the distance between the side band and the fundamental component.

$$f_{\text{sidebands}} = f_s(1 \pm 2ks) \tag{4.1}$$

By analysing these various observed side band frequencies, we can detect easily different types of rolling bearing fault under different loading condition using fast fourier transform with MCSA.

4.4 Fault Detection and Diagnosis using Machine Learning Models

The fault detection and diagnosis of the rolling bearing faults to output classes using machine learning models for all of machine states such as healthy motor, inner race fault, outer race fault and damage bearing cage fault. The total 35 number of input statistical feature and each feature having 10,600 data from all machine state each of all loading conditions. For training the each of machine learning model 75% of total dataset was used and remaining 25% data was used for blind validation of each of model to get normalized confusion matrix which is used to detect the rolling bearing fault of SCIM. After detection of the proper fault we can easily diagnose the bearing fault as the operator action.

4.4.1 Fault Detection using Support Vector Machine (SVM)

The SVM model validation output along with its performance metrics for rolling bearing fault diagnosis of SCIM was shown and explained below. The SVM used selected features from the complete input features as the top 5 higher permutation importance features values to train and test this model. The permutation importance calculated from all the extracted features is shown in Figure 4.13.

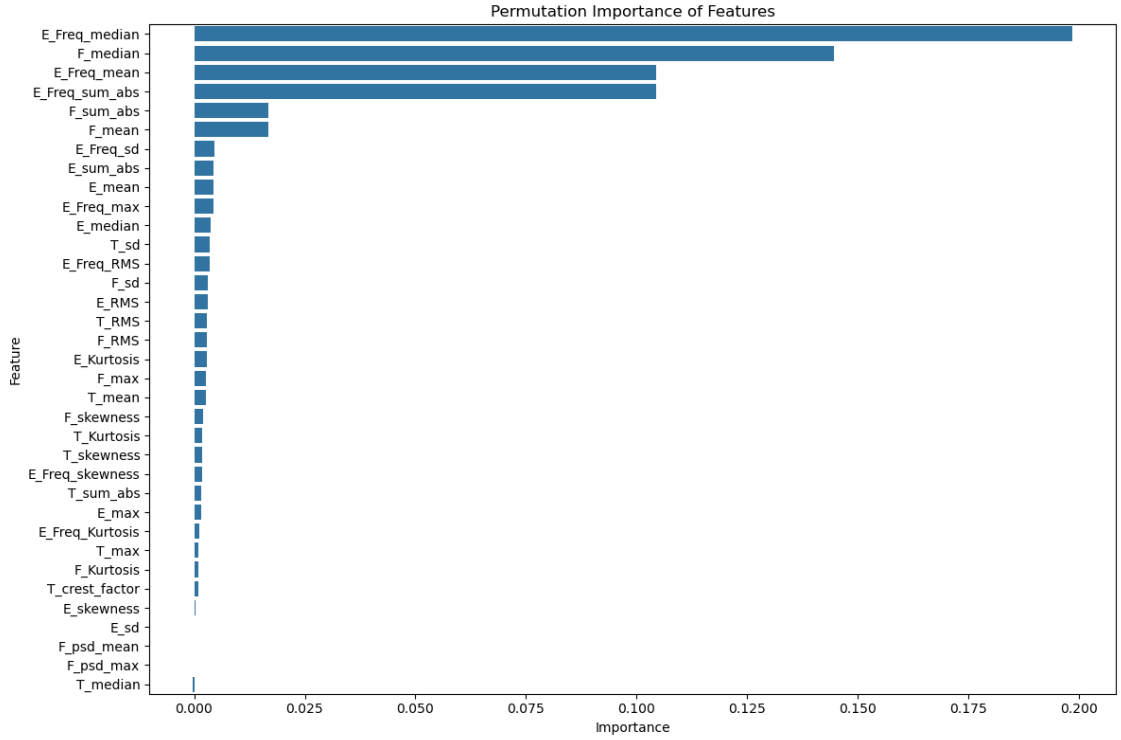

Figure 4.13: SVM with Permutation Importance Plot of Features

This scenario involved discarding the frequency domain mean power spectral density features, the frequency domain maximum power spectral density features and the envelope of the time domain of the standard deviation that had a permutation significance value of zero. The SVM model was trained and tested using the 32 features that had the maximum permutation relevance among the top five features. The remaining 32 features having the highest top 5 permutation importance features were selected to train and test the SVM model. The normalized confusion matrix obtained after blind validation of the SVM network was presented in Figure 4.14.

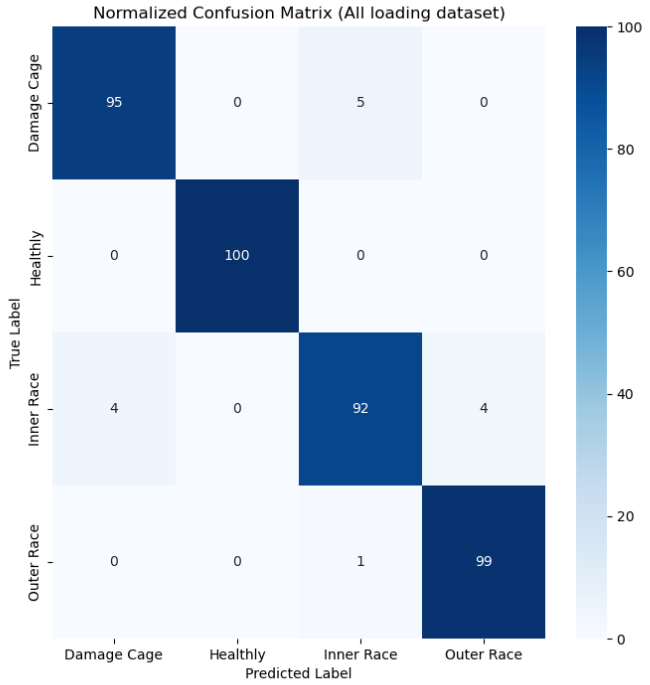

Figure 4.14: SVM with Normalized Confusion Matrix

The Table 4.1 shows various SVM performance metrics for rolling bearing diagnostics. The induction machine rolling bearing fault diagnosis using the SVM network had been performing strongly in classification performance on using the top 5 feature selected conditions. A SVM trained on selected input feature dataset achieved almost an accuracy of 96.5% proving the robustness in the detection of rolling bearing motor faults. The precision, recall and F1-score values remain high across all motor states particularly for the healthy and outer race fault conditions.

Table 4.1: Various SVM Performance Metrics

Optimum feature selection	**State**	**Precision**	**Recall**	**F1-score**	**Accuracy**
Top 5 higher permutation importance selected features	Damage Cage	0.96	0.95	0.95	0.965
	Healthy	1	1	1	
	Inner Race	0.94	0.92	0.93	
	Outer Race	0.96	0.99	0.97	

The top 5 selected feature for SVM model to detection of rolling bearing faults are shown in Table 4.2.

Table 4.2: Top 5 Selected Features for SVM

SVM Model: (Top five features name)	**Feature 1**	**Feature 2**	**Feature 3**
	Envelope of frequency domain signal whose median	Frequency domain signal whose median	Envelope of frequency domain signal whose mean
	Feature 4	**Feature 5**	
	Envelope of frequency domain absolute sum	Frequency domain absolute sum	

Figure 4.15 displays the Receiver Operating Characteristics (ROC) curve plotted for the SVM model. The ROC plot indicates that the SVM classifier was working amazingly well in rolling bearing fault diagnosis with the top 5 selected features having Area Under the Curves (AUCs) of 1.00 for Damage Cage, Healthy and Outer Race faults and 0.99 for Inner Race faults. This reflects near-perfect class separability and implies the goodness of the selected features in capturing fault-specific information. The marginal decrease of the Inner Race class can be a sign of minor overlap with the other classes but the general model shows great generalization and accuracy and demonstrates the SVM feasibility and robustness of feature selection in fault diagnosis.

4.4.2 Fault Detection using Gradient Boosting Machine (GBM)

The Gradient Boosting Machine model validation output along with its performance metrics for rolling bearing fault diagnosis of SCIM was shown and explained below. The GBM used selected features from the complete input features as the top 3 higher permutation importance features values to train and test this model. Figure 4.16 displays the permutation importance of every feature that was extracted.

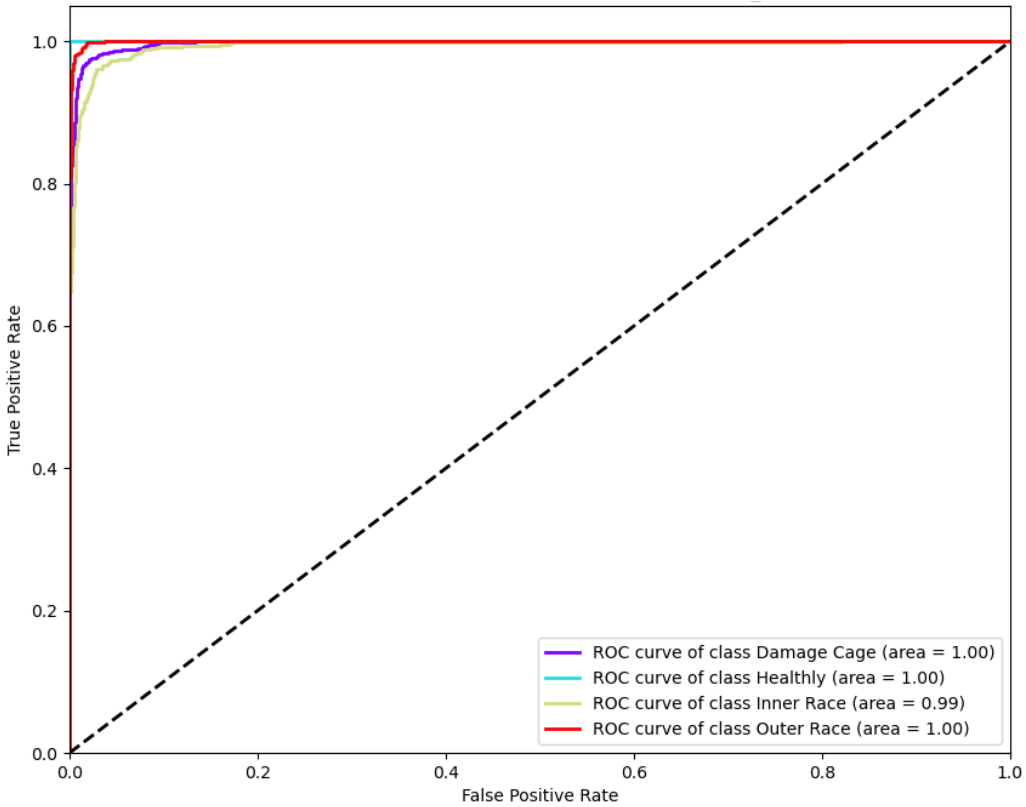

Figure 4.15: SVM Model ROC Curve Plotted Under Top 5 Feature Selected Condition

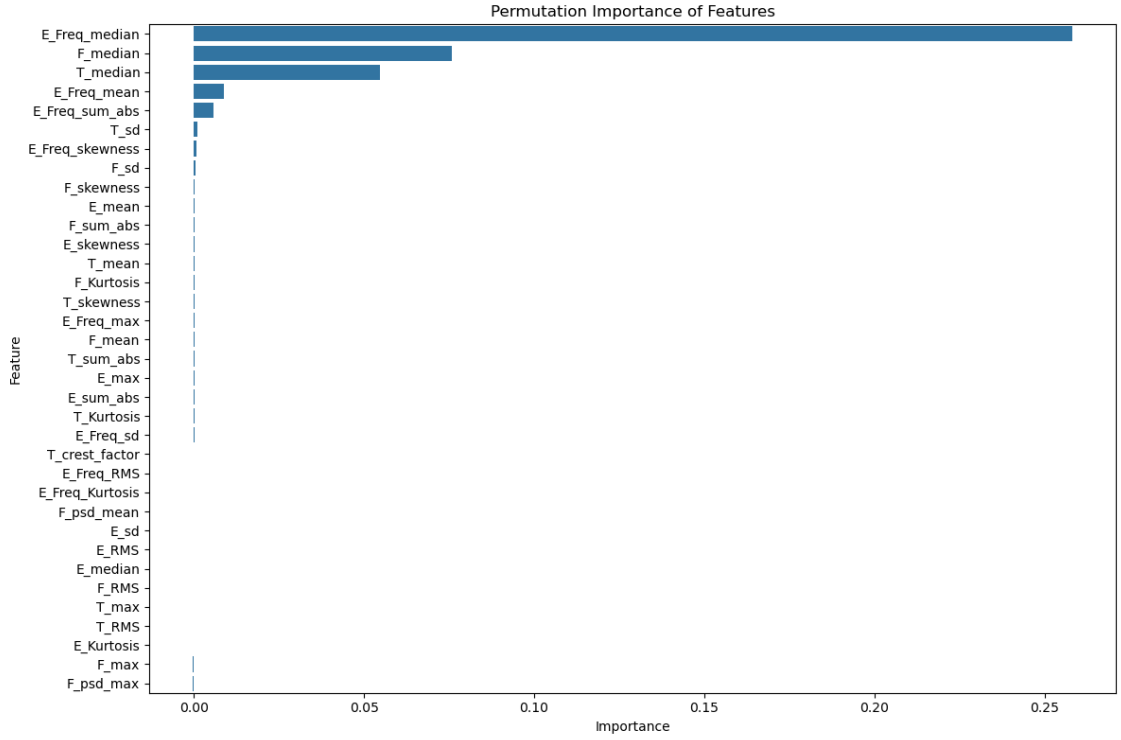

Figure 4.16: GBM with Permutation Importance Plot of Features

The following were excluded in this instance: the frequency domain mean power spectral density features, the frequency domain crest factor envelope, the frequency domain RMS value envelope, the frequency domain kurtosis value envelope, the frequency domain domain median value, frequency domain RMS value, time domain maximum value, time domain RMS value, and the envelope of the time domain kurtosis value with a permutation importance value of zero. To train and test the GBM model, the top three permutation significance features from the other 26 features were chosen. The normalized confusion matrix obtained after blind validation of the GBM network was presented in Figure 4.17

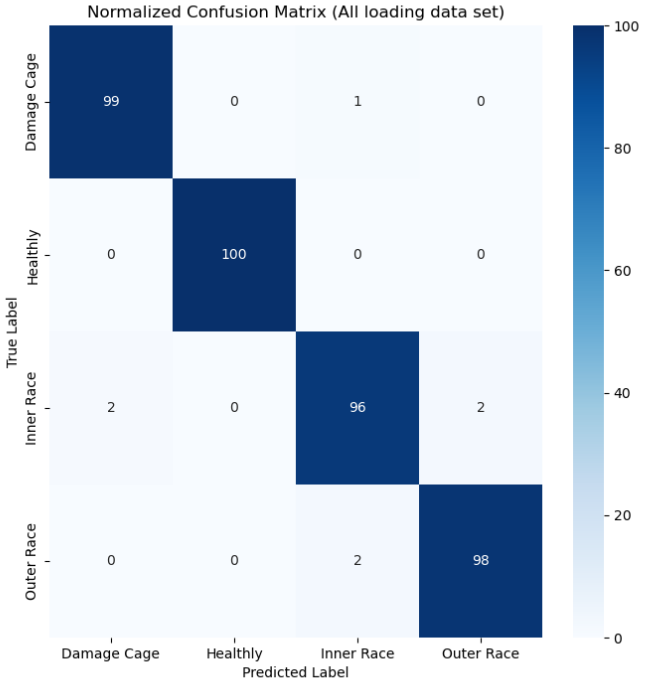

Figure 4.17: GBM with Normalized Confusion Matrix

The Table 4.3 shows various GBM performance metrics for the rolling bearing diagnostics.

Table 4.3: Various GBM Performance Metrics

Optimum feature selection	**State**	**Precision**	**Recall**	**F1-score**	**Accuracy**
Top 3 higher permutation importance selected features	Damage Cage	0.98	0.99	0.99	0.9825
	Healthy	1	1	1	
	Inner Race	0.97	0.96	0.97	
	Outer Race	0.98	0.98	0.98	

The induction machine rolling bearing fault diagnosis using the GBM network had been performing very strongly in classification performance on using the top 3 feature-selected conditions. With an accuracy of 98.25%, a GBM trained on the entire dataset demonstrated the reliability of rolling bearing motor problem detection. In both the healthy and damaged cage fault circumstances, the accuracy, recall and F1 Score values are consistently high throughout all motor states. The top 3 selected feature are shown in Table 4.4.

Table 4.4: Top Three Selected Features for GBM

GBM Model: (Top three features name)	**Feature 1**	**Feature 2**	**Feature 3**
	Envelope of frequency domain signal whose median	Frequency domain signal whose median	Time domain signal whose median

Figure 4.18 displays the Receiver Operating Characteristics (ROC) curve plotted using the GBM model. With the top three features having Area Under the Curves (AUCs) of 1.00 for all Damage Cage, Healthy, Outer Race faults and Inner Race faults, the ROC plot shows that the GBM classifier was doing very well in diagnosing rolling bearing defects. This reflects perfect class separability and implies the very goodness of the selected features in capturing fault-specific information. This indicates GBM has optomal performance even under top 3 selected features.

4.4.3 Fault Detection and Performance Comparison of the Machine Learning Approaches

Support Vector Machine (SVM), Random Forest Classifier (RF), Logistic Regression Classifier (LR) and Gradient Boosting Machine (GBM) performance comparison in rolling bearing fault diagnosis revealed significant variations in classification performance based on the best possible input feature selection. With an accuracy of 96.5%, an average precision of 0.965, a recall of 0.965 and an F1-score of 0.965, the SVM model that was trained utilizing only the top 5 higher permutation significance features demonstrated excellent classification resilience. With an average precision of 0.9775, recall of 0.9775 and F1-score of 0.975, the RF model that was trained utilizing only the top three higher permutation significance features demonstrated excellent classification resilience and reached an accuracy of almost 97%. Using an average precision of 0.98, recall of 0.98 and F1-score of 0.98, the LR model trained using the top 8 higher permutation significance features demonstrated greater classification resilience and about 98% accuracy.On the other hand,

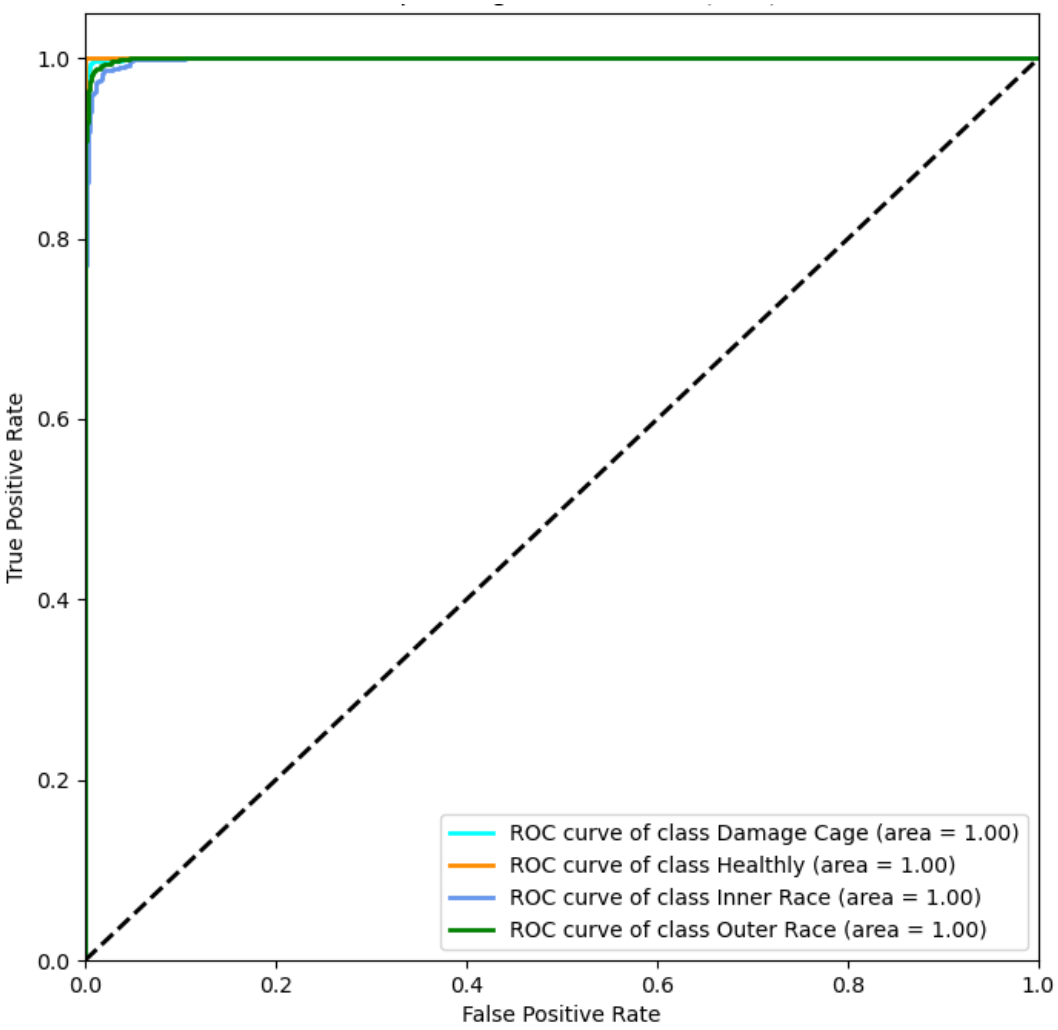

Figure 4.18: GBM Model ROC Curve Plotted Under Top 3 Feature Selected Condition

GBM with the fewest input features (the top three permutation significance) produced the best overall results, outperforming other models with an accuracy of 98.25% and an average precision, recall and F1-score of 0.985. Accordingly, GBM was the best model with the highest classification and the least amount of feature usage. With very few features and strong performance, RF came in second. GBM was the overall best model for fault diagnosis since it performs optimally with low computational complexity. Relative performance of all the machine learning models is shown in Table 4.5

4.4.4 Comparative Result for With and Without Feature Selection in the Machine Learning Models

Feature selection was found to be highly beneficial to rolling bearing fault diagnosis as it significantly reduced the training time by a great margin without a sacrifice in accuracy

Table 4.5: Comparative Performance of Different ML Approaches

Model	Features Used	Accuracy	Average Precision	Average Recall	Average F1-score
SVM	Top 5 selected features	96.5%	0.965	0.965	0.965
RF	Top 3 selected features	97%	0.9775	0.9775	0.975
LR	Top 8 selected features	98%	0.98	0.98	0.98
GBM	Top 3 selected features	98.25%	0.9825	0.9825	0.985

across all the machine learning models. Table 4.6 displayed the training time and model accuracy attained by each machine learning model. Table 4.6 shows that although there

Table 4.6: Comparative Result of MLs for With and without Feature Selection

	With feature selection		Without feature selection	
ML Models(F.S)	**Training Time (seconds)**	**Accuracy (%)**	**Training Time (seconds)**	**Accuracy (%)**
SVM (5)	0.19	96.5	12.20	99.25
RF (3)	1.57	97	397.63	99.99
LR (8)	0.07	98	133.52	99
GBM(3)	12.65	98.25	172.25	99.99

is no substantial difference in the accuracy of the machine learning model with and without feature selection, the computational cost varies greatly. Without feature selection, the training time across all models was extremely high while accuracy was just slightly improved. For instance, GBM model achieved accuracy at 98.5% with feature selection and 99.99% accuracy without feature selection yet the model's training time increased dramatically from 12.65 seconds to 172.25 seconds The same pattern follows for the other model. This means that using all features was not always improving model performance but rather adding complexity and computational expense. In addition, using all features was a risk for overfitting because the model can learn from irrelevant or duplicate information. Therefore, feature selection proved to be an effective approach for optimizing the model efficiency by reducing the training time dramatically without sacrificing competitive accuracy. The computer specification used to process all of the machine learning algorithms is shown in Table 4.7.

4.4.5 GBM Performance With and Without Addition of Gaussian Noise

In both the training and testing datasets of the GBM model, all loading datasets of damaged cage bearing faults were subjected to the medium category Gaussian noise with $\sigma = 0.1$ to 0.3 (moderate perturbations). Next, Table 4.8 displays the GBM model's comparative performance with and without noise.

Table 4.7: Computer Specification to Process Information

Component	Details
System Manufacturer	Acer
System Model	Nitro ANV15-51
BIOS	V1.14 (type: UEFI)
Processor	13th Gen Intel(R) Core(TM) i7-13620H (16 CPUs), 2.4GHz
Memory	16384MB RAM

Table 4.8: GBM Performance With and Without Addition of Noise to Damage Cage Fault Dataset

GBM Model	**Average Precision**	**Average Recall**	**Average F-1 Score**	**Acuracy**
With Noise	0.98	0.98	0.98	98%
Without Noise	0.9825	0.9825	0.985	98.25%

The model's average precision, recall, F1-score and accuracy were all 0.98 (98%) when noise was included. Performance was somewhat lower than that of the noise-free model, which had an average precision, recall, F1-score of 0.9825 and accuracy of 98.25%. Despite data perturbations, the model maintained high accuracy and showed good generalization to real-world settings, as seen by this tiny drop, which showed that it was very insensitive to mild noise.

CHAPTER FIVE: CONCLUSION

The study successfully examined the use of machine learning approaches for diagnosing rolling bearing faults in squirrel cage induction motors (SCIM). In order to attain the best fault detection accuracy, this study compared several machine learning models, such as Support Vector Machines (SVM), Random Forest (RF), Logistic Regression (LR) and Gradient Boosting Machine (GBM), using feature selection based on their permutation importance values.

The result indicated that the SVM model based on the top 5 selected features achieved an acuracy of a 96.5% indicating robust classification performance. The RF and LR models attained good performances with accuracies of 97% and 98% respectively. GBM model, however performed best in attaining the highest accuracy of 98.25% using only the top 3 selected features demonstrating its effectiveness in fault diagnosis with lower computational complexity.

The performance comparison with and without feature selection has confirmed that feature selection efficiently reduced training times without altering model accuracy. This affirmed that feature selection was necessary to improve model efficiency and prevent overfitting threats through eliminating redundant or irrelevant data.

In addition, the inclusion of moderate Gaussian noise (σ = 0.1 to 0.3) in the damaged bearing cage machine state data that the GBM model was highly robust with respect to noise and there was a slight or very few degradation of accuracy. The ability of the model to deliver high performance when operating under noisy environments makes it suitable for real-world applications where data imperfections reign supreme.

As a whole, GBM model stood out as the best among others for rolling bearing fault diagnosis by virtue of having good accuracy, robustness to noise and low computational expenditure. The study highlighted the importance of feature selection in machine learning based diagnostics and offered a valuable resource for induction machine failure identification and maintenance prediction.

REFERENCES

[1] J. A. Rosero, J. Cusido, A. Garcia, J. Ortega, and L. Romeral, "Broken bearings and eccentricity fault detection for a permanent magnet synchronous motor," in *IECON 2006 - 32nd Annual Conference on IEEE Industrial Electronics*, 2006, pp. 964–969.

[2] K. Kudelina, H. A. Raja, M. U. Naseer, S. Autsou, B. Asad, T. Vaimann, and A. Kallaste, "Study of bearing currents in induction machine: diagnostic possibilities, fault detection, and prediction," *Electrical Engineering*, pp. 1–14, 2024.

[3] K. Kudelina, T. Baraškova, V. Shirokova, T. Vaimann, and A. Rassõlkin, "Fault detecting accuracy of mechanical damages in rolling bearings," *Machines*, vol. 10, no. 2, p. 86, 2022.

[4] S. A. Alkadhim, "Three-phase induction motor: Types and structure," 07 2020.

[5] C.-C. Yeh, G. Y. Sizov, A. Sayed-Ahmed, N. A. O. Demerdash, R. J. Povinelli, E. E. Yaz, and D. M. Ionel, "A reconfigurable motor for experimental emulation of stator winding interturn and broken bar faults in polyphase induction machines," *IEEE Transactions on Energy Conversion*, vol. 23, no. 4, pp. 1005–1014, 2008.

[6] A. M. Alturas, "Electrical faults and their effects on induction machines," *Journal of Academic Research*, vol. 15, no. 1, pp. 36–46, 2020, retrieved from https://lam-journal.ly/index.php/jar/article/view/238. [Online]. Available: https://lam-journal.ly/index.php/jar/article/view/238

[7] S. Akbar, T. Vaimann, B. Asad, A. Kallaste, M. U. Sardar, and K. Kudelina, "State-of-the-art techniques for fault diagnosis in electrical machines: Advancements and future directions," *Energies*, vol. 16, no. 17, p. 6345, 2023.

[8] T. Point, "Types of faults in three phase induction motor," 2024. [Online]. Available: https://www.tutorialspoint.com/types-of-faults-in-three-phase-induction-motor

[9] K. N. Gyftakis, P. A. Panagiotou, and D. Spyrakis, "Detection of simultaneous mechanical faults in 6-kv pumping induction motors using combined mcsa and stray flux methods," *IET Electr. Power Appl.*, vol. 15, no. 3, pp. 524–531, Mar. 2021.

[10] K. Kudelina, B. Asad, T. Vaimann, A. Rassõlkin, A. Kallaste, and D. Lukichev, "Main faults and diagnostic possibilities of bldc motors," in *Proceedings of the*

2020 27th International Workshop on Electric Drives: MPEI Department of Electric Drives 90th Anniversary (IWED). Moscow, Russia: MPEI, January 2020.

[11] LFD Group, "Lfd product catalog," 2024, accessed: 2025-03-07. [Online]. Available: http://www.lfd-one.com/media/files/lfd-one-produktkatalog-en.pdf

[12] R. B. Randall and J. Antoni, "Rolling element bearing diagnostics—a tutorial," *Mechanical Systems and Signal Processing*, vol. 25, no. 2, pp. 485–520, 2011.

[13] K. Kudelina, T. Baraškova, V. Shirokova, T. Vaimann, and A. Rassõlkin, "Fault detecting accuracy of mechanical damages in rolling bearings," *Machines*, vol. 10, no. 2, p. 86, 2022.

[14] B. Asad, T. Vaimann, A. Belahcen, A. Kallaste, and A. Rassolkin, "Rotor fault diagnostic of inverter fed induction motor using frequency analysis," in *Proceedings of the 2019 IEEE 12th International Symposium on Diagnostics for Electrical Machines, Power Electronics and Drives (SDEMPED)*, 2019, pp. 127–133. [Online]. Available: https://ieeexplore.ieee.org/document/8864918

[15] A. Kallaste, A. Belahcen, A. Kilk, and T. Vaimann, "Analysis of the eccentricity in a low-speed slotless permanent-magnet wind generator," in *PQ 2012: 8th International Conference - Electric Power Quality and Supply Reliability, Conference Proceedings*, 2012, pp. 47–52. [Online]. Available: https://ieeexplore.ieee.org/document/6256199

[16] K. Kudelina, "Artificial intelligence driven approaches for fault prognostics of electrical machines using vibration spectrum analysis," Ph.D. dissertation, Tallinn University of Technology, 2024, supervised by Toomas Vaimann and Hadi Ashraf Raja. [Online]. Available: https://digikogu.taltech.ee/et/Item/229f1bbb-6178-414a-9e2e-2c98a30a783c

[17] M. Molęda, B. Małysiak-Mrozek, W. Ding, V. Sunderam, and D. Mrozek, "From corrective to predictive maintenance—a review of maintenance approaches for the power industry," *Sensors*, vol. 23, no. 13, p. 5970, 2023. [Online]. Available: https://www.mdpi.com/1424-8220/23/13/5970

[18] K. Kudelina, T. Vaimann, B. Asad, A. Rassõlkin, A. Kallaste, and G. Demidova, "Trends and challenges in intelligent condition monitoring of electrical machines using machine learning," *Applied Sciences*, vol. 11, no. 6, p. 2761, 2021.

[19] C. Liu, K. Chau, and X. Zhang, “An efficient wind-photovoltaic hybrid generation system using doubly excited permanent-magnet brushless machine,” *IEEE Transactions on Industrial Electronics*, vol. 57, no. 3, pp. 831–839, 2010. [Online]. Available: https://ieeexplore.ieee.org/document/5285433

[20] P. Bangalore and L. B. Tjernberg, “An artificial neural network approach for early fault detection of gearbox bearings,” *IEEE Transactions on Smart Grid*, vol. 6, no. 2, pp. 980–987, 2015.

[21] N. Bhole and S. Ghodke, “Motor current signature analysis for fault detection of induction machine–a review,” in *2021 4th Biennial International Conference on Nascent Technologies in Engineering (ICNTE)*, 2021, pp. 1–6.

[22] I. Tsoumas, E. Mitronikas, G. Georgoulas, and A. Safacas, “A comparative study of induction motor current signature analysis techniques for mechanical faults detection,” in *2005 5th IEEE International Symposium on Diagnostics for Electric Machines, Power Electronics and Drives*, 2005, pp. 1–6.

[23] F. J. Villalobos-Pina, J. A. Reyes-Malanche, E. Cabal-Yepez, and E. Ramirez-Velasco, “Electric fault diagnosis in induction machines using motor current signature analysis (mcsa),” in *Time Series Analysis*, J. Rocha, C. M. Viana, and S. Oliveira, Eds. Rijeka: IntechOpen, 2024, ch. 11. [Online]. Available: https://doi.org/10.5772/intechopen.1004002

[24] V. P. Raj, K. Natarajan, and S. T. Girikumar, “Induction motor fault detection and diagnosis by vibration analysis using mems accelerometer,” in *2013 International Conference on Emerging Trends in Communication, Control, Signal Processing and Computing Applications (C2SPCA)*, 2013, pp. 1–6.

[25] M. Tsypkin, “Induction motor condition monitoring: Vibration analysis technique — diagnosis of electromagnetic anomalies,” in *2017 IEEE AUTOTESTCON*, 2017, pp. 1–7.

[26] E. Irgat, E. Çinar, and A. Ünsal, “The detection of bearing faults for induction motors by using vibration signals and machine learning,” in *2021 IEEE 13th International Symposium on Diagnostics for Electrical Machines, Power Electronics and Drives (SDEMPED)*, vol. 1, 2021, pp. 447–453.

[27] G. Devarajan, M. Chinnusamy, and L. Kaliappan, “Detection and classification of mechanical faults of three phase induction motor via pixels analysis of thermal image and adaptive neuro-fuzzy inference system,” *Journal of Ambient Intelligence and Humanized Computing*, vol. 12, 05 2021.

[28] A. K. Bhagat and A. Chauhan, “Thermal image-based fault analysis of induction motors using a novel machine learning model,” in *2022 11th International Conference on System Modeling & Advancement in Research Trends (SMART)*, 2022, pp. 1429–1433.

[29] N. Rajapaksha, S. Jayasinghe, H. Enshaei, and N. Jayarathne, “Acoustic analysis based condition monitoring of induction motors: A review,” in *2021 IEEE Southern Power Electronics Conference (SPEC)*, 2021, pp. 1–10.

[30] S. Sathyan, U. Aydin, and A. Belahcen, “Acoustic noise computation of electrical motors using the boundary element method,” *Energies*, vol. 13, no. 1, 2020. [Online]. Available: https://www.mdpi.com/1996-1073/13/1/245

[31] P. K. N. and I. T.B., “Electromagnetic field analysis of 3-phase induction motor drive under broken rotor bar fault condition using fem,” in *2016 IEEE International Conference on Power Electronics, Drives and Energy Systems (PEDES)*, 2016, pp. 1–6.

[32] A. Choudhary, D. Goyal, and S. S. Letha, “Infrared thermography-based fault diagnosis of induction motor bearings using machine learning,” *IEEE Sensors Journal*, vol. 21, no. 2, pp. 1727–1734, 2021.

[33] I. Zamudio-Ramirez, J. M. Mendoza-Ortiz, R. A. Osomio-Ríos, and J. A. Antonino-Daviu, “Stray flux signal analysis for faults detection in induction motors during startup transient by means of statistical indicators,” in *2023 IEEE 14th International Symposium on Diagnostics for Electrical Machines, Power Electronics and Drives (SDEMPED)*, 2023, pp. 179–185.

[34] P. C. M. L. Filho, D. C. Santos, F. B. Batista, and L. M. R. Baccarini, “Axial stray flux sensor proposal for three-phase induction motor fault monitoring by means of orbital analysis,” *IEEE Sensors Journal*, vol. 20, no. 20, pp. 12 317–12 325, 2020.

[35] K. N. Gyftakis, P. A. Panagiotou, and S. B. Lee, “Generation of mechanical frequency related harmonics in the stray flux spectra of induction motors suffering from

rotor electrical faults," *IEEE Transactions on Industry Applications*, vol. 56, no. 5, pp. 4796–4803, Sep. 2020.

[36] P. A. Panagiotou, I. Arvanitakis, N. Lophitis, J. A. Antonino-Daviu, and K. N. Gyftakis, "On the broken rotor bar diagnosis using time–frequency analysis: 'is one spectral representation enough for the characterisation of monitored signals?'," *IET Electric Power Applications*, vol. 13, no. 7, pp. 932–942, Jul. 2019.

[37] S. Berhausen and T. Jarek, "Method of limiting shaft voltages in ac electric machines," *Energies*, vol. 14, p. 3326, 2021. [Online]. Available: https://doi.org/10.3390/en14063326

[38] M. Sar, S. Barella, A. Gruttadauria, D. Mombelli, and C. Mapelli, "Impact of warm rolling process parameters on crystallographic textures, microstructure and mechanical properties of low-carbon boron-bearing steels," *Metals*, vol. 8, p. 927, 2018. [Online]. Available: https://doi.org/10.3390/met8110927

[39] S. Raadnui and S. Kleesuwan, "Electrical pitting of grease-lubricated rolling and sliding bearings: A comparative study," *Journal of Physics: Conference Series*, vol. 364, p. 012041, 2012. [Online]. Available: https://doi.org/10.1088/1742-6596/364/1/012041

[40] T. Bishop, "Dealing with shaft and bearing currents," *EASA Technical Paper*, 2017, available online: http://www.kyservice.com (accessed on 10 September 2021).

[41] Y. Chen, S. Liang, W. Li, H. Liang, and C. Wang, "Faults and diagnosis methods of permanent magnet synchronous motors: A review," *Applied Sciences*, vol. 9, p. 2116, 2019. [Online]. Available: https://doi.org/10.3390/app9102116

[42] K. Kudelina, T. Vaimann, A. Rassõlkin, and A. Kallaste, "Impact of bearing faults on vibration level of bldc motor," in *IECON 2021 – 47th Annual Conference of the IEEE Industrial Electronics Society*, 2021, pp. 1–6.

[43] N. Bessous, R. Pusca, R. Romary, and S. Salim, "Rolling bearing failure detection in induction motors using stator current, vibration, and stray flux analysis techniques," *Journal of Electrical Engineering & Technology*, vol. 15, no. 6, pp. 2490–2502, 2020.

[44] A. Singhal and M. Khandekar, “Bearing fault detection in induction motor using motor current signature analysis,” vol. Vol. 2, pp. 3258–3264, 07 2013.

[45] J. Faiz and M. Ojaghi, “Unified winding function approach for dynamic simulation of different kinds of eccentricity faults in cage induction machines,” *Electric Power Applications, IET*, vol. 3, pp. 461 – 470, 10 2009.

[46] K. Wang, B. Gao, S. Shan, R. Wang, and X. Wang, “Research on rolling bearing fault diagnosis method based on eca-mranet,” *Applied Sciences*, vol. 14, no. 2, p. 551, 2024. [Online]. Available: https://doi.org/10.3390/app14020551

[47] e. a. Qiao, “Research on the rapid diagnostic method of rolling bearing faults using cloud-edge collaboration frameworks,” *PMC*, 2022. [Online]. Available: https://pmc.ncbi.nlm.nih.gov/articles/PMC9497659/

[48] K. Kudelina, H. A. Raja, V. Rjabtšikov, M. U. Naseer, T. Vaimann, and A. Kallaste, “Signal processing and machine learning techniques for predictive maintenance of rotor bars in induction machine,” in *2023 International Conference on Electrical Drives and Power Electronics (EDPE)*, 2023, pp. 1–7.

[49] K. Kudelina, H. A. Raja, M. U. Naseer, S. Autsou, B. Asad, T. Vaimann, and A. Kallaste, “Study of bearing currents in induction machine: diagnostic possibilities, fault detection, and prediction,” *Electrical Engineering*, vol. 106, no. 6, pp. 7089–7102, 2024.

APPENDIX A: FEATURE DEFINITIONS

Table A.1: Feature Definitions with Calculation Methods and Explanations

Feature Name	**Feature Calculation Method**	**Explanation**
Mean	$\frac{\sum_{n=0}^{N} x_n}{N}$	Sum of the elements divided by the number of elements.
Standard Deviation	$\sqrt{\frac{\sum_{n=0}^{N}(x_n-\bar{x})^2}{N}}$, where $\bar{x}$ is the mean.	Measures the spread of data distribution.
Median	$\begin{cases} x_{N/2}, & \text{if } N\text{:even;} \\ \frac{x_{(N-1)/2}+x_{(N+1)/2}}{2}, & \text{if } N\text{:odd.} \end{cases}$	The middle value of a sorted vector.
Kurtosis	$\frac{1}{N}\sum_{n=0}^{N}\frac{(x_n-\bar{x})^4}{\sigma^4}$, where σ is the standard deviation.	Measures the concentration of data values around the mean.
Root Mean Square (RMS)	$\sqrt{\frac{\sum_{n=0}^{N} x_n^2}{N}}$	Measures the square root of the mean of the squared values.
Skewness	$\frac{\sum_{n=0}^{N}(x_n-\bar{x})^3}{(N-1)\sigma^3}$, where σ is the standard deviation.	Shows the asymmetry degree of data compared to normal distribution.
Maximum Value	$\max(x_n)$	Identifies the maximum value of the signal.
Absolute Sum	$\sum_{n=0}^{N} \lvert x_n \rvert$	Sum of the absolute values of the signal, reflecting the total magnitude regardless of sign.
Time-Domain Crest Factor	$\frac{\max(x_n)}{\text{RMS}}$, where RMS is the root mean square of x.	Indicates the ratio of the peak value to the RMS value.
Frequency-Domain PSD Mean	$\frac{\sum_f P(f)}{M}$, where $P(f)$ is the Power Spectral Density at frequency f, and M is the total number of frequency bins.	Average power distribution across all frequencies.
Frequency-Domain PSD Maximum	$\max(P(f))$, where $P(f)$ is the Power Spectral Density at frequency f.	Identifies the maximum power spectral density value.

APPENDIX B: PUBLICATION

Paper Acceptance Notification from Editorial Team

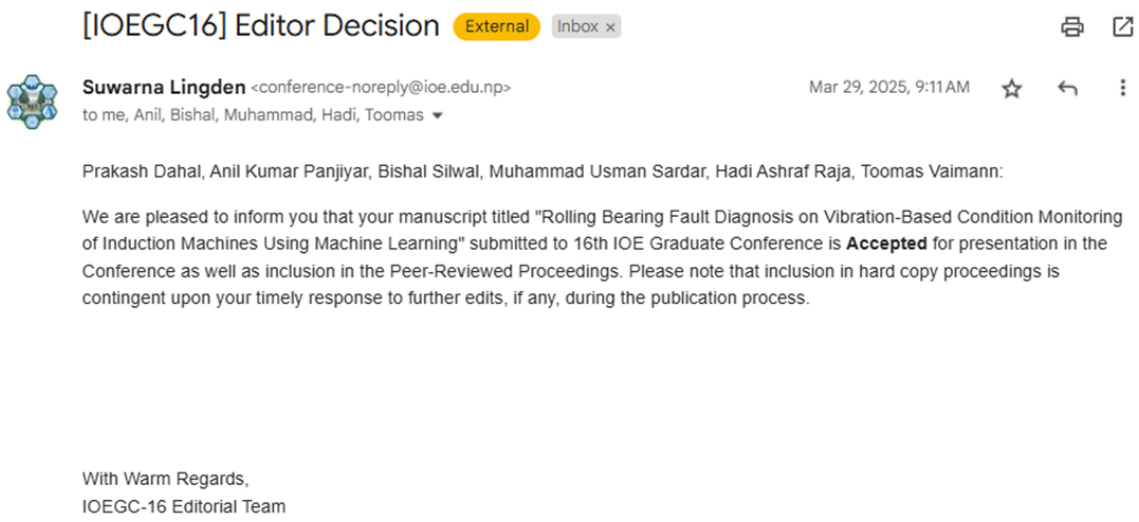

[IOEGC16] Editor Decision External Inbox ×

Suwarna Lingden <conference-noreply@ioe.edu.np> Mar 29, 2025, 9:11 AM

to me, Anil, Bishal, Muhammad, Hadi, Toomas

Prakash Dahal, Anil Kumar Panjiyar, Bishal Silwal, Muhammad Usman Sardar, Hadi Ashraf Raja, Toomas Vaimann:

We are pleased to inform you that your manuscript titled "Rolling Bearing Fault Diagnosis on Vibration-Based Condition Monitoring of Induction Machines Using Machine Learning" submitted to 16th IOE Graduate Conference is **Accepted** for presentation in the Conference as well as inclusion in the Peer-Reviewed Proceedings. Please note that inclusion in hard copy proceedings is contingent upon your timely response to further edits, if any, during the publication process.

With Warm Regards,
IOEGC-16 Editorial Team

Figure A.1: Paper Acceptance Notification from 16th IOE GC Editorial Team

Certification of Participation in 16th IOE Graduate Conference

IOE Graduate Conference

Certificate of Participation

THIS CERTIFICATE IS AWARDED TO

Prakash Dahal

in recognition of an invaluable contribution as

PAPER PRESENTER

at the 16th IOE Graduate Conference

Organized by Tribhuvan University, IOE, Thapathali Campus in association with IOE, Office of the Dean held from April 18-20, 2025 at Thapathali Campus, Kathmandu, Nepal.

Dr. Raj Kumar Chaulagain
Convener
16th IOE Graduate Conference

Dr. Khem Gyanwali
Campus Chief
Thapathali Campus

Prof. Dr. Sushil Bahadur Bajracharya
Dean
Institute of Engineering

Figure A.2: Certificate of Participation in 16th IOE GC Conference

Conference Paper: Proceedings of the 16th IOE Graduate Conference

IOE Graduate Conference
[Placeholder for Publication Information]

Rolling Bearing Fault Diagnosis on Vibration-Based Condition Monitoring of Induction Machines Using Machine Learning

Prakash Dahal [a], Anil Kumar Panjiyar [b], Bishal Silwal [c], Muhammad Usman Sardar [d], Hadi Ashraf Raja [e], Toomas Vaimann [f]

[a,b,c] *Department of Electrical Engineering, Pulchowk Campus, Institute of Engineering, Tribhuvan University, Nepal*
[d, e,f] *Department of Electrical Power Engineering and Mechatronics,Tallinn University of Technology, Tallinn, Estonia*
[a] 078mspse015.prakash@pcampus.edu.np , [b] anil.panjiyar@pcampus.edu.np, [c] bishal.silwal@pcampus.edu.np, [d] muhammad.sardar@taltech.ee, [e] hadi.raja@taltech.ee, [f] toomas.vaimann@taltech.ee

Abstract
Induction machines play a vital role in modern society due to their convenience, safety, reliability, efficiency, power density, and cost-effectiveness. If left undetected, a failure in the rolling bearings can lead to increased vibration, deterioration in machine performance, and eventual catastrophic failure. The most common technique for monitoring induction machine health is Motor Vibration Spectrum Analysis. This paper is dedicated to the investigation of fault detection and diagnosis for rolling bearing of a squirrel cage induction machine based on motor vibration signals at various loading conditions. In this paper, an MLP neural network has been applied to detect outer race, inner race, and cage damage faults. The diagnostic performance of the model is investigated through feature domain optimization and by neglecting the loading condition datasets. The current study extends the application of MVSA to enhance the reliability and efficiency of condition monitoring in induction machines using advanced machine learning techniques.

Keywords
Induction Machine, Bearing faults, Condition Monitoring, Multilayer Perceptron

1. Introduction

1.1 Background

Electrical machines and drive systems are essential in a variety of applications as they significantly boost the system's efficiency and productivity in both modern residential and industrial domains[1].Usually, they have the most important applications in areas such as power generation, manufacturing, and transportation. Their reliability and performance increase safety, simplify operations, and integrate critical processes. As modern society turns to renewable energy, the demand for cost-effective and high-performance electrical machines continues to rise rapidly. Induction motors, especially three-phase motors, are very popular due to their durability, low maintenance, and adaptability to different operating conditions[2]. In order to obtain optimal system performance, effective maintenance strategies are crucial. In traditional methods, the scheduled inspections often lead to resource inefficencies. Advances in predictive maintenance, leveraging condition monitoring and fault prediction that enable effective fault prediction, are transforming operational practices. Vibration analysis plays an important role as a tool for diagnosing, especially mechanical problems. Bearing failures account for approximately 50% of all failures and are a major concern [3]. This study integrates advanced signal processing techniques such as fast Fourier transform and Hilbert transform and machine learning algorithms as MLP to diagnose rolling bearing faults in squirrel cage induction motors.By incorporating real-time condition monitoring, this study aims to enhance overall system reliability, minimize downtime, and reduce maintenance costs [4].

1.2 Condition Monitoring

Induction motors play an important role in various industries, and generally, there are three types of machine maintenance: corrective, preventive, and predictive [5]. Corrective maintenance means a posteriori repairing of the equipment, which can be done at small workstations. Preventive maintenance

includes periodic inspections and servicing to prevent failure; however, it does not possess any prognostic capabilities and hence can result in inefficiency and increased cost. Nowadays, predictive maintenance is in great use by manufacturers, wherein condition monitoring is done to predict the failure of a component based on its operating data. It reduces costs due to shutdowns, reduces downtime, and optimizes resource allocation. Continuous monitoring of current, vibrations, temperature, and magnetic flux, among other parameters, ensures reliable operation [6].

1.3 Causes of rolling bearing faults

When there is an issue with a bearing's rolling elements, outer race, inner race, and cage defects are bound to occur in an induction machine [7]. Such issues are likely to occur on bearings placed on the non-drive end as well. Rolling bearing faults in induction machines are thought to fail by the combination of one or more factors, listed below [8, 9]:

- Mechanical damage is the result of design compromises made by the manufacturer, poor-quality machining processes, assembly errors, and contamination and corrosion in the bearings.
- Material fatigue is the outcome of repeatedly applying stress to a material, which causes subsurface cracks to form, microcracks to proliferate, and surfaces to wear out from inadequate lubrication.
- Because of the abrasive particles, ambient contamination causes corrosion and cam damage when moisture or dirt combines with the lubricant.
- Electrical discharges known as bearing currents generate surface fluting, frosting, pitting, and oxidation, all of which lead to lubrication degradation.

1.4 Bearing fault diagnosis using multilayer perceptron

In recent applications, MLP is widely used in the detection of bearing failures such as inner race, outer race, and cage damage. The MLP-based model processes the vibration signals, uses extracted relevant statistical features, and determines the type of failure using the parameters learned from the network[10].By training the model using a labeled dataset corresponding to various motor states such as healthy, outer race, inner race, and damaged cage and loading conditions such as 0%, 25%, 50%,75% and 100%. With MLP, data moves unidirectionally and without a feedback loop from the input layer to the output layer via intermediate hidden layers. Perceptrons in each layer process the input data by computing the weighted sum, then use the backpropagation technique to improve the weight vector. Bias is then introduced to make the model adaptive. An activation function that enables the network to learn nonlinear relationships determines the perceptron's output[11]. The Sigmoid activation functions are mainly used in the hidden units, which map inputs to [0,1], and the SoftMax function for output units, which converts input vectors into probabilities for multi-classes [12].

2. Methodology

This section describes how experiments are conducted, including the tools used and the steps taken. To classify and diagnose rolling bearing faults in induction machines, the first step is to collect data from laboratory experiments; the second step is to extract and select statistical features; and the last step is to construct models known as multilayer perceptrons of artificial neural networks.

2.1 Approach

The study begins with the literature review of fault diagnostics and condition monitoring techniques, followed by data collection at Tallinn University of Technology, Estonia. Feature extraction from vibration signals is made using DFT and Hilbert transform for statistical features. The permutation importance method is used for feature selection. Then selected features are used for training the multi-layer perceptron neural network to identify faults. The findings are concluded with the methodology summarized in Figure 1.

2.2 Experimental Setup

This paper examined bearing faults in induction machines using an experimental test bench with a testing machine, loading machine, accelerometer, and Dewetron DEWE2-M18 data acquisition system, as depicted in Figure 2. Data collection was performed

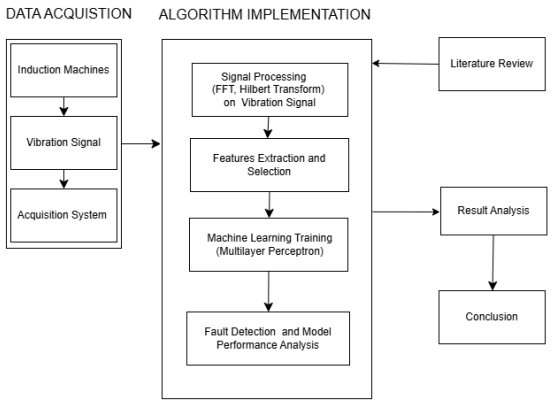

Figure 1: Diagnostic Approach

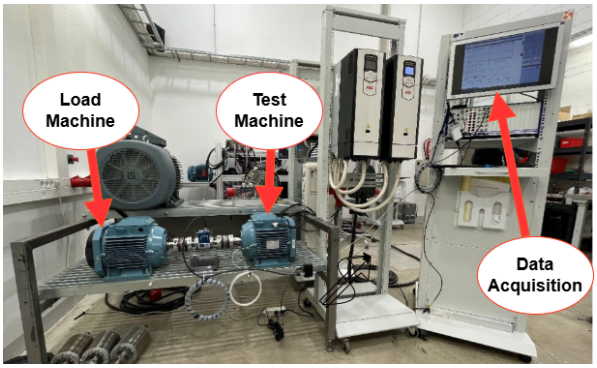

Figure 2: Experimental setup

under DTC and varying load conditions (0–100%), focusing on critical signal segments where fault effects were most pronounced. This approach allowed us to efficiently perform model training and pattern extraction on comprehensive datasets regarding healthy and faulty conditions. For early detection, vibration signals appeared more effective in the case of bearing faults. The vibration signals for both the healthy and faulty states were acquired from the experimental setup at Tallinn University of Technology, Estonia, with specifications of machines used in Table 1.

Table 1: Test Machine Specification

Parameters	Symbols/Units	Value
Number of poles	P	4
Number of Phases	Φ	3
Connection	Y / Δ	Δ
Voltage	V	400
Current	A	15.3
Power	kW	7.5
Speed	rpm	1460
Power factor	cos ϕ	0.79

2.3 Feature Enginnering

The analysis uses a Fast Fourier Transform, which will return the vibration signal in frequency domains from time. Mathematically, the FFT computes the Discrete Fourier Transform (DFT), where

$$X[k] = \sum_{n=0}^{N-1} x[n] e^{-j\frac{2\pi kn}{N}} \tag{1}$$

where $X[k]$ represents the frequency components, N is the number of samples, and k is the frequency index. In this paper, the Fast Fourier Transform (FFT) was used to transform the windowed signal into the frequency domain. The Hann window function was used to reduce spectral leakage. The Hann window is defined mathematically as:

$$w(n) = 0.5\left(1 - \cos\left(\frac{2\pi n}{N}\right)\right) \tag{2}$$

where $w(n)$ is the window function and N is the total number of samples. The Hilbert transform is used to obtain the envelope of a vibration signal either in time domain or in the frequency domain, which helps in extracting features like instantaneous amplitude and phase. The Hilbert transform of a signal $x(t)$ is defined as:

$$\hat{x}(t) = \mathscr{H}\{x(t)\} = \frac{1}{\pi}\mathscr{P}\int_{-\infty}^{\infty}\frac{x(\tau)}{t-\tau}d\tau \tag{3}$$

where $\mathscr{H}$ denotes the Hilbert transform and $\mathscr{P}$ indicates the Cauchy principal value of the integral. The envelope of the signal is then calculated as the instantaneous amplitude:

$$A(t) = \sqrt{x(t)^2 + \hat{x}(t)^2} \tag{4}$$

The feature extraction employed in this research uses a sliding window on the vibration signals of a total duration of 60 seconds. It was performed using a window length of 4 seconds and therefore yielded 80,000 data points in all. It is shifted by 2,000 data points, and hence, the number of data points from 54 seconds onward corresponds to 541 data points from each machine state, uniform at 530 windows for consistency and standardization.

Feature extraction used a sliding window approach with FFT (Hann window) and Hilbert transform. Time-domain features included mean, standard deviation, median, kurtosis, RMS, skewness, maximum value, sum of absolute values, and crest factor. Frequency-domain features included mean,

standard deviation, median, kurtosis, RMS, skewness, maximum value, sum of absolute values, mean power spectral density, and maximum power spectral density. Envelope-based features in both domains included mean, standard deviation, median, kurtosis, RMS, skewness, maximum value, sum of absolute values, mean frequency, frequency standard deviation, frequency median, frequency kurtosis, frequency RMS, frequency skewness, frequency maximum, and sum of absolute frequency components. All 35 features were extracted from 530 windows across different motor states and load levels. In the feature selection process, the permutation importance of all features is calculated, and features with non-zero permutation importance are selected.

2.4 Multilayer Perceptron Architecture

In this work, an MLP model architecture is shown in the following Figure 3. It consists of four hidden

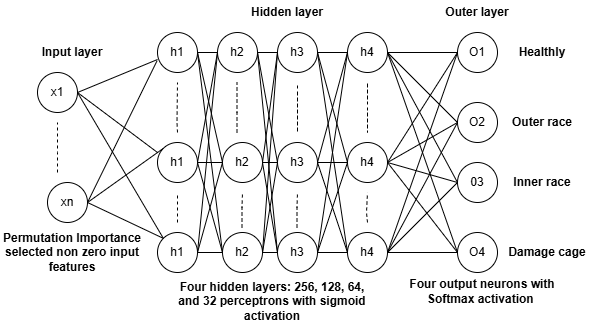

Figure 3: Multilayer Perceptron Architecture

layers and was implemented using TensorFlow and Keras. Extracted statistical features were classified with respect to fault type and load conditions. Feature selection was done using permutation importance, considering only those features whose importance was non-zero for better performance. In order to avoid overfitting, the architecture of the model included four hidden layers of 256, 128, 64, and 32 perceptron's, respectively, with a sigmoid activation function, L2 regularization, batch normalization, and a dropout rate of 50%. The network was trained by minimizing the sparse categorical cross-entropy loss with the Adam optimizer. Early stopping was adopted to prevent overtraining. Correspondingly, the output layer used softmax activation and produced four output neurons for different fault types. The evaluation findings included the normalized confusion matrix, permutation importance graphs, and classification reports that all proved the model efficiently diagnoses the faults with the optimum feature set.

3. Results and Discussion

The MLP network uses the entire dataset with features selected based on non-zero permutation importance. The normalized confusion matrix, obtained after blindly validating the MLP network, is shown in Figure 4.

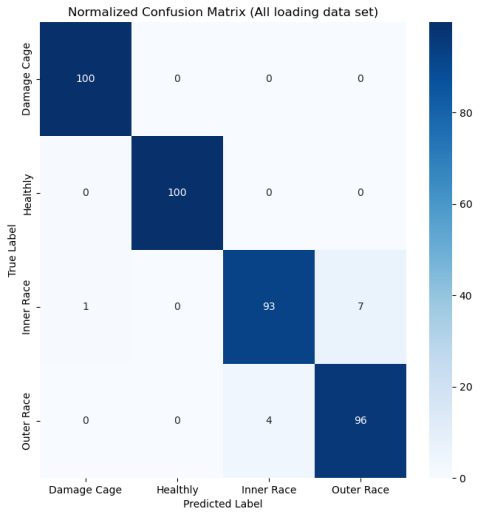

Figure 4: Normalized Confusion Matrix with all loading dataset

In this case, the permutation importance of all of the extracted features is shown in Figure 5.

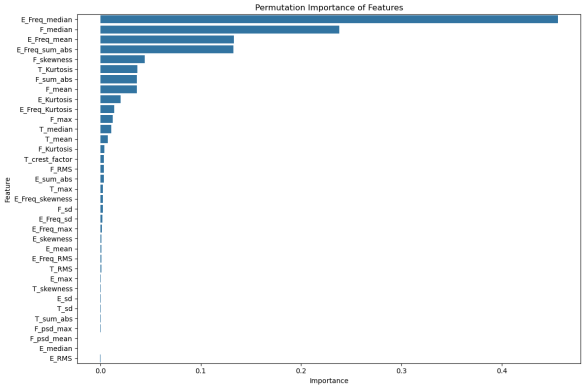

Figure 5: Permutation importance plot of features with considering all loading dataset

In this case, the envelope of the time domain, whose median and the mean of the frequency domain power

spectral density features have a permutation importance value of zero, are discarded. The remaining 33 features, which have a non-zero permutation importance value, are selected for training and testing the MLP model. The classification report of this MLP model is shown in following Table 2.

Table 2: Classification Report of MLP with all loading dataset

Motor States	Precision	Recall	F1-score	Support
Damage Cage	0.99	1.00	0.99	660
Healthy	1.00	1.00	1.00	660
Inner Race	0.96	0.93	0.94	660
Outer Race	0.93	0.96	0.95	660
Accuracy		**0.97**		2640

When the data corresponding to 100% loading for each motor state is discarded, the remaining data, corresponding to lower loading conditions, is used to train and test the multi-layer perceptron (MLP) model. This will have the model trained on a reduced yet representative dataset, helping to assess its performance under varied loading conditions. After discarding data representing 100% loading, the permutation importance of the remaining features is recalculated. In this case, permutation importance refers to the contribution each feature makes to the predictive accuracy of the model as it observes changes in model performance while feature values are shuffled. The features that did not have zero permutation importance were retained since they are important in the diagnosis of motor faults, while features with negligible importance are discarded. This feature selection enhances the model's efficiency to give better predictions with the most relevant attributes on which complex fault diagnosis tasks can be performed. The normalized confusion matrix obtained with this model is depicted in Figure 6.

In this case, the permutation importance of all of the extracted features is shown in Figure 7.

In this case, the envelope of the time domain, whose median, standard deviation, and maximum value features have a permutation importance value of zero, is discarded. The remaining 32 features, which have a non-zero permutation importance value, are selected for training and testing the MLP model. This feature selection process helps reduce dimensionality while retaining relevant information for the model. As a result, the MLP model is expected to achieve better

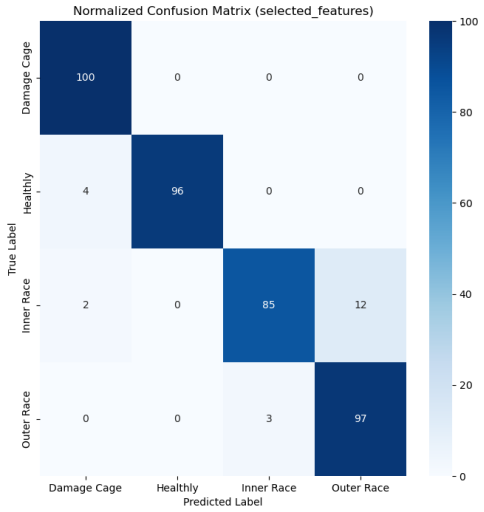

Figure 6: Normalized confusion matrix of MLP with discarded 100% loading dataset

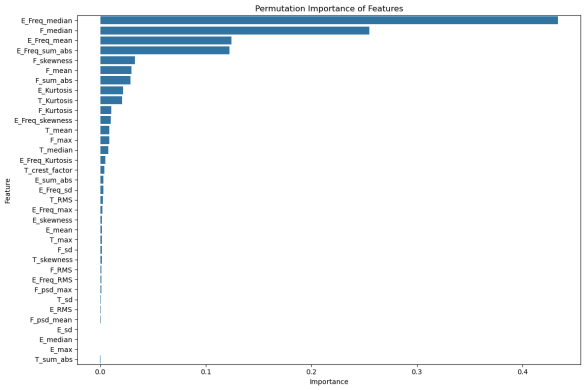

Figure 7: Permutation importance plot of features with discarded 100% loading dataset

generalization and improved predictive accuracy. The classification report of this MLP model is shown in following Table 3.

Table 3: Classification Report of MLP with discarded 100% loading dataset

Motor States	Precision	Recall	F1-score	Support
Damage Cage	0.94	1.00	0.97	528
Healthy	1.00	0.96	0.98	528
Inner Race	0.97	0.85	0.91	528
Outer Race	0.89	0.97	0.93	528
Accuracy		**0.95**		2112

If the data corresponding to 75% loading of each motor state is discarded, the remaining dataset is used to train and test the MLP model. The permutation

importance of all features is recalculated, and features with a non-zero importance value are selected. This refined feature set ensures that only the most relevant variables contribute to the model's performance, potentially improving its accuracy and generalization. By focusing on significant features, the model can reduce the impact of irrelevant or redundant data, enhancing computational efficiency. Additionally, this approach helps in mitigating the risk of overfitting, leading to more robust and reliable predictions. The normalized confusion matrix obtained for this model is shown in Figure 8.

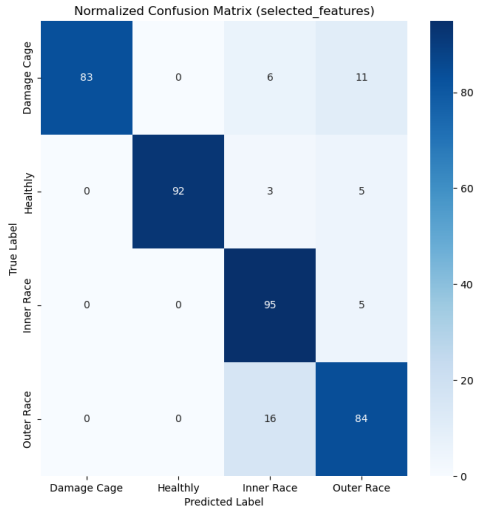

Figure 8: Normalized confusion matrix of MLP with discarded 75% loading dataset

In this case, the permutation importance of all of the extracted features are shown in figure 9.

In this case, the time domain, whose absolute sum feature has a permutation importance value of zero, is discarded. The remaining 34 features, which have a non-zero permutation importance value, are selected for training and testing the MLP model. This selection ensures that only the most relevant features contribute to the learning process, improving the model's efficiency. By eliminating less significant features, the model complexity is reduced, potentially leading to better generalization and performance. The classification report of this MLP model is shown in following Table 4.

The following Table 5 shows a comparative study of MLP performance in all cases of loading conditions. The induction machine rolling bearing fault diagnosis

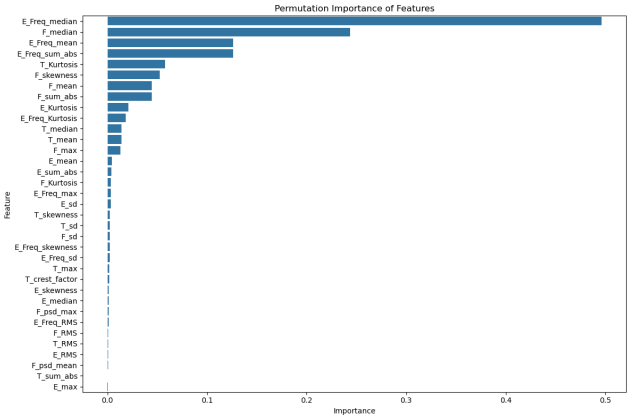

Figure 9: Permutation importance plot of features with discarded 75% loading dataset

Table 4: Classification Report of MLP with discarded 75% loading dataset

Motor States	Precision	Recall	F1-score	Support
Damage Cage	1.00	0.83	0.91	528
Healthy	1.00	0.92	0.96	528
Inner Race	0.79	0.95	0.86	528
Outer Race	0.80	0.84	0.82	528
Accuracy		**0.89**		2112

Table 5: Comparative study of MLP performance in all cases of loading conditions

Dataset Condition	Motor State	Precision	Recall	F1-score	Accuracy
With all Loading Dataset	Damage Cage	0.99	1	0.99	**0.97**
With all Loading Dataset	Healthy	1	1	1	**0.97**
With all Loading Dataset	Inner Race	0.96	0.93	0.94	**0.97**
With all Loading Dataset	Outer Race	0.93	0.96	0.95	**0.97**
Discarding 100% Loading	Damage Cage	0.94	1	0.97	**0.95**
Discarding 100% Loading	Healthy	1	0.96	0.98	**0.95**
Discarding 100% Loading	Inner Race	0.97	0.85	0.91	**0.95**
Discarding 100% Loading	Outer Race	0.89	0.97	0.93	**0.95**
Discarding 75% Loading	Damage Cage	1	0.83	0.91	**0.89**
Discarding 75% Loading	Healthy	1	0.92	0.96	**0.89**
Discarding 75% Loading	Inner Race	0.79	0.95	0.86	**0.89**
Discarding 75% Loading	Outer Race	0.8	0.84	0.82	**0.89**

using the MLP network has been performing very strongly in classification performance on different datasets with varied loading conditions. An MLP trained on the full dataset achieves an accuracy of 97%, proving the robustness in the detection of motor faults. The precision and recall values remain high across all motor states, particularly for the healthy and cage damage conditions. The model has a slight reduction in accuracy to 95% while discarding 100% of the loading data, which may indicate that removing full-load operational data further impairs the model's capability for delineation of subtle fault signatures. The further reduction of the dataset by discarding 75% resulted in a greater drop in accuracy to 89%, reflecting that loading conditions have a high impact

on the feature representation of faults, which makes the distinction between some fault types harder for the MLP.

These results point out the importance of including all varied load conditions while training a machine learning model on fault diagnosis. The removal of high-load data introduces slight misclassifications in inner and outer race faults. However, high classification scores using MLP despite the significantly reduced data volume prove the reliability in the detection of faults under variation of conditions.

4. Conclusion

The results obtained from this study demonstrated that the MLP network was effective in diagnosing rolling bearing problems in induction motors running under various loading conditions. It classified the motor states very precisely with a high recall ratio for all the states. 100% and 75% of the data from loading is removed, yet the model generalizes satisfactorily with just a slight loss in accuracy. Permutation-based feature importance using the permutation technique helps in selecting appropriate features for the MLP model. This further strengthens the robustness in the fault diagnosis system.This will require further research for its applicability to industrial needs and to carry out further optimizations with larger datasets. The study shows that with improved dependability, machine learning-based approaches are of utmost potential in recognizing fault identification and classification so as to reduce maintenance costs.

5. Future Work

Future work can be done with the comparative study of fault detection and prediction models. The comparison between machine learning-based and other traditional methods could provide a selection of suitable techniques for particular applications. Neuro-fuzzy logic algorithm and further development of its web-based application would make this technology more friendly to users while training. Incorporation of real industrial environment complex scenarios for detection and prediction of faults in real time is quite essential for proper implementation.

Acknowledgments

This work was supported by the Department of Electrical Power Engineering and Mechatronics at Tallinn University of Technology, Tallinn, Estonia, under the project "Capacity Enhancement of Electrical Equipment Condition Monitoring and Fault Diagnostics" (CEEECoM).

References

[1] Bin Gou, Yan Xu, Yang Xia, Gary Wilson, and Shuyong Liu. An intelligent time-adaptive data-driven method for sensor fault diagnosis in induction motor drive system. *IEEE Transactions on Industrial Electronics*, 66(12):9817–9827, 2019.

[2] Bilal Asad, Toomas Vaimann, Anton Rassõlkin, Ants Kallaste, and Anouar Belahcen. A survey of broken rotor bar fault diagnostic methods of induction motor. *Electrical, Control and Communication Engineering*, 14:117–124, 12 2018.

[3] J. A. Rosero, J. Cusido, A. Garcia, J.A. Ortega, and L. Romeral. Broken bearings and eccentricity fault detection for a permanent magnet synchronous motor. In *IECON 2006 - 32nd Annual Conference on IEEE Industrial Electronics*, pages 964–969, 2006.

[4] Karolina Kudelina, Bilal Asad, Toomas Vaimann, Anton Rassõlkin, Ants Kallaste, and Dmitri V. Lukichev. Main faults and diagnostic possibilities of bldc motors. In *2020 27th International Workshop on Electric Drives: MPEI Department of Electric Drives 90th Anniversary (IWED)*, pages 1–6, 2020.

[5] M. Molęda, B. Małysiak-Mrozek, W. Ding, V. Sunderam, and D. Mrozek. From corrective to predictive maintenance—a review of maintenance approaches for the power industry. *Sensors*, 23(13), 2023.

[6] Karolina Kudelina, Toomas Vaimann, Bilal Asad, Anton Rassõlkin, Ants Kallaste, and Galina Demidova. Trends and challenges in intelligent condition monitoring of electrical machines using machine learning. *Applied Sciences*, 11(6):2761, 2021.

[7] J. L. H. Silva and A. J. M. Cardoso. Bearing failures diagnosis in three-phase induction motors by extended park's vector approach. In *31st Annual Conference of IEEE Industrial Electronics Society*, pages 2591–2596, 2005.

[8] K. Kudelina, B. Asad, T. Vaimann, A. Rassõlkin, and A. Kallaste. Bearing fault analysis of bldc motor intended for electric scooter application. In *2021 IEEE 13th International Symposium on Diagnostics for Electrical Machines, Power Electronics and Drives (SDEMPED)*, volume 1, pages 427–432, 2021.

[9] K. Kudelina, T. Vaimann, A. Kallaste, B. Asad, and G. Demidova. Induction motor bearing currents—causes and damages. In *Proceedings of the 2021 28th International Workshop on Electric Drives: Improving Reliability of Electric Drives (IWED)*, Moscow, Russia.

[10] Hadi Ashraf Raja, Karolina Kudelina, Bilal Asad, Toomas Vaimann, Ants Kallaste, Anton Rassõlkin, and Huynh Van Khang. Signal spectrum-based machine learning approach for fault prediction and maintenance of electrical machines. *Journal of Electrical Engineering and Technology*, 2024.

[11] Ian Goodfellow, Yoshua Bengio, and Aaron Courville. *Deep Learning*. MIT Press, 2016. Online. Available: https://www.deeplearningbook.org/.

[12] Michael A. Nielsen. *Neural Networks and Deep Learning*. Determination Press, 2015.

APPENDIX D: PLAGIARISM TEST REPORT

Prakash Dahal

Rolling Bearing Fault Diagnosis on Vibration-Based Condition Monitoring of Induction Machines Using

Tribhuvan University

Document Details

Submission ID
trn:oid:::3117:450646053

Submission Date
Apr 20, 2025, 8:40 AM GMT+5:45

Download Date
Apr 20, 2025, 8:43 AM GMT+5:45

File Name
Prakash_Thesis_Plag_Final_Check.pdf

File Size
9.1 MB

67 Pages

16,659 Words

91,062 Characters

13% Overall Similarity

The combined total of all matches, including overlapping sources, for each database.

Filtered from the Report

- Bibliography

Match Groups

185 Not Cited or Quoted 11%
Matches with neither in-text citation nor quotation marks

33 Missing Quotations 2%
Matches that are still very similar to source material

0 Missing Citation 0%
Matches that have quotation marks, but no in-text citation

2 Cited and Quoted 0%
Matches with in-text citation present, but no quotation marks

Top Sources

9% Internet sources
11% Publications
0% Submitted works (Student Papers)

Integrity Flags

1 Integrity Flag for Review

Replaced Characters
9 suspect characters on 4 pages
Letters are swapped with similar characters from another alphabet.

Our system's algorithms look deeply at a document for any inconsistencies that would set it apart from a normal submission. If we notice something strange, we flag it for you to review.

A Flag is not necessarily an indicator of a problem. However, we'd recommend you focus your attention there for further review.

Match Groups

- **185** Not Cited or Quoted 11%
  Matches with neither in-text citation nor quotation marks
- **33** Missing Quotations 2%
  Matches that are still very similar to source material
- **0** Missing Citation 0%
  Matches that have quotation marks, but no in-text citation
- **2** Cited and Quoted 0%
  Matches with in-text citation present, but no quotation marks

Top Sources

9% Internet sources
11% Publications
0% Submitted works (Student Papers)

Top Sources

The sources with the highest number of matches within the submission. Overlapping sources will not be displayed.

1	Internet	mdpi-res.com <1%
2	Internet	www.mdpi.com <1%
3	Publication	Ruqiang Yan, Jing Lin. "Equipment Intelligent Operation and Maintenance", CRC P... <1%
4	Publication	Subrata Karmakar, Surajit Chattopadhyay, Madhuchhanda Mitra, Samarjit Sengu... <1%
5	Internet	www.science.gov <1%
6	Publication	R. N. V. Jagan Mohan, B. H. V. S. Rama Krishnam Raju, V. Chandra Sekhar, T. V. K. P... <1%
7	Internet	core.ac.uk <1%
8	Internet	aaltodoc.aalto.fi <1%
9	Internet	www.researchgate.net <1%
10	Internet	accentsjournals.org <1%

11 Internet
conference.ioe.edu.np <1%

12 Internet
link.springer.com <1%

13 Publication
Slobodan N. Vukosavic. "Electrical Machines", Springer Science and Business Medi... <1%

14 Internet
www2.mdpi.com <1%

15 Publication
Dinesh Goyal, Bhanu Pratap, Sandeep Gupta, Saurabh Raj, Rekha Rani Agrawal, I... <1%

16 Internet
pdffox.com <1%

17 Publication
Mohamed A. El-Sharkawi. "Electric Energy - An Introduction", CRC Press, 2019 <1%

18 Internet
dokumen.pub <1%

19 Publication
Karolina Kudelina, Tatjana Baraškova, Veroonika Shirokova, Toomas Vaimann, An... <1%

20 Publication
"Proceedings of Data Analytics and Management", Springer Science and Business... <1%

21 Publication
"Intelligent Communication, Control and Devices", Springer Science and Business... <1%

22 Publication
"Proceedings of the 4th International Conference on Electrical Engineering and C... <1%

23 Internet
eprints-phd.biblio.unitn.it <1%

24 Internet
arxiv.org <1%

25 Internet
ijarsct.co.in <1%

26 Internet
research.aalto.fi <1%

27 Internet
open.uct.ac.za <1%

28 Internet
pubmed.ncbi.nlm.nih.gov <1%

29 Internet
etheses.whiterose.ac.uk <1%

30 Internet
file.scirp.org <1%

31 Internet
livrepository.liverpool.ac.uk <1%

32 Internet
www.giiresearch.com <1%

33 Publication
Bashir Mahdi Ebrahimi, Jawad Faiz. "Feature Extraction for Short-Circuit Fault Det... <1%

34 Publication
Israel Zamudio-Ramirez, Roque A. Osornio-Rios, Jose A. Antonino-Daviu, Jonathan... <1%

35 Publication
Jarosław Duda, Jacek Leśkow, Paweł Pawlik, Witold Cioch. "CMAFI — Copula-base... <1%

36 Publication
Paulo C. M. Lamim Filho, Deivity C. Santos, Fabiano B. Batista, Lane M. R. Baccarin... <1%

37 Internet
assets-eu.researchsquare.com <1%

38 Internet
community.intel.com <1%

39 Internet
oak.ulsan.ac.kr <1%

40 Internet
tel.archives-ouvertes.fr <1%

41 Internet
123dok.net <1%

42 Publication
A Cryogenic Engineering Conference Publication, 1996. <1%

43 Publication
Dimitrios A. Moysidis, Georgios D. Karatzinis, Yiannis S. Boutalis, Yannis L. Karnav... <1%

44 Publication
John Bird, John Bird. "Electrical and Electronic Principles and Technology", Routle... <1%

45 Publication
R Supangat, N Ertugrul, W L Soong, D A Gray, C Hansen, J Grieger. "Estimation of t... <1%

46 Publication
Zhang, Yue. "Cyber-Physical Augmentation for Robust and Scalable Occupant Mo... <1%

47 Internet
library.acadlore.com <1%

48 Internet
www.ijraset.com <1%

49 Publication
Marco Antonio Cotrina-Teatino, Jairo Jhonatan Marquina-Araujo, Jose Nestor Ma... <1%

50 Publication
Wangjie Lang, Yihua Hu, Chao Gong, Xiaotian Zhang, Hui Xu, Jiamei Deng. "Artifici... <1%

51 Internet
downloads.hindawi.com <1%

52 Internet
www.naturalspublishing.com <1%

53 Publication
Karolina Kudelina, Toomas Vaimann, Anton Rassolkin, Ants Kallaste, Bilal Asad, G... <1%

54 Publication
Paulo C. M. Lamim Filho, Lane M. Rabelo Baccarini, Fabiano B. Batista, Ana C. Ara... <1%

55 Internet
api.deepai.org <1%

56 Internet
os.zhdk.cloud.switch.ch <1%

57 Publication
Karolina Kudelina, Hadi Ashraf Raja, Viktor Rjabtšikov, Muhammad Usman Nasee... <1%

58 Publication
Mohamed Boudiaf Koura, Ahmed Hamida Boudinar, Ameur Fethi Aimer. "Improv... <1%

59 Publication
Yejvander Thakur, Geetesh Goga, Vipin Shrivastava. "A review study on the impro... <1%

60 Internet
dadun.unav.edu <1%

61 Internet
ruor.uottawa.ca <1%

62 Publication
Cem Ekin Sunal, Vladimir Dyo, Vladan Velisavljevic. "Review of Machine Learning ... <1%

63 Publication
Lydiah Aywa Sikinyi, Christopher Muriithi Maina, Livingstone Ngoo. "Condition M... <1%

64 Publication
Mohamed Esam El-Dine Atta, Doaa Khalil Ibrahim, Mahmoud I. Gilany. "Broken B... <1%

65 Publication
Pavithra R, Prakash Ramachandran. "An Overview Of Predictive Maintenance For ... <1%

66 Internet
docslib.org <1%

67 Internet
journals.plos.org <1%

68 Internet
papers.phmsociety.org <1%

69 Internet
repository.library.noaa.gov <1%

70 Internet
www.ijsrd.com <1%

71 Internet
www.jatit.org <1%

72 Internet
www.preprints.org <1%

73 Internet
5dok.net <1%

74 Publication
Mikhail Tsypkin. "Induction motor condition monitoring: Vibration analysis techn... <1%

75 Publication
Minh-Quang Tran, Meng-Kun Liu, Quoc-Viet Tran, Toan-Khoa Nguyen. "Effective F... <1%

76 Publication
Nikita Bhole, ShrutiSandip Ghodke. "Motor Current Signature Analysis for Fault D... <1%

77 Publication
Rodriguez, P.V.J.. "A simplified scheme for induction motor condition monitoring"... <1%

78 Internet
conservancy.umn.edu <1%

79 Internet
ntnuopen.ntnu.no <1%

80 Internet
openrepository.aut.ac.nz <1%

81 Internet
oulurepo.oulu.fi <1%

82 Internet
pure.tue.nl <1%

83 Internet
sageuniversity.edu.in <1%

84 Internet
sfera.unife.it <1%

85 Internet
www.bestpartstore.co.uk <1%

86 Internet
www.diva-portal.org <1%

87 Internet
www.rs.tus.ac.jp <1%

88 Publication
"Deep Learning", Walter de Gruyter GmbH, 2020 <1%

89 Publication
Bing Zhang. "A Novel Blind Deconvolution De-Noising Scheme in Failure Prognosi... <1%

90 Publication
Gunapriya Devarajan, Muniraj Chinnusamy, Lakshmi Kaliappan. "Detection and cl... <1%

91 Publication
J J. Saucedo-Dorantes, D. A. Elvira-Ortiz, A. Y. Jaen-Cuellar, J. A. Antonino-Daviu, R. ... <1%

92 Publication
Karolina Kudelina, Bilal Asad, Toomas Vaimann, Anton Rassolkin, Ants Kallaste. "... <1%

93 Publication
Lourembam Ranjita Devi, Sreenu Sreekumar, Rohit Bhakar, Dileep G., Sanjeeviku... <1%

94 Publication
Megha Singh, Abdul Gafoor Shaik. "Bearing fault diagnosis of a three phase induc... <1%

95 Publication
Merve Ertargin, Ahmet Orhan, Ozal Yildirim, Turan Gurgenc. "Automated fault cla... <1%

96 Publication
Mikko Tahkola, Victor Mukherjee, Janne Keranen. "Transient Modelling of Inducti... <1%

97 Publication
Noureddine Bessous. "Reliability Surveys of Fault Distributions in Rotating Electri... <1%

98 Publication
Rajeev Kumar, RS Anand. "Health Monitoring and Fault Analysis of Induction Mot... <1%

99 Publication
S. Nandi, H.A. Toliyat, X. Li. "Condition Monitoring and Fault Diagnosis of Electrica... <1%

100 Publication
Seho Son, Hyunseung Lee, Dayeon Jeong, Kyung ho Sun, Ki-Yong Oh. "Digital twin... <1%

101 Publication
Siegel, D.. "Novel method for rolling element bearing health assessment-A tach... <1%

102 Internet
clok.uclan.ac.uk <1%

103 Internet
dias.library.tuc.gr <1%

104 Internet
digitalcommons.usf.edu <1%

105 Internet
journal.esrgroups.org <1%

106 Internet
journals.pan.pl <1%

107 Internet
secure.ai.org.mx <1%

108 Internet
sndbx.library.tuc.gr <1%

109 Internet
trepo.tuni.fi <1%

110 Internet
wiredspace.wits.ac.za <1%

111 Internet
www.hindawi.com <1%

112 Internet
www.ijosi.org <1%

113 Internet
www.intechopen.com <1%

114 Internet
www.rroij.com <1%

115 Internet
www.worldscientificnews.com <1%

116 Publication
Bhumichai, Dhanasak. "Hybrid Deep Learning-Based Model for Eclipse Attack Det... <1%

117 Publication
Jorge Bonet Jara. "A precise, General, Non-Invasive and Automatic Speed Estimati... <1%

118 Publication
Kah Keng Wong. "Ensemble machine learning and tree-structured Parzen estimat... <1%

119 Publication
Muhammad Amir Khan, Bilal Asad, Karolina Kudelina, Toomas Vaimann, Ants Kall... <1%

120 Publication
Xiangjin Song, Jingtao Hu, Hongyu Zhu, Jilong Zhang. "A bearing outer raceway fa... <1%

121 Internet
doi.org <1%

122 Publication
"Improving Productivity through Automation and Computing", 2019 25th Interna... <1%

123 Publication

Anurag Choudhary, Deepam Goyal, Shimi Sudha Letha. "Infrared Thermography ... <1%

124 Publication

Jorge E. Salas-Robles, Vicente Biot-Monterde, Jose A. Antonino-Daviu. "Current an... <1%

125 Publication

Nipuna Rajapaksha, Shantha Jayasinghe, Hossein Enshaei, Nirman Jayarathne. "A... <1%

126 Publication

Sujata Dash, Subhendu Kumar Pani, Joel J. P. C. Rodrigues, Babita Majhi. "Deep Le... <1%

127 Publication

Z. Ye, A. Sadeghian, B. Wu. "Mechanical fault diagnostics for induction motor with... <1%